P-03-102

# Forsmark site investigation

# Interpretation of petrophysical surface data

# Stage 1 (2002)

Hans Isaksson, Håkan Mattsson,
Hans Thunehed, Mikael Keisu
GeoVista AB

February 2004

**Svensk Kärnbränslehantering AB**
Swedish Nuclear Fuel
and Waste Management Co
Box 5864
SE-102 40 Stockholm Sweden
Tel 08-459 84 00
+46 8 459 84 00
Fax 08-661 57 19
+46 8 661 57 19

ISSN 1651-4416
SKB P-03-102

# Forsmark site investigation

# Interpretation of petrophysical surface data

# Stage 1 (2002)

Hans Isaksson, Håkan Mattsson,
Hans Thunehed, Mikael Keisu
GeoVista AB

February 2004

*Keywords:* Petrophysics, Gamma-ray spectrometry, Anisotropy, Magnetic susceptibility, AMS, Density, Porosity, Resistivity, Induced polarisation.

# Contents

# 1 Introduction

This document reports *interpretation of petrophysical surface data,* which is one of the activities performed within the site investigation at Forsmark. The work was conducted according to activity plan AP PF-400-02-47 (SKB internal controlling document), by GeoVista AB; Hans Isaksson, Håkan Mattsson and Hans Thunehed. Mikael Keisu has been responsible for delivery of data.

The work carried out in this stage, stage 1, comprises petrophysical data collected during 2002. A revision will be carried out after collecting new petrophysical data during 2003.

No field work has been performed.

# 2 Objective and scope

The purpose of petrophysical measurements is to gain knowledge of the physical properties of different rock types. This information is used to increase the understanding of geophysical measurements and to support the geological mapping.

The work comprises statistical processing and evaluation of results from the 2002 petrophysical sampling and gamma ray spectrometry measurements on outcrops /1/. The analyses were made with respect to rock type characteristics and the geographical distributions of the measured properties. Data from the magnetic susceptibility measurements carried out during the geological mapping 2002 /2/ are also included in the report. A special study on the anisotropy of magnetic susceptibility (AMS) of rocks is presented. The AMS method gives 3D-oriented information related to deformational rock fabrics.

In some figures, contour maps based on interpolation methods of petrophysical parameters are presented. In some cases, the interpolation of petrophysical data is questionable, but it is performed in this report in order to better visualize the spatial variations in the data. Detailed variations in these contour maps should be ignored.

# 3 Input data and geological coding

The following laboratory measurements have been carried out: magnetic susceptibility, remanent magnetization, anisotropy of magnetic susceptibility (AMS), density, porosity, electric resistivity and induced polarization. Measurements of natural gamma radiation with a portable gamma-ray spectrometer were performed in situ on outcrops. A description of the collection of samples, laboratory measurement techniques, sample and data handling and the performance of in situ gamma-ray spectrometry measurements is given in /1/. Each sampling (measurement) location was assigned an identity code "PFMXXXXXX" (where XXXXXX is a serial number) followed by a rock order number, which correspond to the location identity code and the rock order number used for the bedrock mapping /2/. The rock order number is followed by a specimen number, which separates the different drill cores (samples) collected at each location.

The selection of sampling (measurement) locations was performed in co-operation with the responsible geologist Michael B. Stephens (Geological Survey of Sweden). A geological coding system was established containing four major rock groups (A, B, C and D) and sub-groups of rock types for each rock group respectively. Each rock sample was classified according to this system, which is presented below.

**Group A. Supracrustal rocks**

A1. Felsic to intermediate metavolcanic and metavolcanoclastic rocks

A2. Fe-rich mineralization

A3. Veined gneiss (paragneiss?)

**Group B. Ultramafic, mafic, intermediate and quartz-rich felsic (granitoid) meta-intrusive rocks**

B1. Meta-ultramafic rock

B2. Metagabbro

B3. Metadiorite, quartz-bearing metadiorite, metadioritoid

B4. Amphibolite

B5. Metatonalite

B6. Metatonalite to metagranodiorite

B7. Metagranodiorite

B8. Metagranodiorite to metagranite

B9. Metagranite

B10. Metagranite, aplitic

**Group C. Quartz-rich felsic (granitoid) meta-intrusive rock, fine- to medium-grained. Occurs as dykes and lenses within rocks belonging to Groups A and B**

(No subgroups)

**Group D. Granite, pegmatitic granite, pegmatite. Occurs as dykes and minor intrusive bodies within rocks belonging to Groups A and B. Pegmatites display variable time relationships to Group C**

D1. Granite

D2. Pegmatitic granite

D3. Pegmatite

The field-geologists who performed the bedrock mapping carried portable instruments for in situ measurements of the magnetic susceptibility /2/. Eight readings were taken on each rock type at the observed outcrops, which has created a unique database of 853 locations and 1602 rock types covering a large part of the Forsmark area. A compilation of this data is presented in Chapter 9.

# 4 Density and magnetic properties

Different rock types vary in composition and this leads to variations in their petrophysical properties. The rock density and magnetic properties (susceptibility and remanence) are therefore often used as supportive information when classifying rocks. These properties are important for the interpretation of geophysical data and they also constitute input parameters when modelling gravity and magnetic data.

## 4.1 Data processing

In order to get a better picture of the data and to increase the possibility to compare different data sets and data from different rock types, certain sub-parameters are often calculated from the density, the magnetic susceptibility and the magnetic remanence. Two such sub-parameters are the silicate density and the Q-value (Königsberger ratio). The silicate density /3/ provides an estimation of the rock composition and is calculated by correcting the measured total density for the content of ferromagnetic minerals (e.g. magnetite and pyrrhotite) by use of the magnetic susceptibility. The Q-value /4/ is the quotient between the remanent and induced magnetization:

$$Q = \frac{M_R}{M_I} = \frac{M_R}{KH} = \frac{M_R \mu_0}{KB}$$

where

$M_R$ = Remanent magnetization intensity (A/m)
$M_I$ = Induced magnetization (A/m)
$K$ = Magnetic susceptibility (SI)
$H$ = Magnetic field strength (A/m)
$B$ = Magnetic flux density (T)
$\mu_0$ = Magnetic permeability in vacuum ($4\pi\ 10^{-7}$ Vs/Am)

The Q-value thus indicates the contribution of the remanent magnetization to the measured anomalous magnetic flux density and is therefore an important parameter when interpreting and modelling ground and airborne magnetic data. The Q-value is also grain size dependent and indicates what ferromagnetic minerals that are present in the rock.

In this investigation the so called density-susceptibility rock classification diagrams (see for example Figure 4-1) were used. The Y-axis in these diagrams displays the magnetic susceptibility on the left hand side and the estimated magnetite content to the right. It has been shown that in rocks in which the magnetic susceptibility is primarily governed by magnetite, there is a fairly good correlation between the magnetic susceptibility and the magnetite content /5/. However, the scatter is fairly high so predictions of the volume-percent magnetite in rocks based on the magnetic susceptibility should be used with caution.

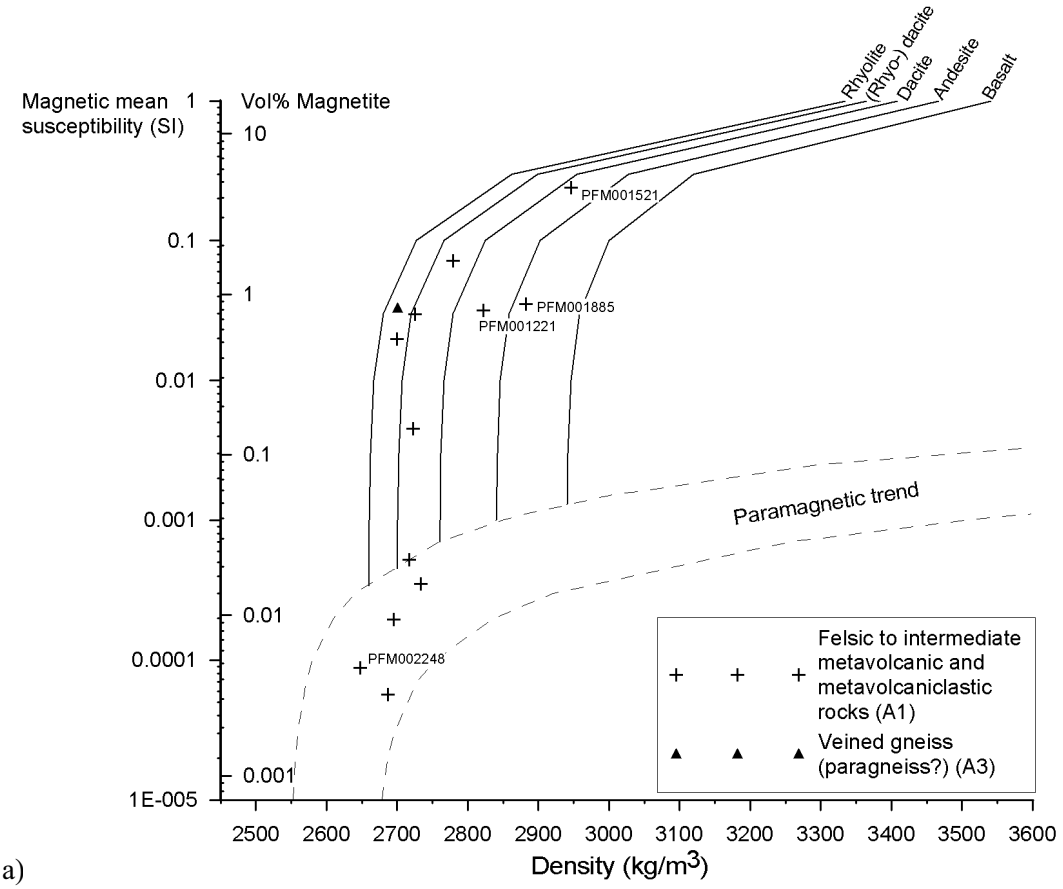
Magnetic mean susceptibility (SI)
Vol% Magnetite
Rhyolite
(Rhyo-) dacite
Dacite
Andesite
Basalt
PFM001521
PFM001885
PFM001221
PFM002248
Paramagnetic trend
Felsic to intermediate metavolcanic and metavolcaniclastic rocks (A1)
Veined gneiss (paragneiss?) (A3)
Density (kg/m3)

a)

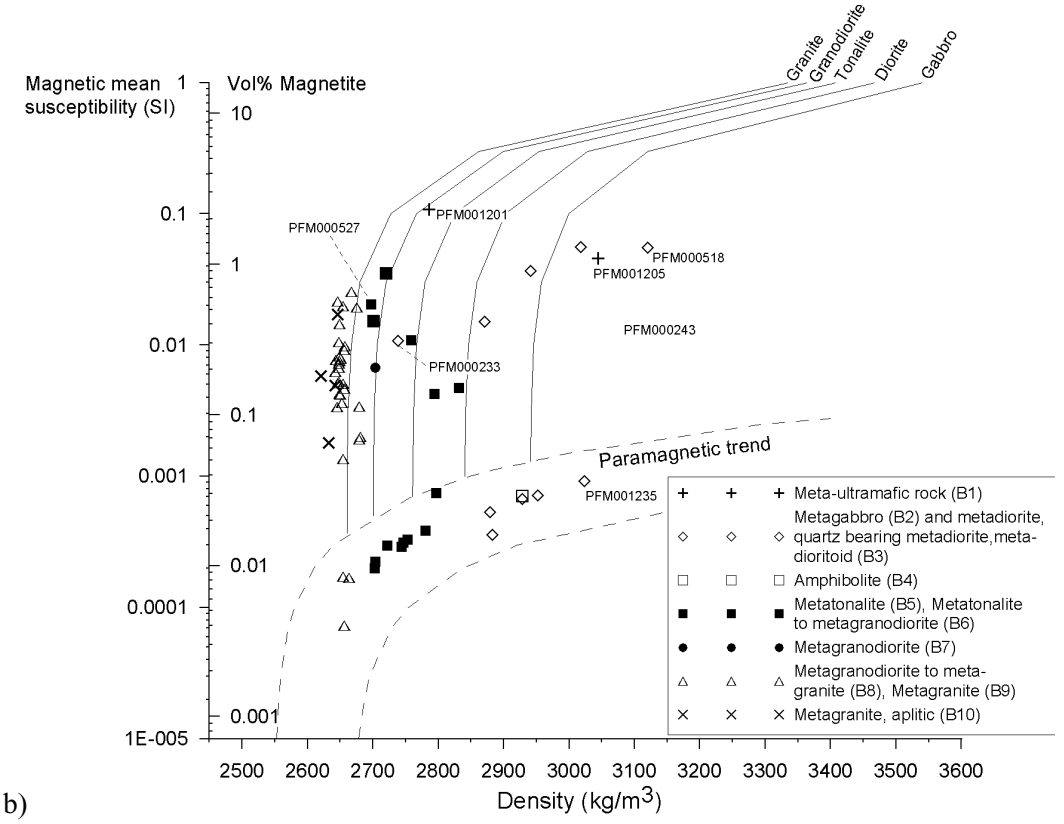
Magnetic mean susceptibility (SI)
Vol% Magnetite
Granite
Granodiorite
Tonalite
Diorite
Gabbro
PFM000527
PFM001201
PFM000518
PFM001205
PFM000243
PFM000233
PFM001235
Paramagnetic trend
Meta-ultramafic rock (B1)
Metagabbro (B2) and metadiorite, quartz bearing metadiorite,meta-dioritoid (B3)
Amphibolite (B4)
Metatonalite (B5), Metatonalite to metagranodiorite (B6)
Metagranodiorite (B7)
Metagranodiorite to meta-granite (B8), Metagranite (B9)
Metagranite, aplitic (B10)
Density (kg/m3)

b)

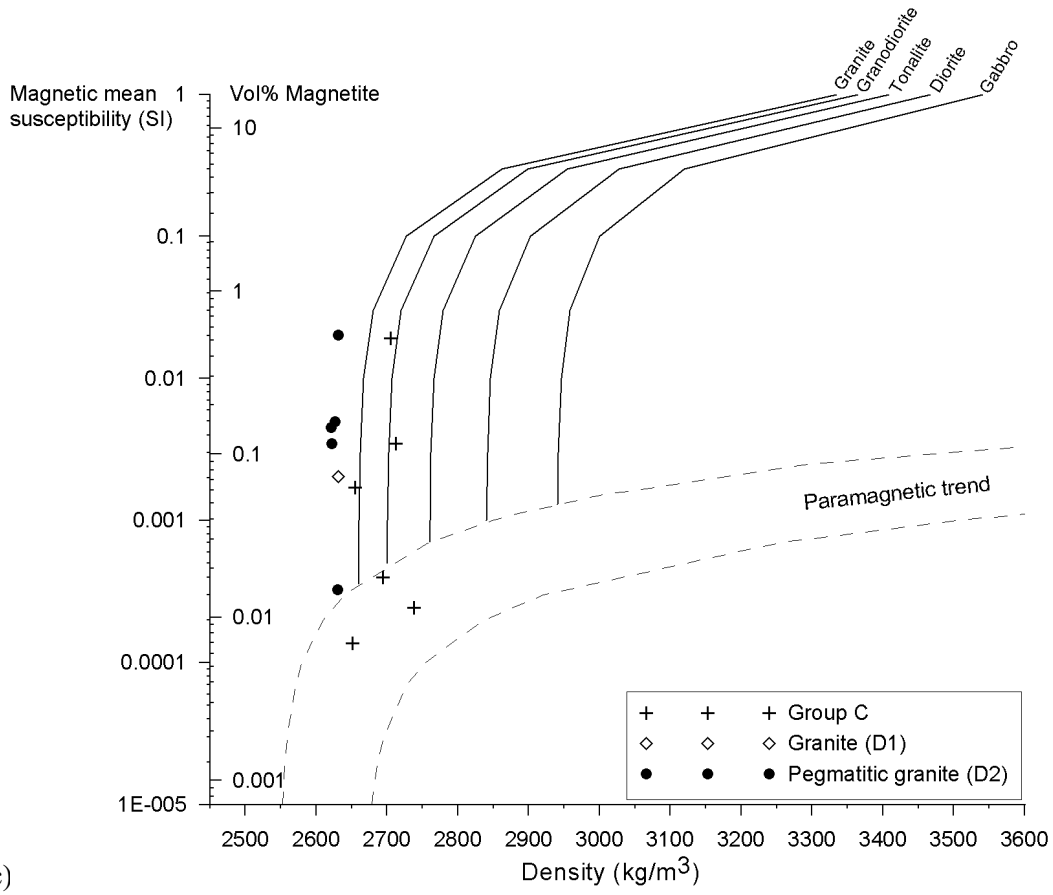


***Figure 4-1.*** *Density-susceptibility rock classification diagrams for the rocks of the Forsmark area. See the text for explanation.*

The silicate density curves are based on equations from Henkel 1991 /3/, and the average densities of each rock type originate from Puranen 1989 /6/. The diagram should be read in the way that if a rock sample plots on, or close to, a "rock type curve" it is indicated that the rock should be classified according to the composition of this rock type. Since there is often a partial overlap of the density distributions of different rock types, there is always a certain degree of uncertainty in the classification. A sample plotting in between, for example, the granite and granodiorite curves should thus be classified as granite to granodiorite.

## 4.2 Results

The classification of the volcanic rocks, groups A1 and A3, indicates that a majority of the rocks should be classified as rhyodacite to dacite (Figure 4-1a). If the three samples from the Fe-rich mineralizations are excluded, the rock densities average at c 2750 kg/m$^3$ (Figure 4-2a). The rock at PFM002248 has a significantly lower density and is classified as rhyolite whereas the rocks at the sites PFM001221 (rock order number 5) and PFM001521 classify as dacite to andesite. At site PF001885 the rock density is 2882 kg/m$^3$, which indicates that the rock should be classified as andesite to basalt. It appears to be two subgroups of high and low magnetic susceptibility rocks within the felsic to intermediate metavolcanic group (A1).

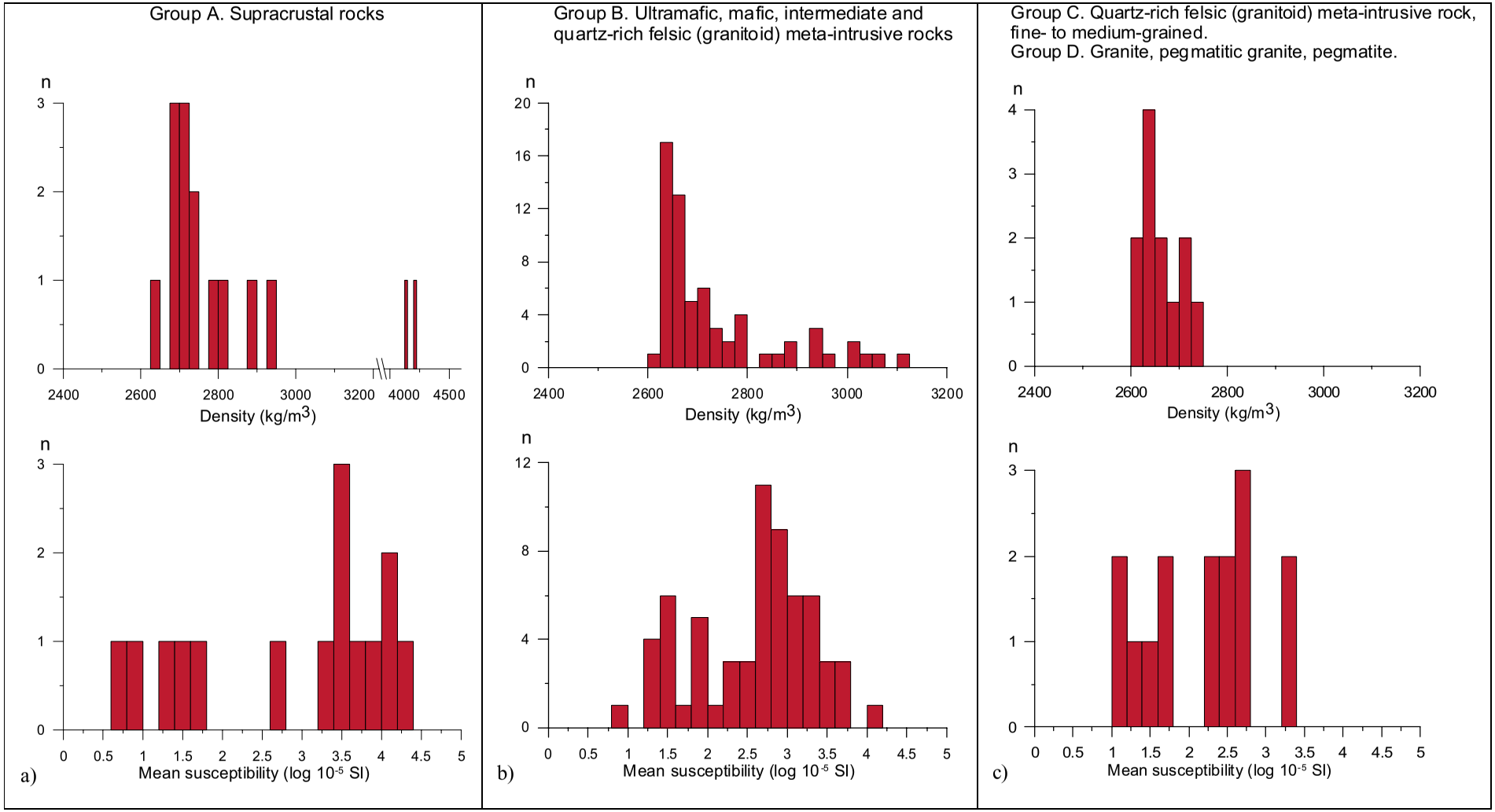


*Figure 4-2. Histograms showing the distribution of density and magnetic susceptibility of the rocks in the Forsmark area.*

The group B rocks vary greatly in composition, ranging from leucocratic granite to ultramafic rocks. However, a majority of the rocks falls close to the granite and granodiorite classification curves (Figures 4-1b and 4-2b). The meta-ultramafic rock at site PFM001201 has suffered from alteration (serpentinization) which has lowered its density to a value corresponding to a granodiorite composition. The rocks at the sites PFM000243, PFM00518 and PFM001205 have densities ranging from 3045 kg/m$^3$ to 3120 kg/m$^3$, which are fairly high, compared to the average density of 2940 kg/m$^3$ used for classifying gabbro rocks. This indicates that the rocks have compositions corresponding to ultramafic rocks. The rock at site PFM001235 also plots rather far to the right of the gabbro classification curve but is anyhow classified as a gabbro. At site PFM000233, which belongs to the metadiorite, quartz bearing metadiorite, metadioritoid group (B3) the rock density indicates a composition between granodiorite and tonalite. The rock at site PFM000527 classifies as granite to granodiorite due to its comparatively low density of 2697 kg/m$^3$.

There is an indication in the diagram (Figure 4-1b) that the metatonalite to metagranodiorite rocks (groups B5 and B6) can be divided into two “magnetic subgroups”, one group containing a fair amount (0.1–1 volume percent) of magnetite and the other containing no, or only a small amount, of ferromagnetic minerals. This may be important for future work involving for example modelling of magnetic data. A similar “magnetic” grouping is also indicated for the metagabbro, metadiorite, quartz bearing metadiorite, metadioritoid groups (B2 and B3) and slightly indicated for the metagranodiorite-metagranite to metagranite rock groups (B8 and B9).

The metagranodiorite-metagranite to metagranite rock groups (B8 and B9) have an average density of 2655 ± 11 kg/m$^3$, which is slightly lower than what is expected for “normal” granite.

The quartz-rich felsic granitoids (group C) mainly classify as granodiorite, whereas the rocks of group D (granite, pegmatitic granite and pegmatite) generally have lower densities and are classified as leucocratic granite (Figures 4-1c and 4-2c).

A contour plot of the geographical distribution of wet densities for the main rocks in the Forsmark area is presented in Figure 4-3 (gridding performed with Surfer 8, ™ Golden Software), inverse distance to the power of 2, cell size = 200 m, search radius = 1000 m). The data indicates that the candidate area is dominated by low densities (2625 kg/m$^3$ to 2675 kg/m$^3$) corresponding to granite rocks. A “tongue” of higher densities, related to the metatonalite rock, crosscuts the north-eastern boundary of the candidate area. Along the south-eastern boundary of the candidate area there is a fairly sharp density contrast and there is a well defined increase in density south-westward.

The geographical distribution of the main rock types classified on basis of the silicate density indicates that a vast majority of the rocks of the sampling locations within the candidate area, where the bedrock is mainly mapped as granite to granodiorite, classify as rocks with a composition corresponding to granite (Figure 4-4). There is a generally good agreement between the silicate density classifications and the geological map, but minor differences do occur. It must be emphasized that the silicate density is only an indicator of the composition of rocks, and deviations between the silicate density classification and the geological classification will always occur. An interesting observation is the scatter in silicate densities of the rocks of the four sampling locations within the metatonalite-metagranodiorite that crosscuts the north-eastern boundary of the candidate area. The silicate densities vary from 2698 kg/m$^3$ to 2780 kg/m$^3$, which may indicate fairly large compositional variations within this rock unit.

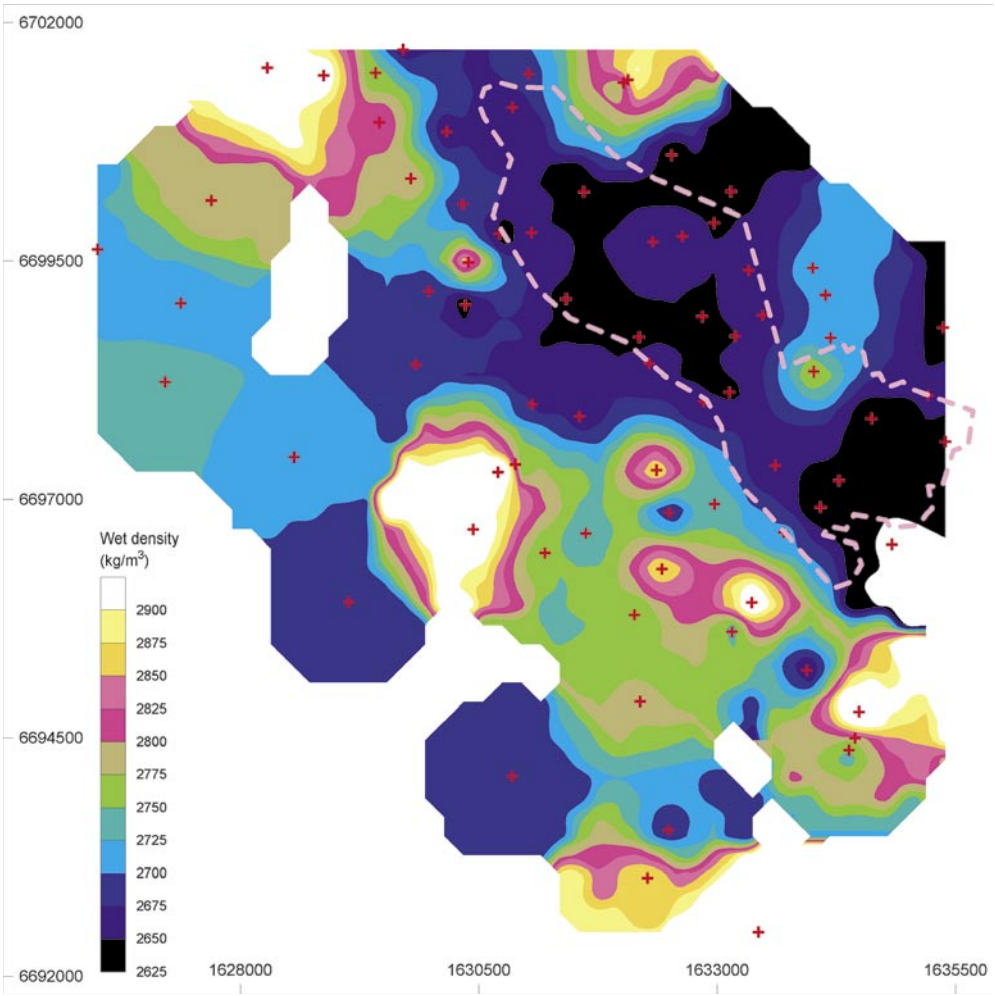


***Figure 4-3.*** *Contour plot of wet density distribution for the main rocks (rockorder number 1) in the Forsmark area. Mineralized rocks (group A2) and granitoid dykes (group C) are excluded. Red crosses denote sampling locations.*

A vast majority of all measured rock samples have Q-values below 0.5, which indicates that magnetic anomalies mainly reflect the magnetization induced by the present earth magnetic field. However, the obtained Q-values are high enough to recommend that the direction and intensity of the remanent magnetization should be accounted for in modelling of magnetic data from the area. At three sites there are indications of extremely high Q-values; Q = 25.5 (metagabbro PFM000243), Q = 14.9 (Fe-mineralization PFM000336) and Q = 15.9 (Fe-mineralization PFM000446). The Q-value of the metagabbro is calculated using susceptibility and remanence intensity data from two different specimens within the site, which makes this result a bit uncertain. However, it is reasonable to believe that the Q-values of all the three rock types may be very high, which may have a significant effect on the shape and intensity of related magnetic anomalies.

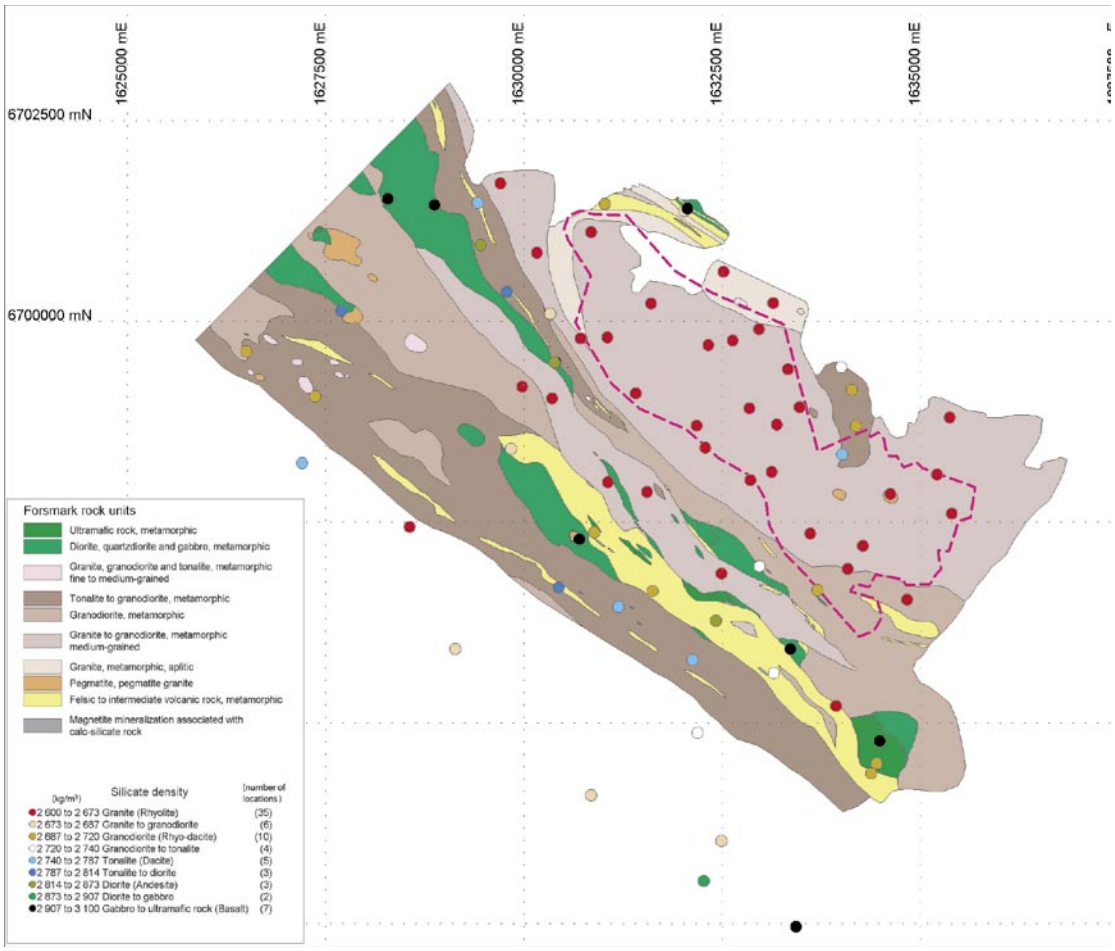


***Figure 4-4.*** *Geographical distribution of rock classification based on silicate density for the main rocks (rockorder number 1) in the Forsmark area plotted on the present geological map. Mineralized rocks (group A2) and granitoid dykes (group C) are excluded.*

The diagram of natural remanence intensity versus magnetic susceptibility for the volcanic group of rocks (groups A1–A3, Figure 4-5a) indicates that the previously suggested magnetic subgroups within the felsic to intermediate metavolcanic rocks (group A1) do not differ significantly in Q-values. In fact, the low susceptibility group has a slightly higher average Q-value than the high susceptibility group. This suggests that the varying susceptibility is only related to variations in magnetite content within the rocks. This is also valid for the metagranodiorite to metagranite group (B8 and B9). However, the high susceptibility specimens of the metatonalite to metagranodiorite rocks (groups B5 and B6; PFM000777, PFM001217, PFM000774, PFM000891, PFM000527 and PFM000808) have significantly higher Q-values than the low susceptibility specimens (PFM001860, PFM001859, PFM000804, PFM001861, PFM001510, PFM000380, PFM001162 and PFM002056) ($Q_{high\ sus} = 0.39$, $Q_{low\ sus} = 0.07$), which indicates that the two groups may have different magnetic mineralogy, or that different grain sizes of magnetite govern their magnetization (Figure 4-5b). This is also valid for the metagabbro, metadiorite, quartz bearing metadiorite, metadioritoid groups (B2 and B3). Both explanations given above of these groupings may be of importance for the understanding of the geology of the area. For example, all four sites within the metatonalite-metagranodiorite rock, previously mentioned, that crosscuts the north-eastern boundary of the candidate area all have low Q-values and low susceptibilities, to be compared with the larger variance in silicate density in the same samples.

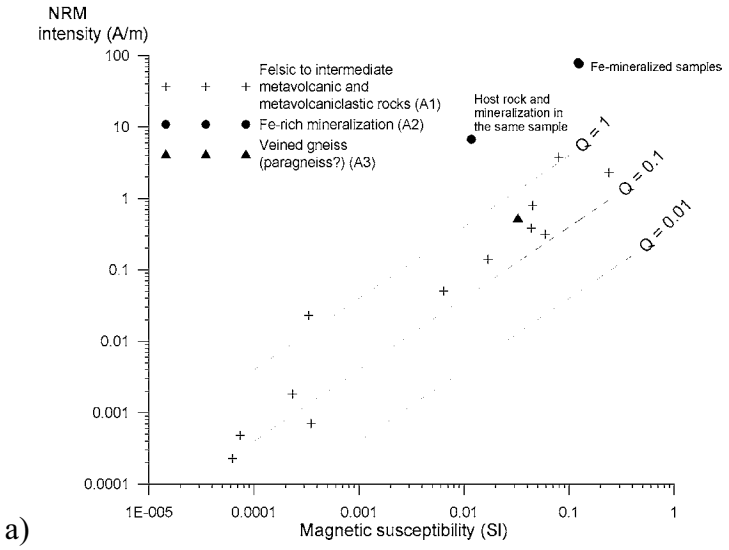


a)

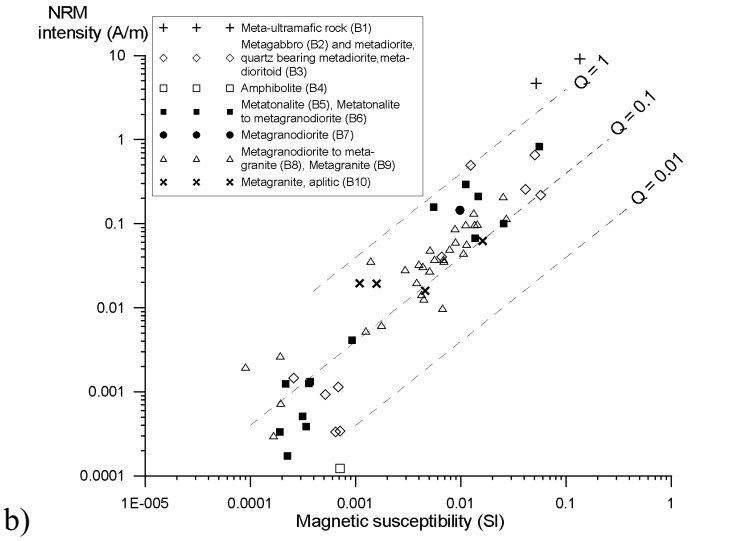


b)

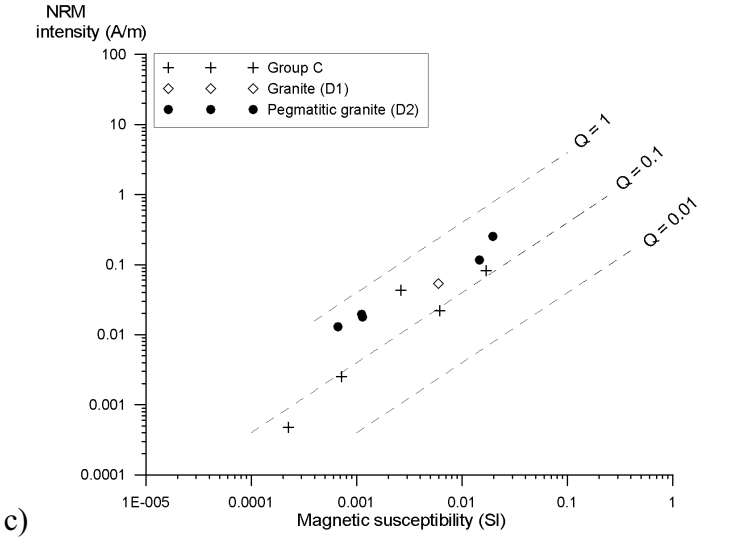


c)

*Figure 4-5. Natural remanent magnetization (NRM) intensity versus magnetic susceptibility for the rocks from the Forsmark area. See the text for explanation.*

The NRM-directions of the investigated rocks show moderate to steep inclinations and scattered declinations, without any sign of clustering (Figure 4-6a). No significant grouping is found for the different rock groups A, B, C or D. The large number of samples plotting in the south east direction (Figure 4-6b), parallel to the maximum strain indicated by the magnetic lineations (Figure 5-4), suggests that the NRM-directions are affected by the deformation of the rocks. Otherwise a majority of the NRM-directions ought to fall closer to the direction of the present earth magnetic field (approximate declination = 358° and inclination = 72°).

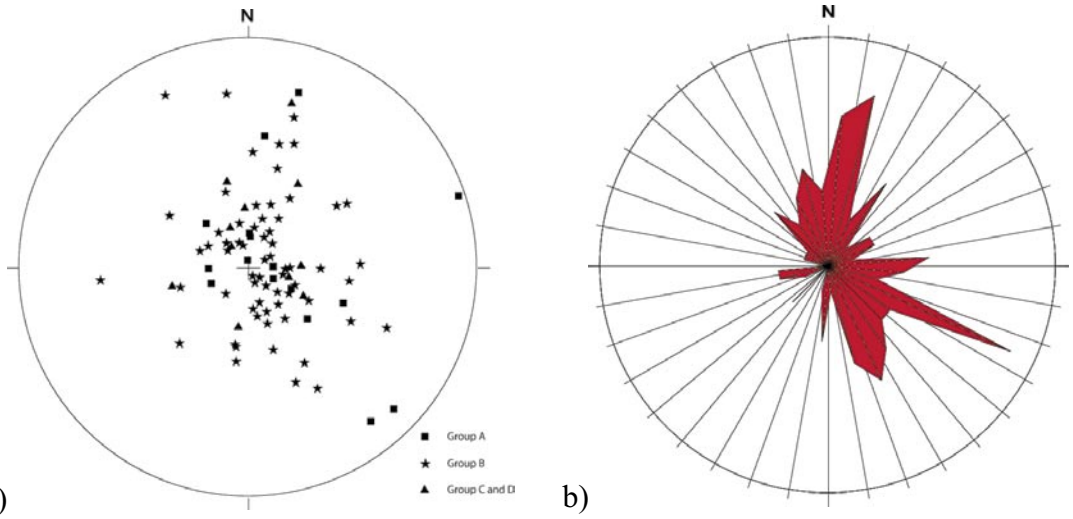


a) b)

***Figure 4-6.*** *a) Equal area projection diagram and b) rose diagram of NRM-directions of rock samples from the Forsmark area.*

# 5 Anisotropy of magnetic susceptibility (AMS)

## 5.1 The method

Since the anisotropy of magnetic susceptibility (AMS) is a fairly new and unknown method, this paragraph gives a brief introduction to its origin and application. A more complete description of AMS can be found in, for example, /7/.

The magnetic anisotropy of rock forming minerals basically originates from two sources, the grain shape and the crystallographic structure /8/. Magnetite is ferromagnetic and carries strong shape anisotropy, whereas pyrrhotite and hematite are governed by crystalline anisotropy due to their antiferromagnetic origin. Paramagnetic minerals (e.g. biotite, hornblende) and diamagnetic minerals (e.g. quartz, feldspars) are also carriers of magneto-crystalline anisotropy. The orientation of the anisotropy of magnetic susceptibility coincides with the crystallographic axes for most rock forming minerals, and it is therefore possible to directly transfer “magnetic directions” to “tectonic directions” (foliation and lineation) measured in the field.

Since magnetite carries a very high magnetic susceptibility in comparison to most other rock forming minerals, even a low grade tends to dominate the magnetic properties, including the anisotropy of a rock. However, for e.g. “non-magnetic” granites the magnetic anisotropy is mainly governed by biotite and other paramagnetic minerals.

The magnetic susceptibility ***K*** is generally written as a constant of proportionality between the applied field ***H*** and the induced magnetisation ***M***. However, the susceptibility responds differently to different directions of the applied field. It is anisotropic and *K* can not be described as a simple scalar, but has to be written as a symmetric 3×3 tensor /9/:

$$\begin{bmatrix} M_x \\ M_y \\ M_z \end{bmatrix} = \begin{bmatrix} k_{11}k_{12}k_{13} \\ k_{21}k_{22}k_{23} \\ k_{31}k_{32}k_{33} \end{bmatrix} \begin{bmatrix} H_x \\ H_y \\ H_z \end{bmatrix}$$

where x, y and z stands for three perpendicular directions in a right handed co-ordinate system. The tensor *K* is termed the anisotropy of magnetic susceptibility (AMS) tensor (on matrix form). It is a symmetric tensor implying that

$$k_{12} = k_{21}; k_{13} = k_{31}; k_{23} = k_{32}$$

By the use of linear algebra it is possible to calculate the eigenvalues and the eigenvectors of K. The eigenvectors are termed principal directions (p1, p2, p3) and the eigenvalues principal susceptibilities K1 (or kmax), K2 (or kint), and K3 (or kmin), where K1 ≥ K2 ≥ K3. The principal susceptibilities can graphically be described by an ellipsoid, with K1 representing the long axis, K2 the intermediate and K3 the short axis (Figure 5-1).

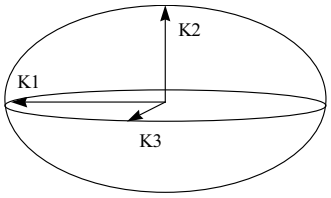


***Figure 5-1.*** *The anisotropy ellipsoid, K1 = maximum axis, K2 = intermediate axis, K3 = minimum axis.*

The degree of anisotropy is usually characterised by P = K1/K3. The degree of foliation is F = K2/K3 and the degree of lineation is L = K1/K2. The shape of the anisotropy ellipsoid is defined by the shape parameter T, see below. For $-1<T<0$ the ellipsoid is prolate (cigar-shaped) and for $0<T<1$ the ellipsoid is oblate (disc-shaped). If T = 0 the ellipsoid is neutral.

$$T = \frac{2\ln K2 - \ln K1 - \ln K3}{\ln K1 - \ln K3}$$

The magnetic susceptibility indicates the volumetric content and type of magnetic minerals in a rock. For primary low-magnetic granitoids in which the susceptibility is carried primarily by iron-bearing silicates (biotite and hornblende), the susceptibility is proportional to the iron content and can be used as a petrography index /10/. If different rock types vary in mineralogy they may be identified by means of variations in their magnetic susceptibility. However, when dealing with altered or deformed rock types containing ferromagnetic minerals (e.g. magnetite, hematite or pyrrhotite) the link between the susceptibility and petrography is complex. Brittle deformation of rocks causes fracturing and in the vicinity of the fractures magnetite oxidizes to hematite, which decreases the magnetic susceptibility giving rise to low magnetic zones. Also plastic deformation affects the magnetic mineralogy but the result is more complex since the deformation may lead to a destruction of magnetite, but flowing of hydrothermal fluids may lead to a creation, recrystallization, of magnetite as well.

An unaltered rock carries a primary AMS fabric that corresponds to the rock type, its mineral composition and the environment in which it was formed. Sedimentary rocks generally show an oblate shaped AMS ellipsoid orientated parallel to the bedding plane, thus with the minimum principal susceptibility axis orthogonal to the bedding. A lineation can be developed if the grains were deposited in a slope or in running water /7/, otherwise the K1 and K2 axes form a girdle pattern. AMS is a well-known indicator of the direction of magma flow in basic dykes and the method has been used in several studies to define flow fabrics (for example /11, 12 and 13/). Basic sills and dikes and basaltic lava flows usually carry a degree of AMS of less than 10% and the fabric of sub horizontal sills reminds of that of sedimentary rocks. AMS has been applied to many granite plutons for kinematical reconstruction of their emplacement /14 and 15/. A primary magnetic fabric can generally be related to the shape of the intrusion /7/ and preferred orientations of feldspars (known as geological magma flow indicators) tend to be parallel to the magnetic foliation plane, for example /16/. If the magnetic foliation of a granite pluton is parallel to a regional foliation, the pattern may be due to large scale deformation.

The deformation of a rock produces strain that imposes a secondary magnetic fabric. A brittle deformation basically gives rise to rigid grain rotation and fracturing whereas a plastic deformation mainly causes changes of the grain shape that result in a tectonic foliation and lineation. Therefore, plastic deformation must be considered as the main

producer of secondary magnetic fabrics. However, /17/ reported deformational AMS structures in two monzonite plutons that lack visible tectonic structures. From the general theory of magnetic anisotropy we can see that small changes of the distances between atoms, ions or crystal lattices are enough to change the anisotropy and therefore the magnetic susceptibility can be more sensitive to minor deformations that are not visible to the eye.

Attempts to connect the degree of anisotropy to the degree of strain are reported by for example /7, 17, 18 and 19/. Examples of good correlation have been found over a limited range of strain, but there are large problems to overcome, such as growth or recrystallisation of minerals. Also, measurements of the AMS reflect the properties of an entire rock and not just a specific grain fraction. In general, if the primary rock fabric is determined by AMS, if the degree of deformation is low and if there is no recrystallisation of minerals, it should be possible to determine the amount of strain by use of the AMS. However, these criteria are not easily achieved.

## 5.2 Data processing

The sampling for AMS analyses in Forsmark includes 88 rock objects at 80 sites /1/, and generally 4 drill cores were collected at each object. One specimen was cut from each drill core and the AMS measurements were performed, which produced four data readings per object. The four measurements on an individual rock object allow a calculation of mean directions of the principal AMS axes (called the site mean direction) and corresponding "site mean value" of the degree of anisotropy (P), degree of lineation (L), degree of foliation (F) and ellipsoid shape (T). When calculating the site mean values of the P, L, F and T parameters, the orientations of the ellipsoids of each specimen are taken into account. Vector addition is applied to the three susceptibility axes of the four specimens from the site, which results in a "site mean ellipsoid". The site mean values of the anisotropy parameters thus give information of the site as a whole and are not just "simple" average values. According to statistical demands at least six measurements (specimens) are required for estimating uncertainty regions of the calculated mean directions. No such calculations were therefore performed. Instead, the data quality of each site was evaluated by visual inspection and site mean directions based on scattered specimen directions were rejected (about 10% of the data were rejected). At four sites, only two specimens gave measurable results and if the corresponding principal axes fell close to each other the mean direction was accepted as a site mean direction. If the principal directions of the two specimens were far apart, no mean direction could be established, and the data were rejected.

## 5.3 Results

The average mean susceptibility of all measured rock specimens shows a distinct bimodal distribution, which indicates two populations of magnetic carriers (Figure 5-2a). The low-magnetic specimens average at c $50\times10^{-5}$ SI, which suggests no, or very little, content of ferromagnetic minerals such as magnetite, hematite or pyrrhotite. The group of specimens with higher susceptibilities has an average value of c $1000\times10^{-5}$ SI, which clearly indicates the presence of ferromagnetic minerals (most likely magnetite). Histograms of the susceptibility of different rock units (Figure 4-2) indicate that both low ($10^{-4}$ SI) and high ($10^{-2}$ SI) susceptibilities also occur within the group of meta-granitiod (group B) rocks that dominate the bedrock of the investigated area.

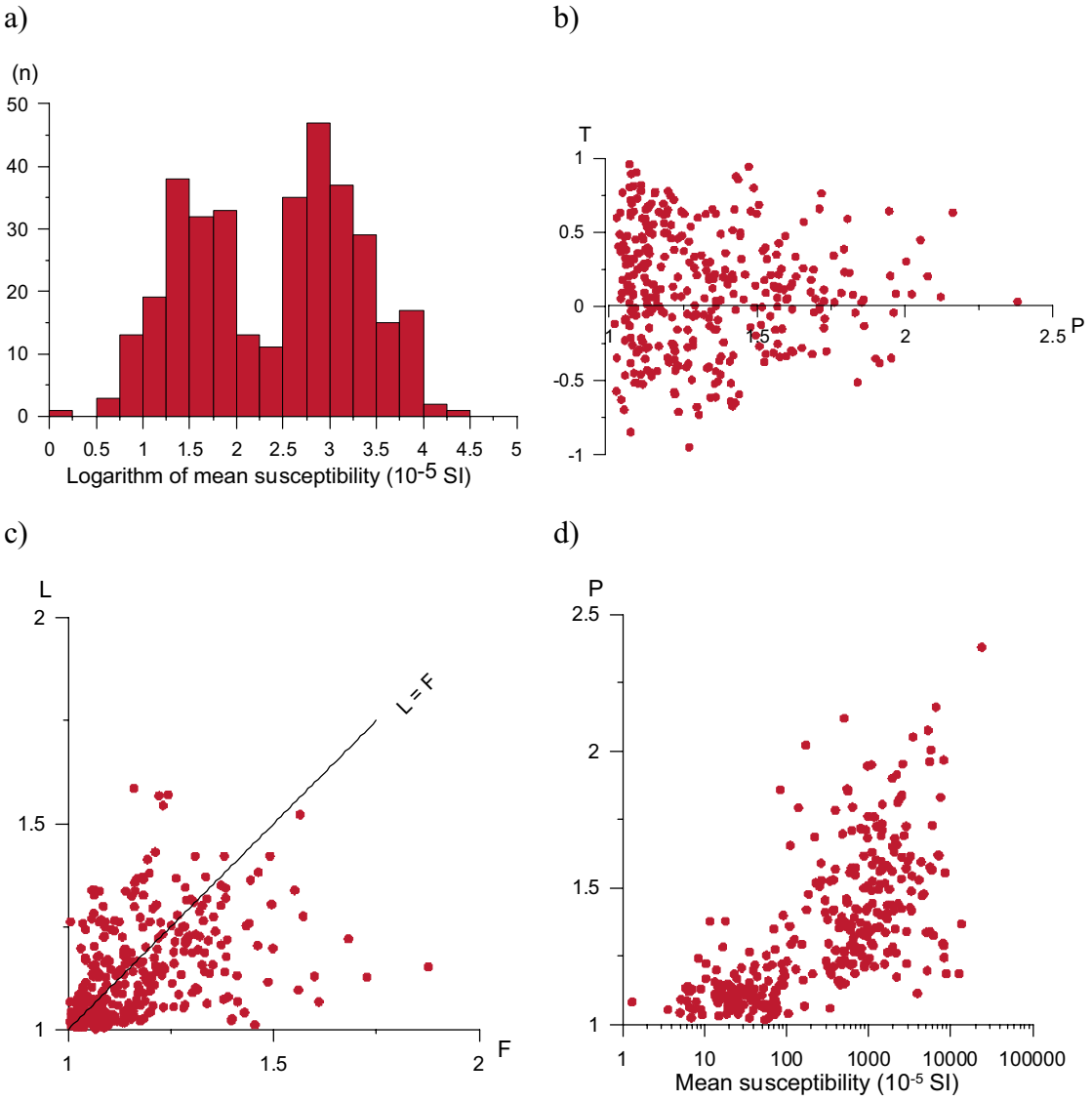


***Figure 5-2.*** *Anisotropy of magnetic susceptibility parameters for individual specimens from all sampling sites. a) Histogram of the mean susceptibility, b) Shape parameter (T) versus degree of anisotropy (P), c) Degree of lineation (L) versus degree of foliation (F) and d) Degree of anisotropy (P) versus mean susceptibility.*

The average degree of anisotropy is P = 1.36, which is a fairly high value, and about 60% of the specimens have a degree of anisotropy P > 1.2 (Figure 5-2b). This indicates that a majority of the investigated rocks have been affected by plastic deformation most likely related to the regional deformation and metamorphism of the area. However, a correlation is seen between the degree of anisotropy and the volume susceptibility, which indicates that the P-parameter is dependent (at least from a statistical point of view) on the concentration of magnetite and can not be directly connected to the degree of tectonic strain (Figure 5-2d). This correlation is also seen in the site mean data and it is most likely related to an interaction between magnetite grains. Since there is a wish to identify areas within the site investigation area that have suffered from a high degree of deformation, an attempt was made to "correct" the degree of anisotropy for the dependence to the volume susceptibility.

The magnetite content, as well as the concentration of other magnetic minerals, is often rock type dependent. Therefore, only the group B rocks, with the exception of the mafic rocks (sub-groups B1, B2 and B4) were selected for the correction, which includes a total number of 54 sampling locations. It is assumed that the P-parameter depends on a linear combination of the two components grain shape and volume susceptibility, and a principal component analysis (PCA) is applied to the P-parameter and corresponding mean susceptibility data. By calculating eigenvectors and eigenvalues for the data it is possible to mathematically separate the two components from each other; one solely dependent on the volume susceptibility, the other independent of the susceptibility and in theory mainly dependent on the grain shape of the minerals. The geographical distribution of the "corrected" degree of anisotropy is presented as a contour plot in Figure 5-3a. The data broadly indicates three northwest-southeast trending regions of varying degrees of anisotropy. Northeast of the candidate area the rocks are dominated by moderate degrees of anisotropy. In the central part there is domination of low degrees and in the south-western part many rocks carry moderate to high degrees of anisotropy. The result suggests that the lowest strained rocks are found in the central part of the candidate area and the highest strained rocks occur southwest of the candidate area. In Figure 5-3b a contour plot of the ellipsoid shape parameter (T) is presented. The T-parameter shows no correlation to the mean susceptibility and has therefore not been altered. The rocks of the candidate area are dominated by weakly prolate to neutral shaped ellipsoid, whereas the rocks to the west of the candidate area, together with the metatonalite rock crosscutting the northern boundary, have AMS-ellipsoids dominated by weak to strong oblate shapes. Oblate shaped ellipsoids (S-tectonites) seem to be related to rocks with a high degree of anisotropy.

An equal area projection plot of site mean directions of the minimum (poles to foliation) and maximum (lineation) AMS axes for all investigated sites shows a fairly uniform pattern where the minimum axes form a girdle pattern, however with a cluster in the northeast sub horizontal direction, and the maximum axes cluster in the southeast direction with moderate to steep dips (Figure 5-4). A general interpretation of the distribution of the AMS axes is that a majority of the rocks have suffered from a dominant NE-SW directed compressive deformation with a maximum strain in the southeast direction, dipping downwards c 45°.

The division of the sampling sites into the four rock groups A, B, C and D (where A = Supracrustal rocks, B = Ultramafic, mafic, intermediate and quartz-rich felsic (granitoid) meta-intrusive rocks, C = Quartz-rich felsic (granitoid) meta-intrusive rock, fine- to medium-grained and D = Granite, pegmatitic granite, pegmatite) shows that the general AMS fabric seems to dominate also the individual A, B and C groups but not the D group (Figure 5-5). The girdle distribution of the minimum axes (poles to foliation) is only present in group B and it indicates a folded geometry. The estimated orientation of the fold axis defined from the average intersection point of the planes belonging to each of the poles falls at Declination = 134° and Inclination = 43° (Figure 5-5). The magnetic lineation of group B are clustered and display a mean direction of Declination = 134° and Inclination = 50°, which indicates that the direction of the fold axis is parallel to the direction of the lineation.

a)

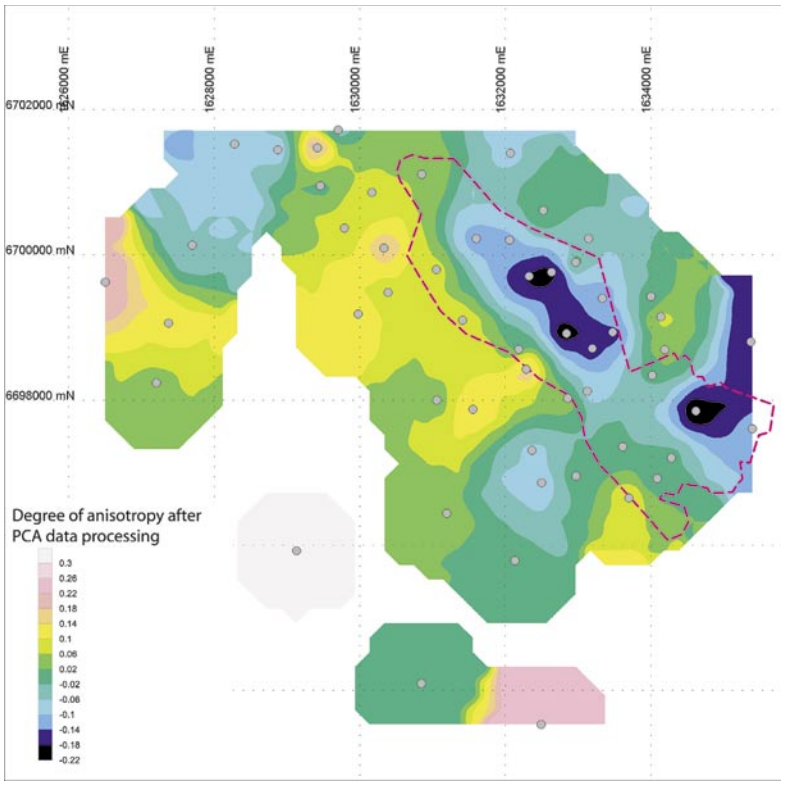


b)

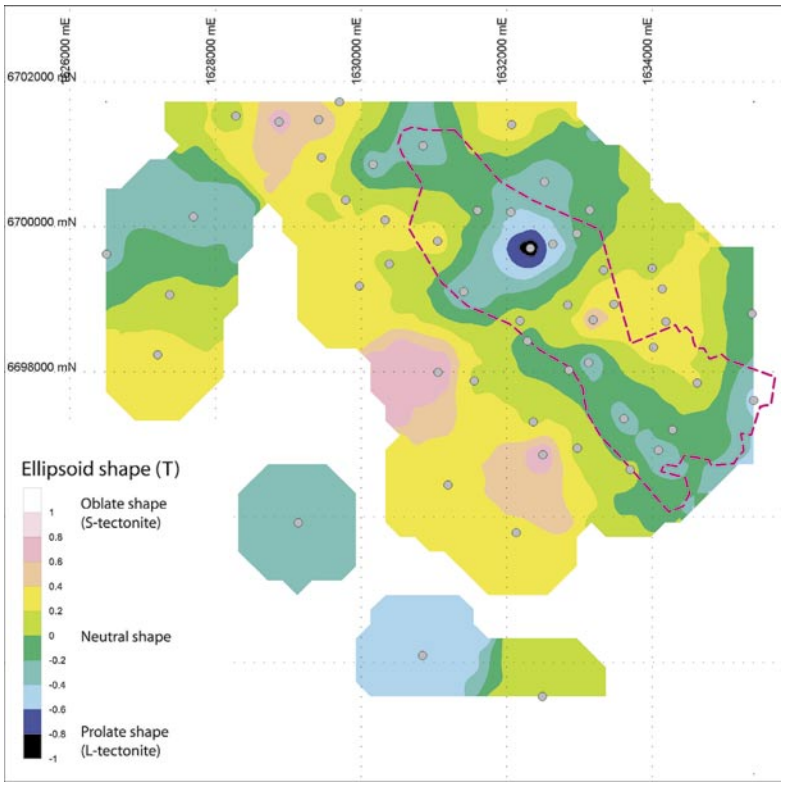


***Figure 5-3.*** *Contour plots of a) normalized degree of magnetic anisotropy and b) ellipsoid shape parameter (T) of the rocks in the Forsmark area. The sampling locations are indicated by a grey dot. See the text for explanation. The candidate area outlined with a dashed red line.*

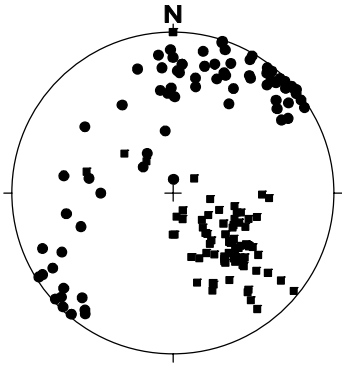


***Figure 5-4.*** *Equal area projection plot of the site mean Kmax (lineation) and Kmin (pole to foliation) AMS axes for all investigated sites in the Forsmark area. Squares = lineation and dots = poles to foliation.*

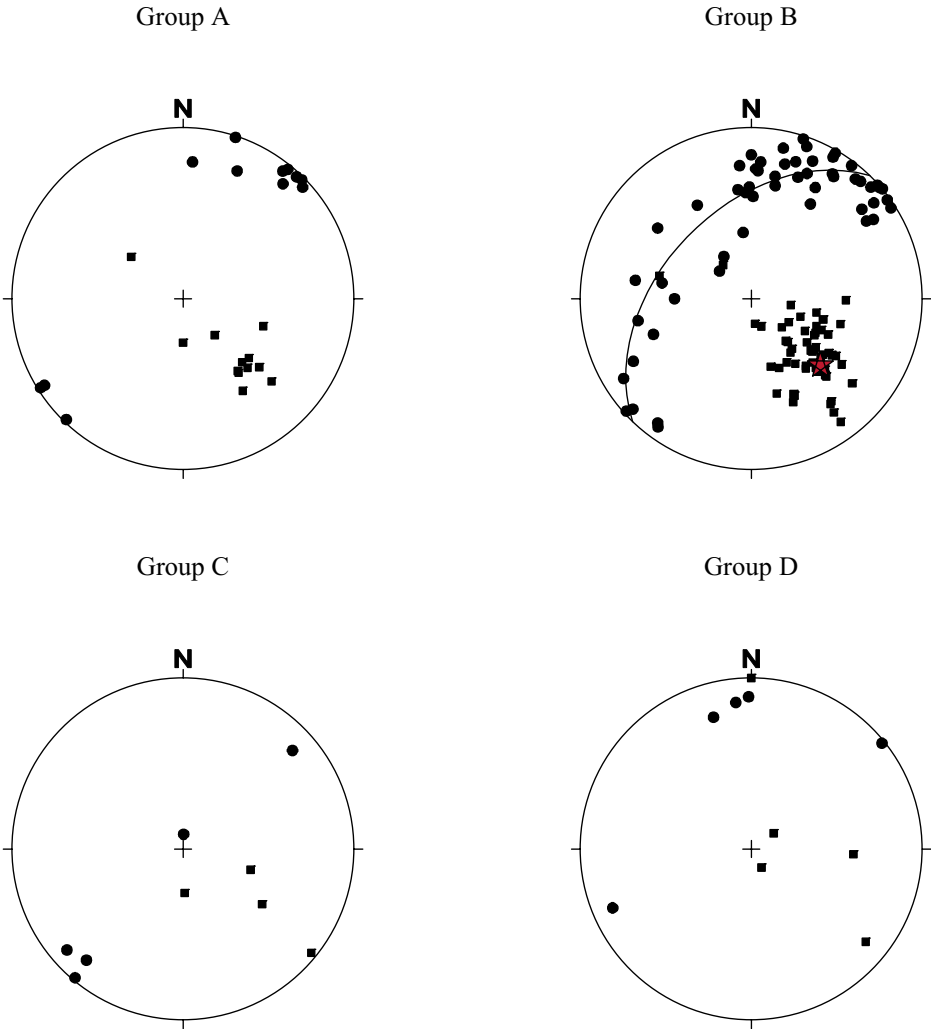


***Figure 5-5.*** *Equal area projection plots of AMS lineation and poles to foliation for each of the four geological groups A, B, C, and D respectively (site mean data). Squares = lineation and dots = poles to foliation. The red star in the group B plot indicates the estimated fold axis.*

The magnetic foliation poles of group D are a bit scattered, but three sites cluster close to the horizontal north direction, which indicates foliation planes with a mean east-west strike direction and a vertical dip. This direction is significantly different in orientation from the groups A, B and C, and it may indicate that these three rocks from group D have suffered from a deformation of different orientation. However, when analyzing the geographical distribution of the sites it seems as if these rocks belong to the folded geometry indicated for the B group (Figure 5-7).

The geographical distribution of the lineation and foliation plane orientations shows a consistent pattern (Figures 5-6 and 5-7). In the figures the group A and B rocks are represented by black symbols and the groups C and D rocks are represented by red symbols. Plus-symbols indicate sites where no mean direction could be established. A majority of the lineation have a southeast directed orientation and they dip c 45°–60°. The lineation dips of the rocks within the candidate area appear to be approximately 10° steeper than in the rocks outside. In the central part of the lens there is an obvious counter clockwise rotation of c 20°–30° of the lineation, which is most likely related to the fold geometry indicated by the orientation of the foliation planes (Figure 5-7).

Except for the rotation of the foliation planes within the central part of the lens, the foliations display very consistent mainly southeast oriented strike directions with sub vertical dips toward southwest, which agrees very well with the general structural rock fabric of the area as indicated by aeromagnetic data. The dips of the foliation planes in the vicinity of the folded geometry, and in the metatonalite rock nearby, are significantly shallower than for the rocks at the other sampling locations. Within the indicated fold the dips vary from c 20° to 50°.

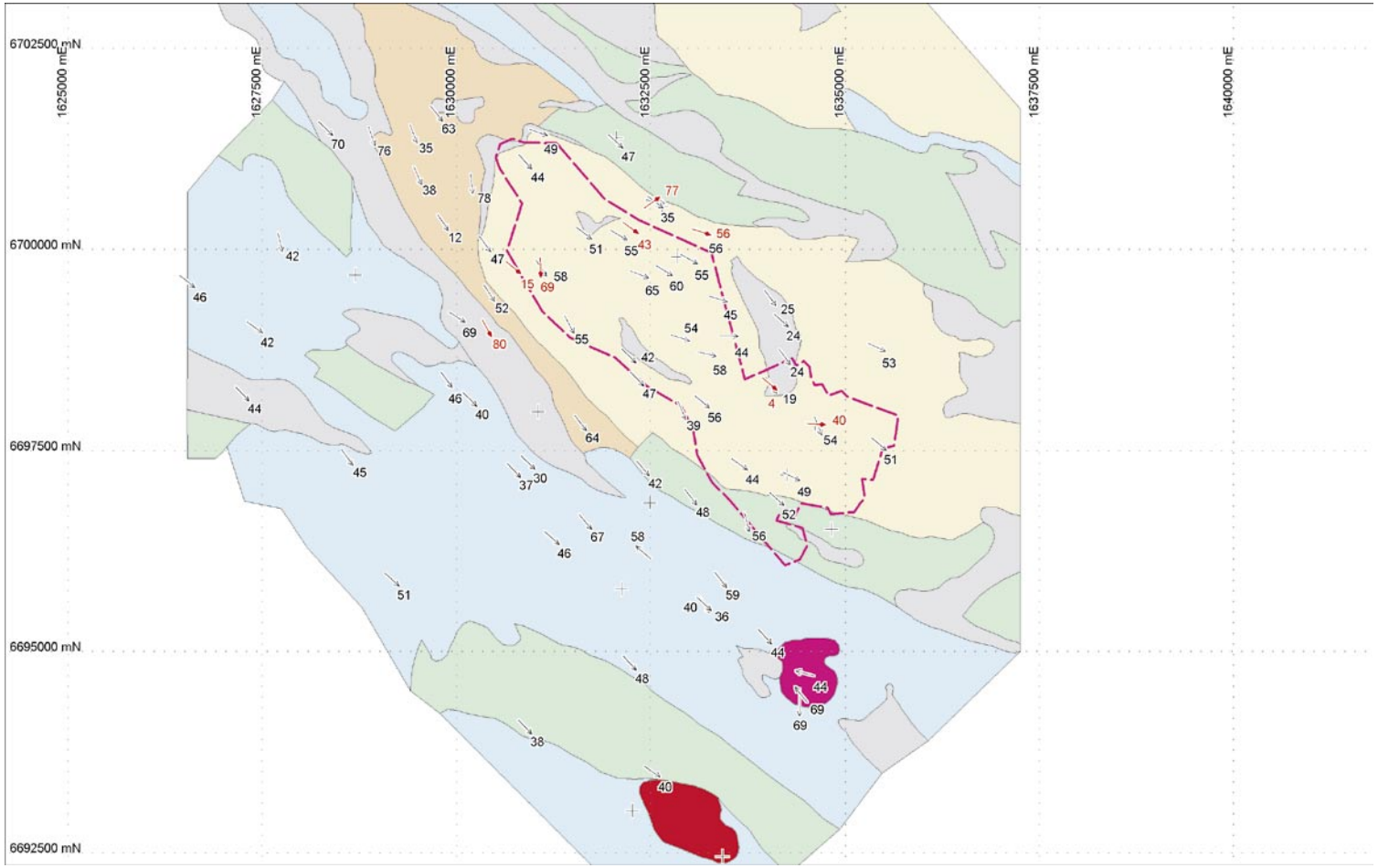


***Figure 5-6.*** *Site mean magnetic lineation (strike and dip) of the rocks in the Forsmark area. See the text for explanation. The background information shows areas with different structural magnetic anomaly patterns (from /20/).*

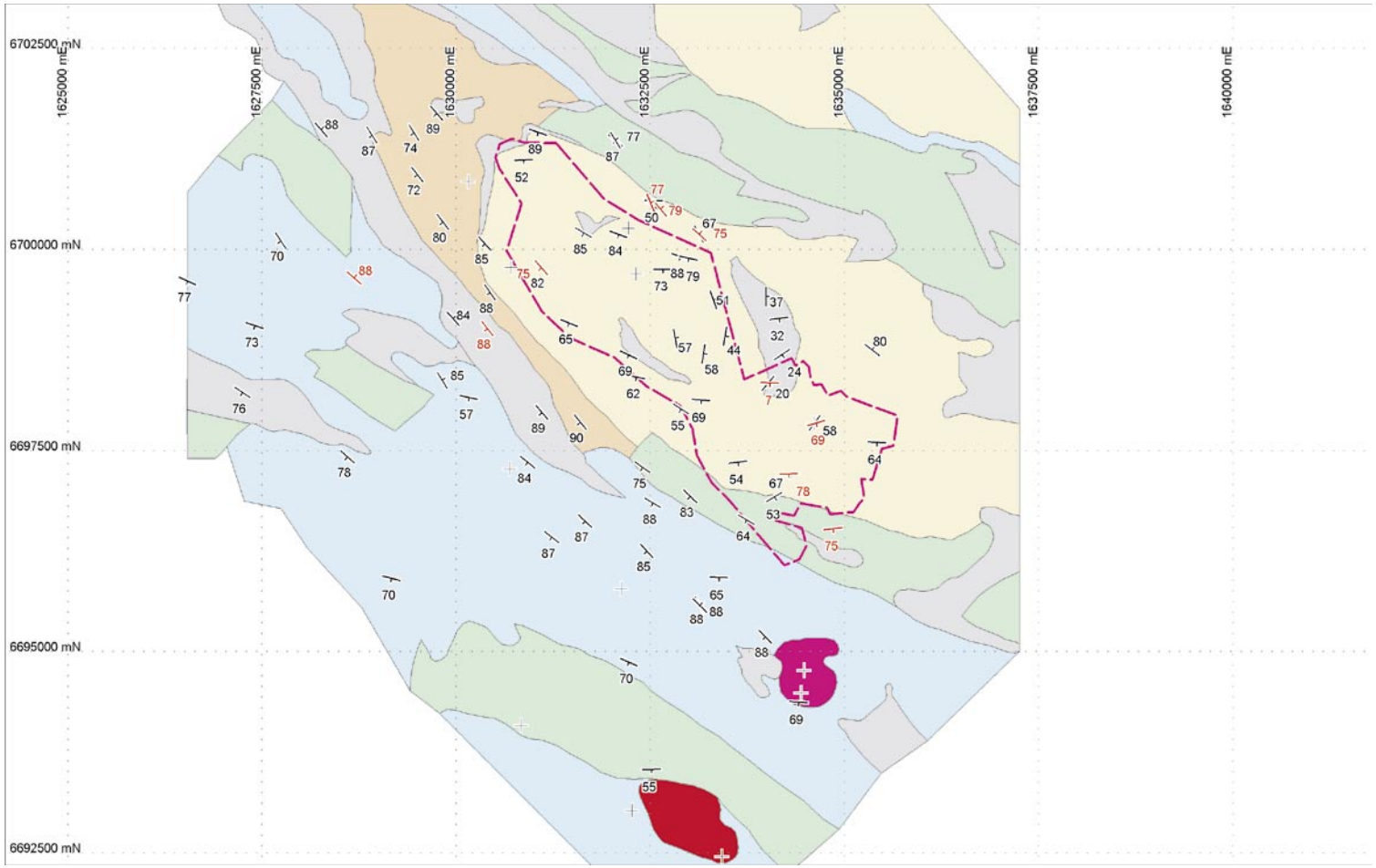


***Figure 5-7.*** *Site mean magnetic foliations (strike and dip) of the rocks in the Forsmark area. See the text for explanation. The background information shows areas with different structural magnetic anomaly patterns (from /20/).*

# 6 Electrical properties and porosity

### *Electric resistivity*

The contrast in resistivity (ρ) between silicate minerals and more conducting media like water or sulphides/graphite is extremely high. The bulk resistivity of a rock is therefore more or less independent of the type of silicate minerals that it contains. Electric conduction will be almost purely electrolytic if the rock is not mineralised. Archie's law /21/ is frequently used to calculate the conductivity (1/ρ) of sedimentary rocks.

$$\sigma = a \cdot \sigma_w \cdot \phi^m \cdot s^n$$

where

$\sigma$ = bulk conductivity (=1/ρ, S/m)
$\sigma_w$ = pore water conductivity (S/m)
$\phi$ = volume fraction of pore space
s = fraction of pore space that is water saturated
a, m, n = dimensionless numbers, $m \approx 1.5$ to 2.2, $a \geq 1$

Archie's law has proved to work well for rocks with a porosity of a few percent or more. Old crystalline rocks usually have a porosity of 0.1 to 2% and sometimes even less. With such low porosity the interaction between the electrolyte and the solid minerals becomes relevant. Some solids, especially clay minerals, have a capacity to adsorb ions and retain them in an exchangeable state /22/. This property makes clays electrically conductive but the same property can to some degree be found for most minerals. The resulting effect, surface conductivity, can be accounted for by the parameter *a* in Archie's law. Surface conductivity will be greatly reduced if the pore water is salt. The amount of surface conductivity is dependent upon the grain size and texture of the rock. Fine grained and/or mica-rich, foliated rocks are expected to have a large relative portion of thin membrane pore spaces that contribute to surface conductivity.

The electric resistivity is in reality not a simple scalar. Most rocks show electric anisotropy and the resistivity is thus a tensor. On a micro-scale the anisotropy is caused by a preferred direction of pore spaces and micro fractures.

### *Induced polarisation*

The IP effect can be caused by different mechanisms of which two are the most important. When the electric current passes through an interface between electronic and electrolytic conduction there is an accumulation of charges at the interface due to the kinetics of the electrochemical processes involved. This will occur at the surface of sulphide, oxide or graphite grains in a rock matrix with water filled pores. The second mechanism is related to electric conduction through thin membrane pore spaces. In this case an accumulation of charges will occur at the beginning and end of the membrane. The membrane polarisation is thus closely related to the surface conduction effect mentioned above for electric resistivity. Fine grained and/or mica rich, foliated rocks are therefore expected to show membrane polarisation. Also, the membrane polarisation is greatly reduced in salt water in the same way as surface conductivity.

Since the polarisation is caused by several complicated processes it is not possible to describe the frequency or time dependence of IP with any analytical function. It is however common to model the complex resistivity of a rock material with the empirical Cole-Cole model:

$$\rho(\omega) = \rho_0\left[1 - m\left(1 - \frac{1}{1 + (i\omega\tau)^c}\right)\right]$$

where

$\rho_0$ = resistivity at zero frequency (Ωm)
$\omega$ = angular frequency (rad/s)
m = chargeability
$\tau$ = time constant (s)
c = shape factor
i = $\sqrt{-1}$

The complex resistivity is thus described by $\rho_0$, m, $\tau$ and c. High chargeability is expected for rocks containing significant amounts of conductive minerals but also for rocks with clay alteration or considerable membrane pore space. The frequency at which the IP effect is strongest is related to the time constant. IP caused by conductive minerals or clay will in general give IP with long time constants whereas membrane polarisation will cause IP with short time constants that might be just of the order of milliseconds. The time constant is also texture dependent, where coarse grained rocks in general will cause IP with longer time constants than fine grained rocks. Field surveys are usually performed at 0.1 to 10 Hz (or equivalent times if performed in the time domain). They will therefore mainly detect IP sources with long time constants.

### *Measurement procedure*

The sample handling and laboratory procedure has been described in /1/ and is therefore only treated briefly here.

The electric properties were measured on 90 rock samples. Out of the generally four drill cores that were collected for each rock type at each site, one was selected for electric measurements. The measurements were then performed with an in-house two electrode equipment of Luleå University of Technology, which uses a saw-tooth wave-form at three base frequencies (0.1, 0.6 and 4 Hz). The complex resistivity was measured on the samples in accordance with SKB MD 230.001. The samples were first soaked in tap water and measured and then soaked in salt water (125 g NaCl per 5 kg of water) and measured once more. It should be noted that the 48 hours minimum that the samples were soaked in salt water might not be enough to completely saturate all pore spaces with salt water. However, the resulting accuracy of the measurements is expected to be good enough for the application of the data to bedrock mapping.

The porosity of the samples was calculated by measuring the weight of the samples water saturated, dry and suspended in water. This procedure also gives input for calculation of wet and dry density. Porosity and density measurements were performed on all drill cores of a rock type from each site assembled together.

## 6.1 Data processing

A correction for drift caused by drying of the sample during measurements is done automatically by the instrumentation software by comparing the harmonics of low frequency measurements with the base frequency result of the next higher frequency.

The resistivity data were compared with the measured porosity in order to make a fit in accordance to Archie's law. It should however be noted that the porosity measurements in this study were performed on all samples of a rock type from a site assembled together, whereas the electric properties were measured on one sample only. This will introduce some uncertainty in the fit to Archie's law.

Estimates of the contribution of surface conductivity to the overall bulk conductivity of the samples were estimated in two ways. Assuming a reasonable value of the parameter *m* in Archie's law and using the known values of $\sigma$, $\sigma_w$ and $\phi$, an apparent value of the parameter *a* was calculated. High values will correspond to a large contribution from surface conductivity and vice versa. Also, the ratio of the resistivity of a sample in fresh water to the resistivity in salt water was calculated. Low values correspond to a large contribution of surface conductivity in fresh water measurements.

The measurements, including harmonics, ranged from 0.1 to 30 Hz. This makes accurate fits of data to the Cole-Cole model possible for samples with a time constant of around 5 milliseconds to 1.7 seconds. Since it was obvious that samples with both shorter and longer time constants exist in the study, fits were only performed for a few samples to obtain typical values of the Cole-Cole parameters. The fit was performed with a GeoVista in-house procedure based on Monte-Carlo inversion. A simple estimate of the IP frequency characteristics was however obtained by calculating the ratio of the phase angle at 4 Hz to the phase angle at 0.1 Hz. Large ratios will then correspond to short time constants and vice versa.

## 6.2 Results

### *Porosity*

The distribution of measured porosities can be seen in Figure 6-1. The range of porosities is, with a few exceptions, rather narrow. Most samples have porosity between 0.3 and 0.6%. The low number of samples with higher porosity might be due to the fact that mainly fresh rock was sampled in this study. The two samples of group A with very high porosity are from the Fe-mineralizations (PFM000336 and PFM000446) south of the Forsmark candidate area and the two high porosity samples of group B are from altered ultra-mafic rocks (PFM001201 and PFM001205). Although the porosity ranges of the groups overlap, some differences can be noted. Group A has lower porosity than the other groups with a median value of 0.335%. Group B has slightly higher porosity with a median value of 0.417%. Group C and D have even higher median values of 0.459 and 0.498% respectively, but since the number of samples of these rock groups is small, the difference might not be significant.

Within group B there is a weak tendency that the mafic samples have slightly lower porosity than the felsic samples. The median porosity of the B2/B3 group combined is 0.365% whereas the corresponding values for B5/B6 combined and B8/B9 combined is 0.395% and 0.433% respectively. However, these differences are hardly statistically significant.

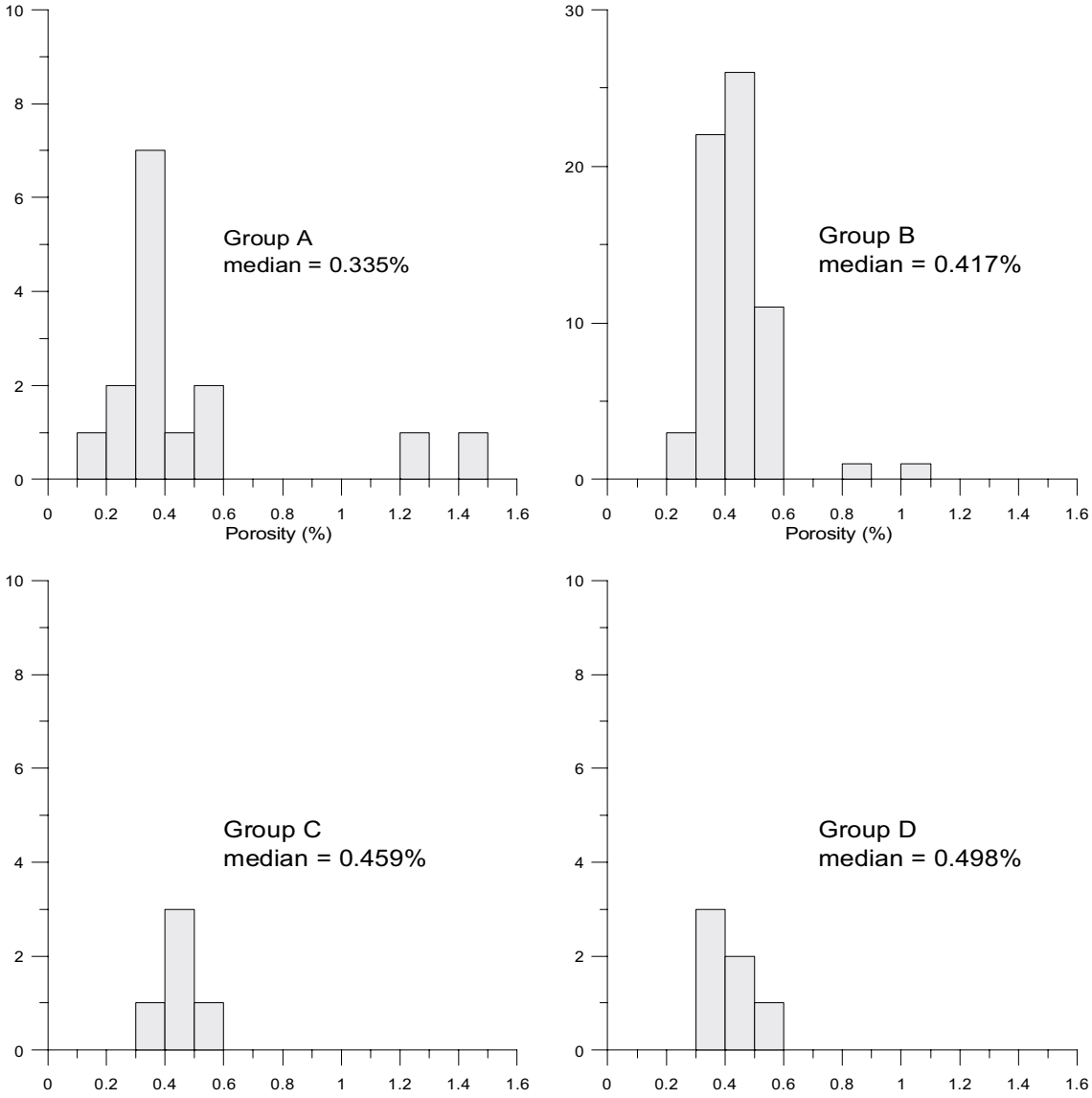


***Figure 6-1.*** *Histograms showing distribution of measured porosities for the rock groups A, B, C and D.*

Figure 6-2 shows the spatial distribution of porosity values. The candidate area is quite uniform with most samples having porosity between 0.4% and 0.52%. A few samples with higher values can be found along the north-eastern border of the candidate area and smaller values can be found north-east of Bolundsfjärden. Samples from the areas south and west of the candidate area have lower porosity. This is not entirely due to the presence of A type rocks; also the B type rocks have lower porosity here, which might be an effect of the ductile deformation of the rock.

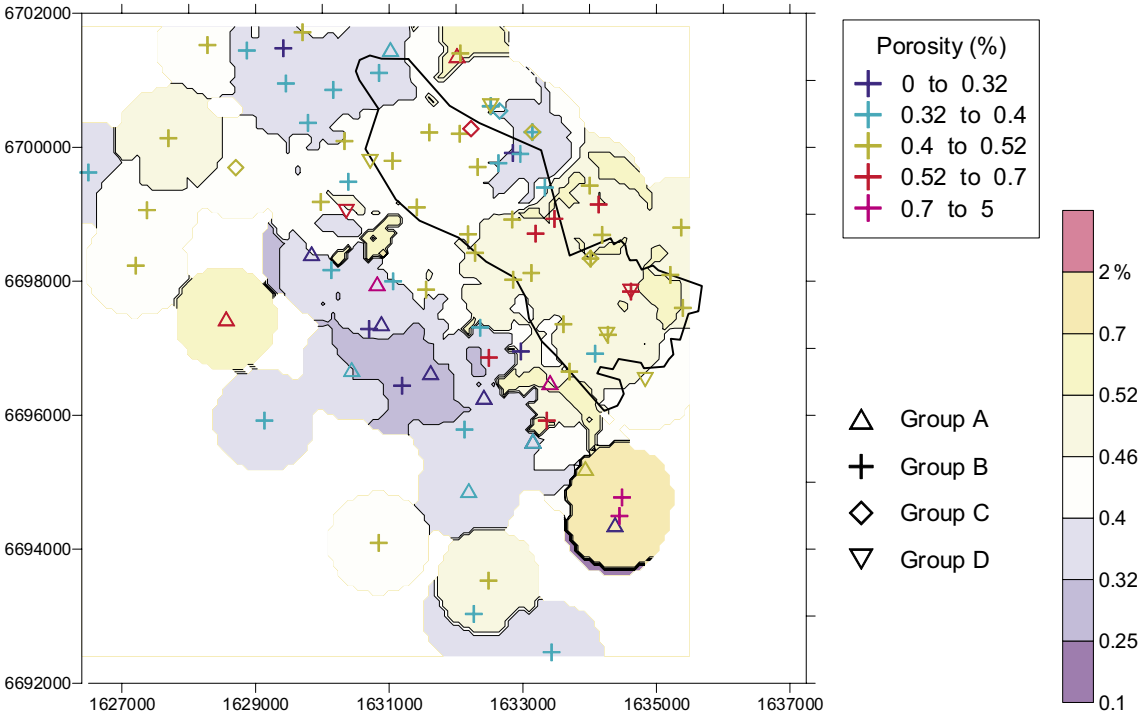


***Figure 6-2.*** *Map showing the measured porosity of the samples. The contour lines have been interpolated by taking the median value of values within a search radius of 800 m. The candidate area is shown with a black line. The different rock groups are indicated with different symbols with the measured porosity indicated by the symbol colour.*

### *Electrical properties*

The spatial distribution of electrical properties and the properties of different rock groups have been analyzed.

The IP effect as a function of resistivity in fresh water can be seen in Figure 6-3. With a few exceptions the samples have resistivities from 8000 to 35,000 Ωm and IP-values from 5 to 18 mrad. Both ranges can be considered to be quite normal for non-mineralized crystalline rocks.

Four samples have significantly different properties compared to the others. They show unusually low resistivity and very high IP values. Two of the samples are from Fe-mineralizations at PFM000336 and PFM000446 and the other two are from meta-ultramafic rocks at PFM001201 and PFM001205. High grades of magnetite explain the low resistivity and high IP of these samples. Only two more samples have IP values above 30 mrad, one belonging to the A group and one belonging to the B group of rocks. Both these are samples from mafic rocks with high density and high magnetic susceptibility (PFM001521 and PFM000850). Apart from the above mentioned samples there is a tendency that the samples with the highest resistivities have slightly higher IP than the ones with lower resistivity. This is probably due to membrane polarization in samples with low porosity.

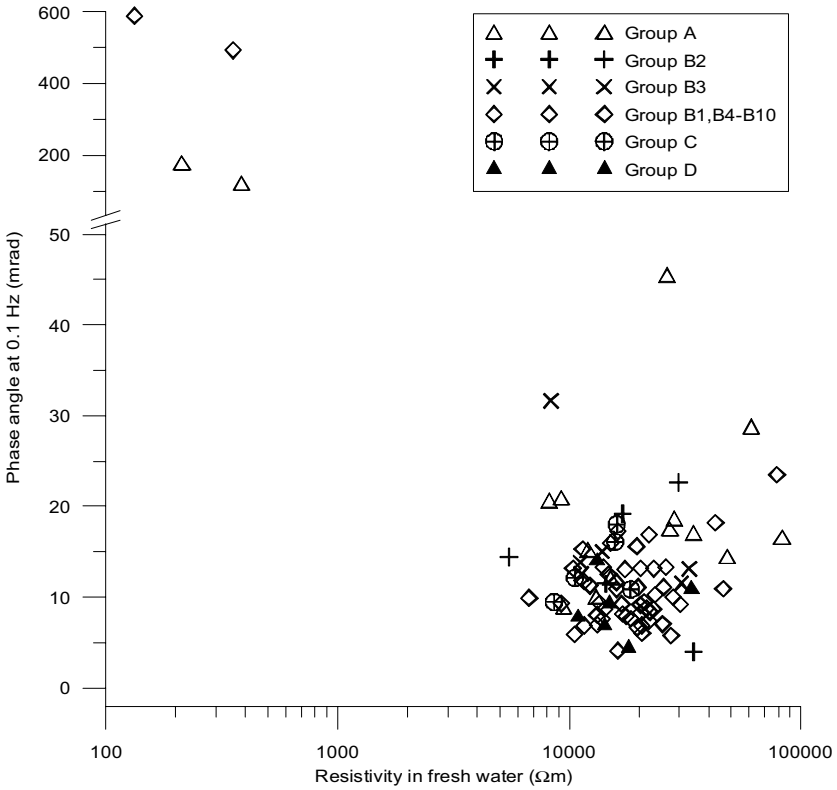


***Figure 6-3.*** *Resistivity and IP-effect (phase angle) for samples soaked in tap water.*

No significant difference in resistivity can be seen between the different rock groups. All four groups have a median resistivity of around 16,000 Ωm. However, within the B group there is a difference so far as the mafic subgroups have slightly lower resistivity than the felsic ones. B2/B3 combined has a median resistivity of 14,400 Ωm, whereas the corresponding values for B5/B6 combined and B8/B9 combined are 15,000 Ωm and 20,670 Ωm respectively. The higher value for B8/B9 is significant.

The ranges of IP values for the rock groups overlap but the group A has a higher median value (18.1 mrad) compared to the others (B: 10.9 mrad, C: 10.4 mrad, D: 8.4 mrad). Within the B group there is a difference between the mafic and the felsic rocks where the latter ones have lower IP although the ranges overlap. The median value for the B2/ B3 combined is 15.9 mrad whereas the corresponding value for the B5/B6 combined and the B8/B9 combined are 11.9 and 9.2 mrad respectively.

Maps showing the resistivity and IP values of the samples can be seen in Figure 6-4 and 6-5. Contour lines have been interpolated by taking the median measured value within a search radius of 800 m. The central and northern part of the candidate area show fairly uniform resistivity values. No resistivities above 25,000 Ωm or below 8000 Ωm have been measured on samples from this area. Resistivities above 25,000 Ωm can be found for some samples along the southern border of the candidate area. The ductile deformed belt south of the candidate area shows more variable resistivities where both high and low resistivity values can be found.

Almost all samples with IP below 8 mrad can be found in the candidate area or just south of this area. The northern part of the candidate area has slightly higher values and the same applies for the ductile deformation belt in the south, even though there are several exceptions from this pattern.

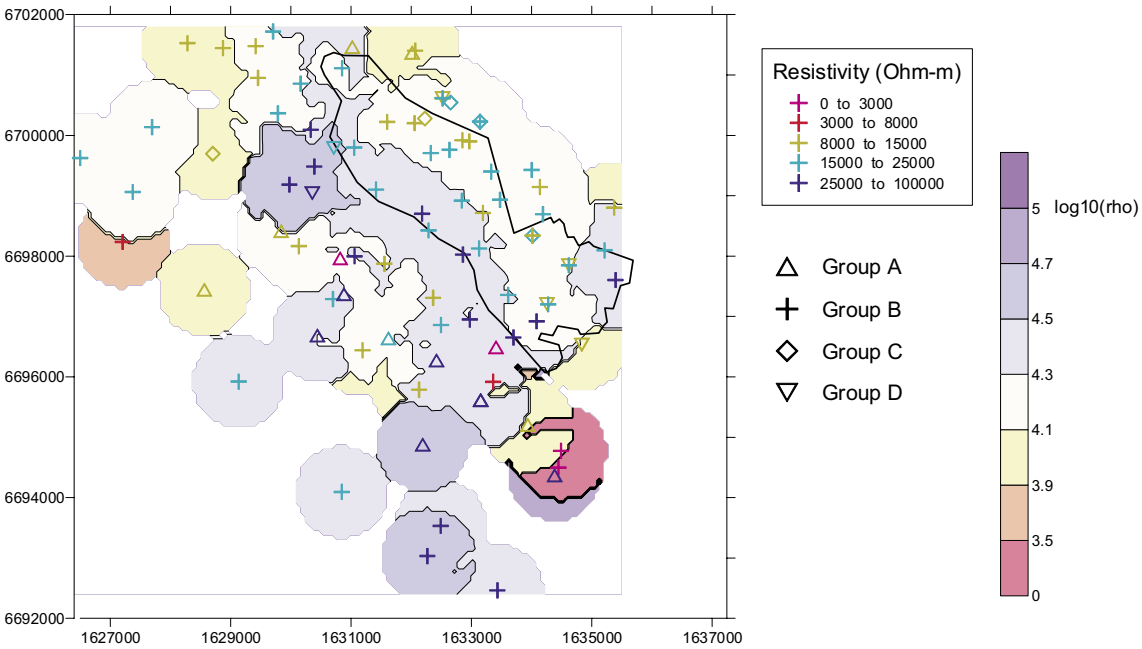


***Figure 6-4.*** *Map showing the resistivity of samples measured in fresh water. The contour lines have been interpolated by taking the median value of values within a search radius of 800 m. The candidate area is shown with a solid black line.*

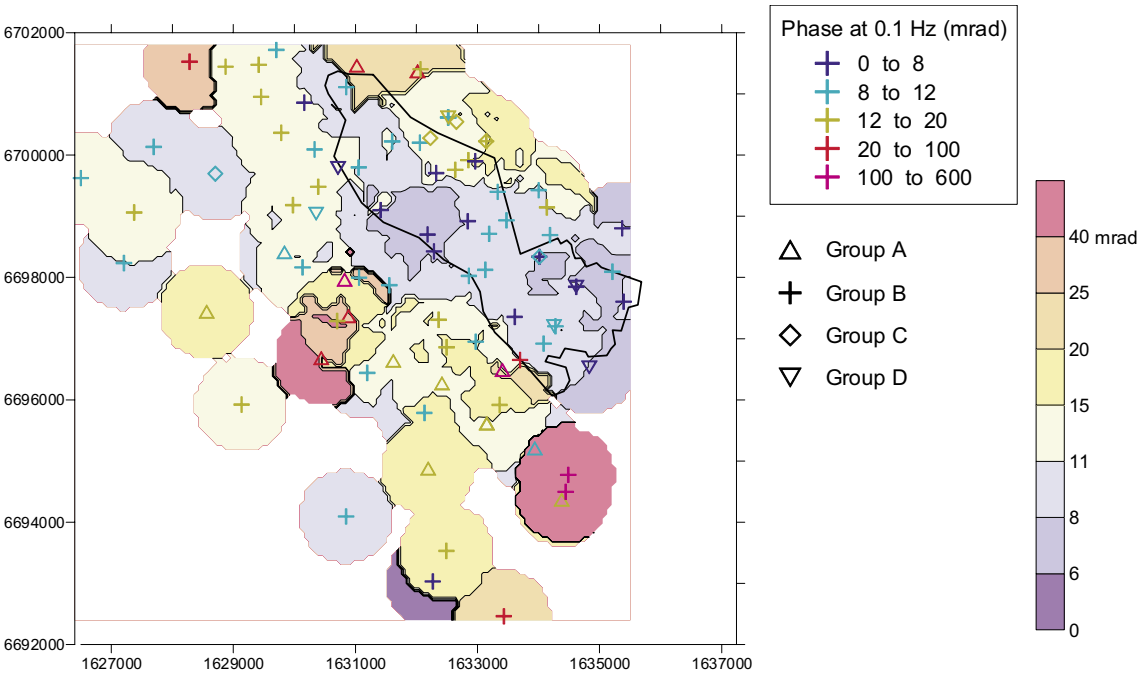


***Figure 6-5.*** *Map showing the IP effect (phase angle) of samples measured in fresh water. The contour lines have been interpolated by taking the median value of values within a search radius of 800 m. The candidate area is shown with a solid black line.*

The measured resistivity as a function of porosity is plotted in Figure 6-6. A negative correlation might be expected since high porosity should correspond to low resistivity and vice versa. This relationship can be modelled with Archie's law according to the discussion in Section 6.1. However, it is hardly possible to see such a correlation in Figure 6-6. There are some possible reasons for this. Firstly, the porosity has been measured on all drill cores from a site assembled to one sample in order to get a high accuracy, whereas the resistivity has been measured on one drill core only. This procedure will introduce some scatter in the plot in Figure 6-6. However, it can hardly entirely explain the lack of correlation. A second reason is that samples have different surface conductivity properties, even if they belong to the same rock group. Samples where the porosity to a relatively large degree consists of thin membranes will have a lower resistivity than a sample with the same porosity but wider pore spaces. A third reason for the poor correlation in Figure 6-6 is that the samples might be anisotropic. It has only been possible to measure the resistivity in one direction for each sample. The porosity is a simple scalar and this means that the position of a sample in the plot in Figure 6-6 to some degree might be dependent on the drill core orientation relative rock foliation and rock lineation. Finally it should be noted that the range of porosities seen in the measured samples is quite narrow. It is likely that a better correlation to the resistivity could be seen if samples with higher and lower porosities had been available.

The resistivity measured in salt water as a function of porosity can be seen in Figure 6-7. The salt concentration is 125 g NaCl per 5 kg of water. This is not a saturated solution and even if the effect of surface conductivity is reduced by the salt, it might not be completely removed. The correlation between porosity and resistivity is rather poor also for this case and no reliable fit to Archie's law can be made.

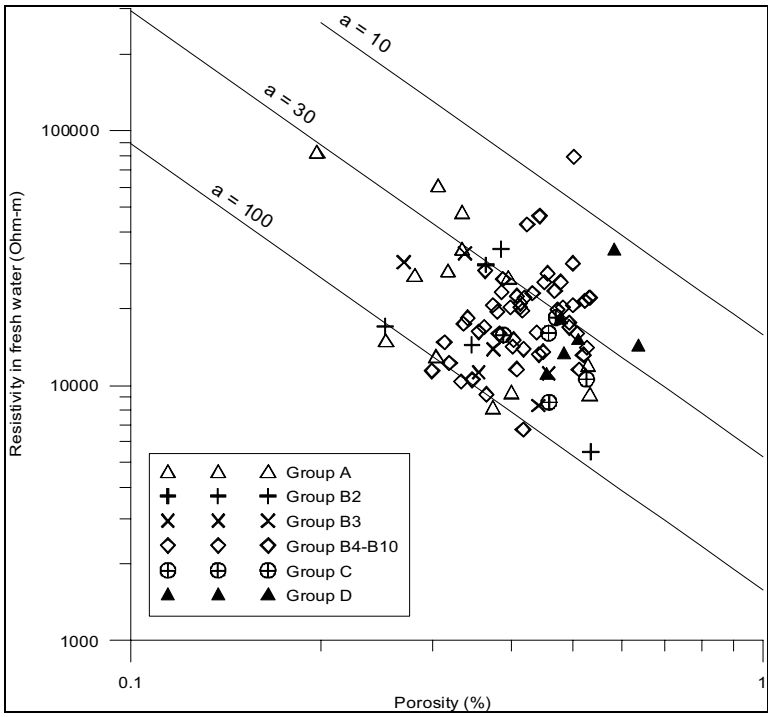


***Figure 6-6.*** *Measured resistivity as a function of porosity for samples soaked in tap water. The three straight lines represent the resistivity according to Archie's law calculated for m = 1.75 and* $\sigma_w$ *= 0.02 S/m. The samples then show different apparent a-values which might correspond to different amounts of surface conductivity.*

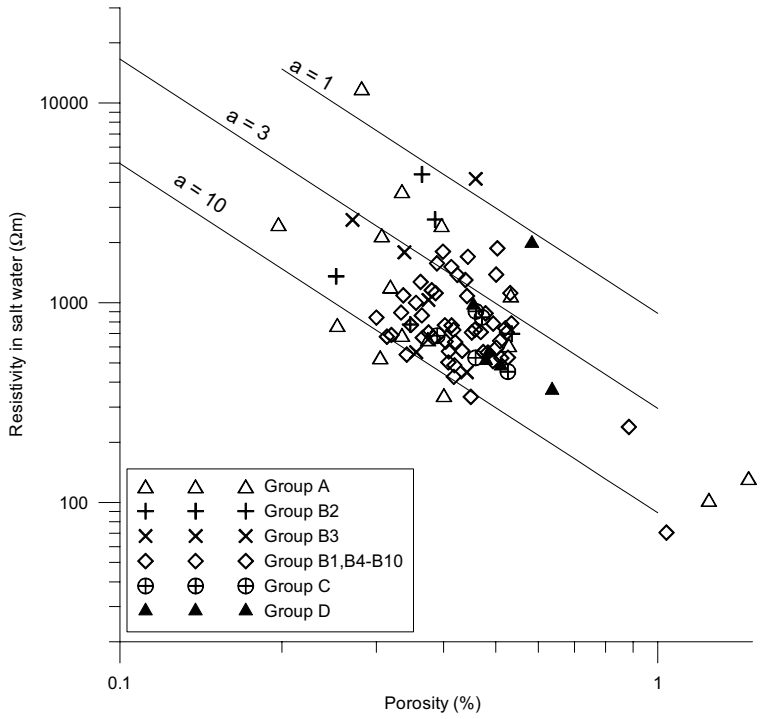


***Figure 6-7****. Measured resistivity as a function of porosity for samples soaked in salt water. The three straight lines represent the resistivity according to Archie's law calculated for m = 1.75 and* $\sigma_w$ *= 3.57 S/m. Apparent a-values equal to one would then correspond to no surface conductivity.*

Assuming a reasonable value of 1.75 for *m* in Archie's law and calculating the value of *1/a* for the fresh water data, we end up with values ranging from around 0.01 to 0.1. Low values would then possibly correspond to a large contribution of surface conductivity to the bulk conductivity of the samples. These apparent *1/a*-values for rocks of the B-group are shown on a map in Figure 6-8. Most samples from the belt of ductile deformation have low values of *1/a* as might be expected. However, there are also a number of samples in the northern part of the candidate area with low values. This might indicate some kind of textural anomaly although the number of samples is rather small. This area partly coincides with the area of low porosity in Figure 6-2.

Another way of investigating the influence of surface conductivity is to compare the resistivity measured in fresh and salt water respectively, Figure 6-9. The contrast in resistivity between the fresh and salt water is around 180. However, the average ratio in sample resistivity measured in fresh and salt water respectively is only 22. Since the surface conductivity effect to a large extent is removed in salt water, the ratio of resistivity values can be taken as a measure of the relative contribution of surface conductivity in the fresh water measurements. In Figure 6-9 we can see that the four low resistivity samples of the Fe-mineralizations and ultramafic rocks plot rather close to the solid line corresponding to

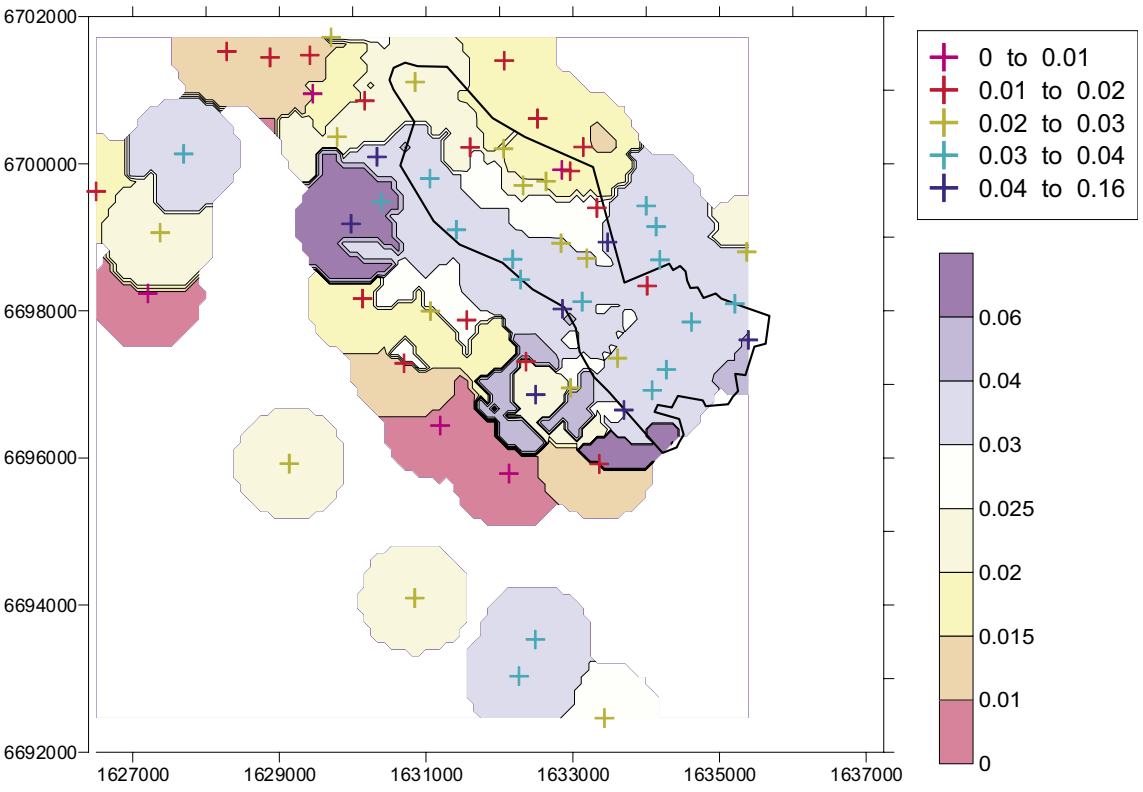


***Figure 6-8.*** *Map showing apparent 1/a-values in fits to Archie's law, assuming m = 1.75. Only rocks of the B2 to B10 groups are shown. Low values might correspond to large contributions of surface conductivity. The contour lines have been interpolated by taking the median value of values within a search radius of 800 m. The candidate area is shown with a black line.*

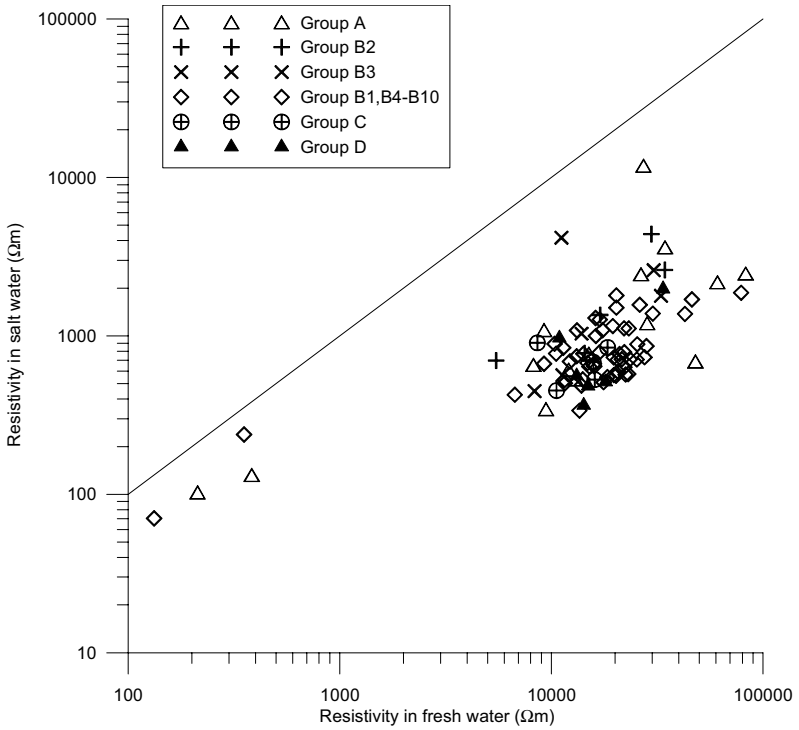


***Figure 6-9.*** *Resistivity measured with the samples soaked in fresh and salt water. The straight line corresponds to equal resistivity for the two cases. The contrast in resistivity between the fresh and salt water was around 180 whereas the contrast in resistivity for most of the samples was just between 15 and 25.*

equal resistivity for fresh and salt water measurements. This is due to the fact that electronic conduction is dominating over electrolyte conduction in these samples. One high resistivity sample of group A (PFM001885) and one from group B (PFM001235) also plots close to the line. It is possible that these samples have been poorly saturated with salt water but it is also possible that electronic conduction in oxide or sulphide minerals is significant. The PFM001885 sample has a fairly high magnetic susceptibility.

A map showing the ratio of resistivities measured in fresh and salt water respectively can be seen in Figure 6-10. Low values are found in the ductile deformation belt south of the Forsmark lens as might be expected. However, low values are also found in the northern part of the candidate area for more or less the same samples that had low *1/a*-values in fits to Archie's law. The low resistivity ratios might also indicate some kind of texture anomaly in this area.

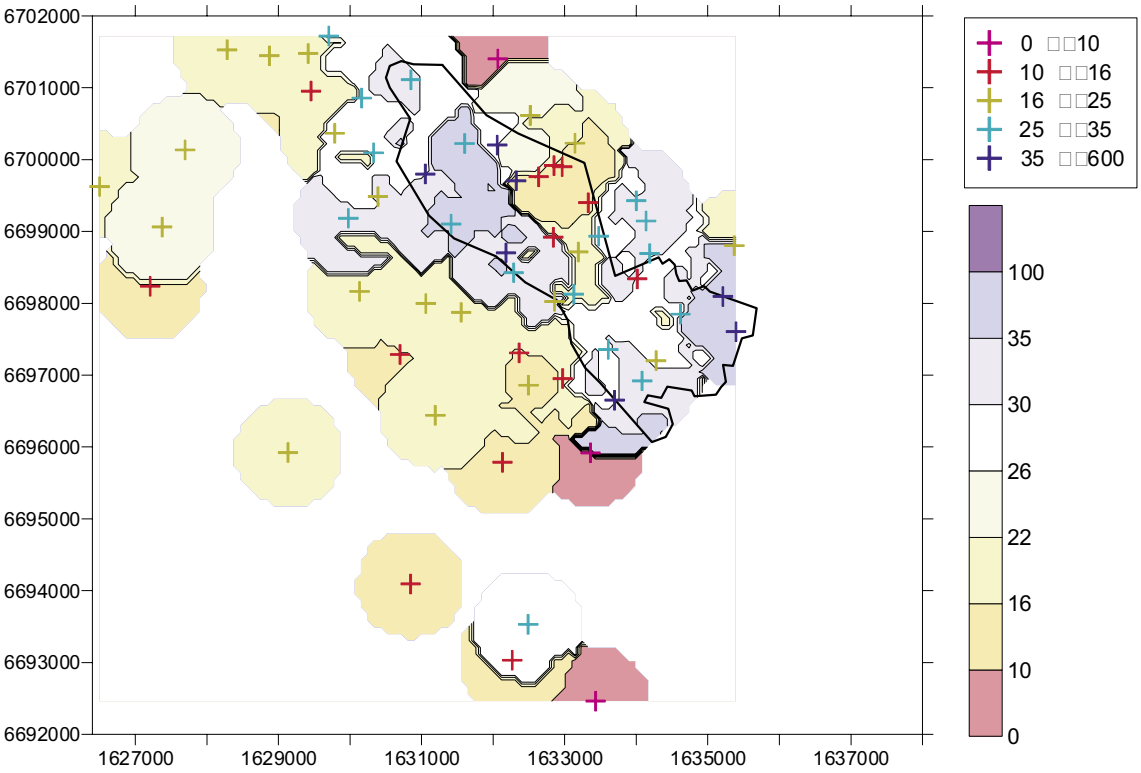


***Figure 6-10.*** *Map showing ratio of resistivity measured in fresh and salt water respectively. Only rocks of the B2 to B10 groups are shown. Low values might correspond to large contributions of surface conductivity. The contour lines have been interpolated by taking the median value of values within a search radius of 800 m. The candidate area is shown with a black line.*

The relation between IP measured in fresh and salt water can be seen in Figure 6-11. Most samples have very low IP in salt water indicating that the IP in fresh water is due to membrane polarisation. The samples with significant IP effect in salt water are all from the belts with ductile deformation south and north of the candidate area. With a few exceptions these samples have high magnetic susceptibility and the likely explanation for their IP effect is magnetite. However, four low-magnetic samples show some IP in salt water for which the cause is unknown, namely PFM002056, PFM002087, PFM001235 and PFM001156.

The IP-effect has been plotted for two different frequencies in Figure 6-12. Stronger IP in the higher frequency compared to the lower frequency indicate IP with a short time constant. Most samples plot close to the straight line indicating equal IP for the two cases. All samples with significantly higher IP in the higher frequency are from the ductile deformation belt south of the candidate area. Most of them also have high magnetic susceptibility and IP in salt water, indicating presence of magnetite. Exceptions are PFM000240, PFM000253 and PFM000259. A few samples have lower IP for the high frequency. Some of these samples have noisy IP-data for the high frequency. However, the ultra-mafic rocks with very high IP at PFM001201 and PFM001205 have higher IP for the low frequency and thus long time constants and so have two samples of the A group from PFM000725 and PFM001156. The latter two samples have low magnetic susceptibility and the cause of the anomalous IP properties has not yet been examined.

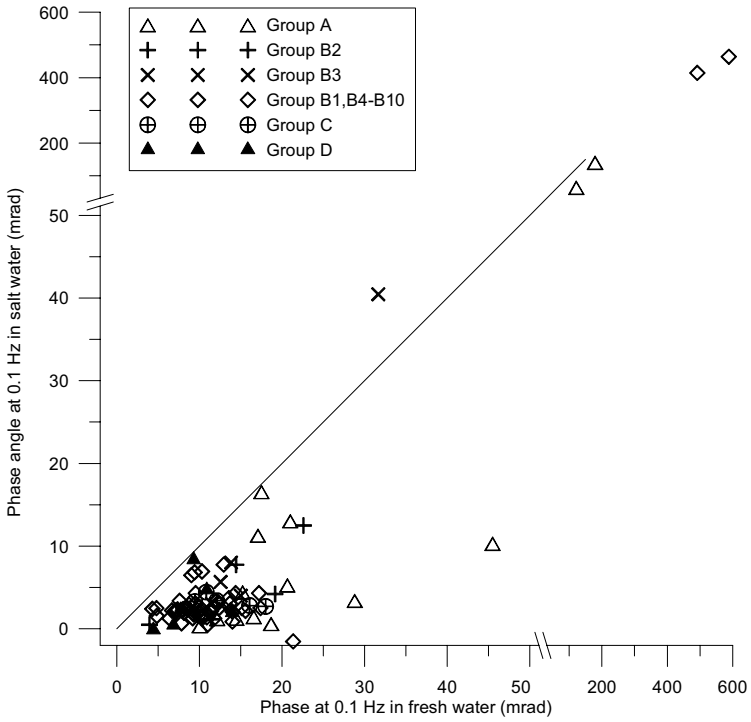


***Figure 6-11.*** *IP-effect measured with the samples soaked in fresh and salt water. The straight line indicates equal IP for the two cases. Most samples show low IP in salt water indicating that membrane polarisation is the dominating IP effect in fresh water. With a few exceptions, the samples with significant IP in salt water have high magnetic susceptibility indicating that magnetite is the cause to this IP-effect*

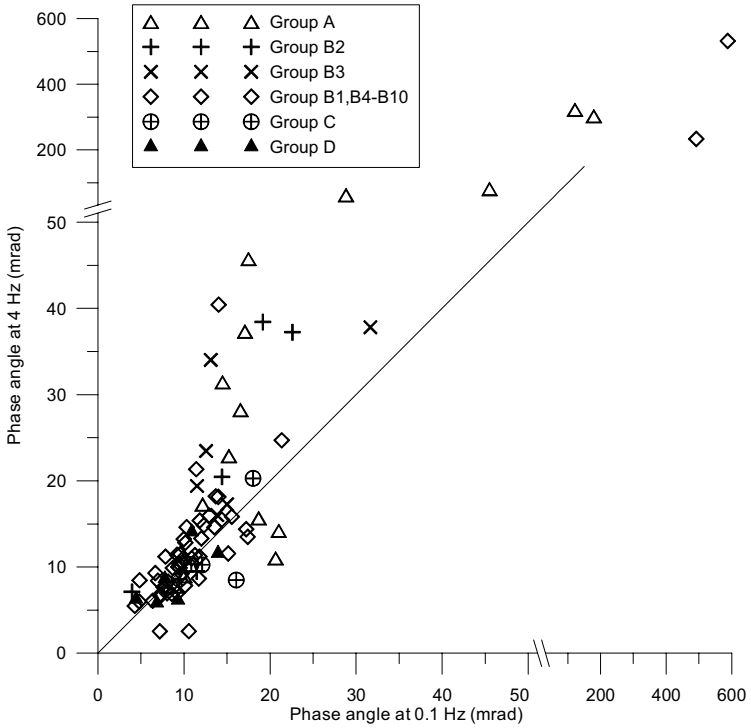


***Figure 6-12.*** *IP-effect as phase angle for two frequencies. Samples that plot above the straight line are expected to have short time constants.*

Cole-Cole parameters have been calculated for a few samples to give an idea of what values to expect from different types of rocks. The results are shown in Table 6-1. It should be remembered that fits to the Cole-Cole model not are accurate for very short and very long time constants due to the limited frequency range of the measurements. The sample PFM000695 is of the B9 group from the candidate area and the sample PFM000739 is of the B10 group from just north of the candidate area. These can be seen as samples with fairly typical complex resistivities of granitic rocks in the candidate area. They have low chargeability, medium long time constants and high resistivity. Two samples (PFM000240 and PFM001521) are of the A group from the ductile deformation belt south of the candidate area selected for their fairly strong IP-effect. Both samples have high resistivity, high chargeability and short time constants. One sample (PFM000725) is from the deformation belt north of the candidate area and was selected for having anomalous IP properties. This sample has a very long time constant, low chargeability and moderate resistivity. The last sample (PFM001201) is of the B1 group and it has a very long time constant, high chargeability and low resistivity.

**Table 6-1. Estimated Cole-Cole parameters for some selected samples with different electrical properties. Note that the estimates are very rough for samples with time constants shorter than 5 ms or longer than 1.7 s.**

| Sample | $\rho_0$ (Ωm) | $\tau$ (s) | m | c | Rock group |
|---|---|---|---|---|---|
| PFM000240 | 64,640 | 0.00097 | 0.617 | 0.304 | A1 |
| PFM001521 | 31,100 | 0.013 | 0.623 | 0.229 | A1 |
| PFM000725 | 9,495 | 62.76 | 0.181 | 0.257 | A1 |
| PFM001201 | 1,170 | 44.67 | 0.913 | 0.389 | B1 |
| PFM000739 | 17,290 | 0.371 | 0.146 | 0.255 | B10 |
| PFM000695 | 25,980 | 0.015 | 0.085 | 0.22 | B9 |

# 7 Gamma ray spectrometry on outcrops

## 7.1 Data processing

The individual gamma-ray measurements previously performed /1/ in connection with the bedrock mapping project /2/, have been treated statistically. Site averages have been calculated and plotted as histograms and as hue-saturation plots. Site locations are shown in Figure 7-1.

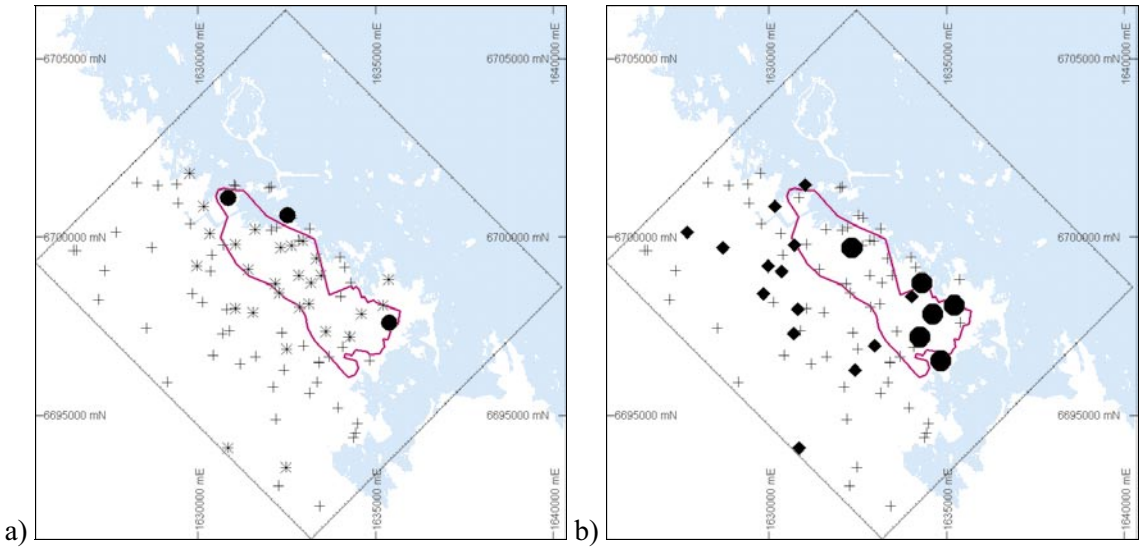


***Figure 7-1.*** *In situ, gamma ray spectrometry, site locations.*
a) ∗ *metagranodiorite-metagranite,* • *metagranite - low potassium, + other site location*
b) ♦ *pegmatitic granite and pegmatite. U-dominant and high natural exposure rate*
• *pegmatitic granite and pegmatite. Th, K-dominant and normal natural exposure rate*
*+ other site location*

## 7.2 Results

The distribution of potassium (K), uranium (U) and thorium (Th) in the bedrock is discussed in conjunction with the histograms and hue-saturation plots in Figure 7-2 and 7-3.

The felsic to intermediate metavolcanic and metavolcanoclastic rocks (group A1) show scattered potassium content, from 0.4–3.7%. The group A1 shows an average content of 1.9% K, 4 ppm U and 10 ppm Th, based on measurements at 12 sites. One differing site in group A is a veined gneiss (group A3), which shows a high potassium content, 5.1%, depending on its high K-feldspar content.

The potassium, uranium and thorium contents for ultramafic to mafic rocks are commonly low, which is also the case in Forsmark. Ultramafic rocks (group B1), measured at two sites show 0% K, 0 ppm U and 0 ppm Th. The metagabbro to metadiorite (group B2/B3) show an average content of 0.8% K, 1 ppm U and 2 ppm Th, based on measurements at 11 sites. The metatonalite-metagranodiorite, group B5/B6, shows an average content of 1.9% K, 4 ppm U and 9 ppm Th, based on measurements at 14 sites. Of interest is that this result is very similar to the contents for the felsic to intermediate metavolcanic and metavolcanoclastic rocks in group A1.

Metagranite-metagranodiorite, group B8/B9, shows a normal distribution common for granites, with an average of 3.0% K, 5 ppm U and 15 ppm Th, based on measurements at 31 sites, Figure 7-2 and Figure 7-3a. However, a few sites located at the margin of the Forsmark candidate area show depletion in the potassium content, see Figure 7-1.

Measurements on the aplitic metagranite show a very scattered result with a potassium content ranging from 0.8% to 4.1% and a thorium content ranging from 9 ppm to 28 ppm. The uranium content is normal for granite rocks, 5.5 ppm in average on 6 sites. In general the aplitic metagranite is more Th-dominant than typical granite.

The felsic, meta-intrusive granitoid, group C, indicates two populations. One population is based on 4 sites, and show low potassium, 1–2%, and moderate uranium and thorium contents, 2–8 and 10–12 ppm respectively. Two sites with a metagranodiorite-metagranite composition, show potassium and uranium contents normal for granite rocks. However, the thorium contents are anomalous, 22–27 ppm.

The pegmatitic granite and pegmatite show a bimodal distribution. One part is uranium-dominant and shows a high natural exposure rate. The other part is thorium and potassium dominant and shows only slightly higher natural exposure rate compared to the metagranite. The surface distribution of this latter group shows that the sites predominantly occur within the Forsmark candidate area and close to Storskäret, in the southeastern part of the candidate area. The first group mainly occurs, southwest and west of the candidate area, see Figure 7-1.

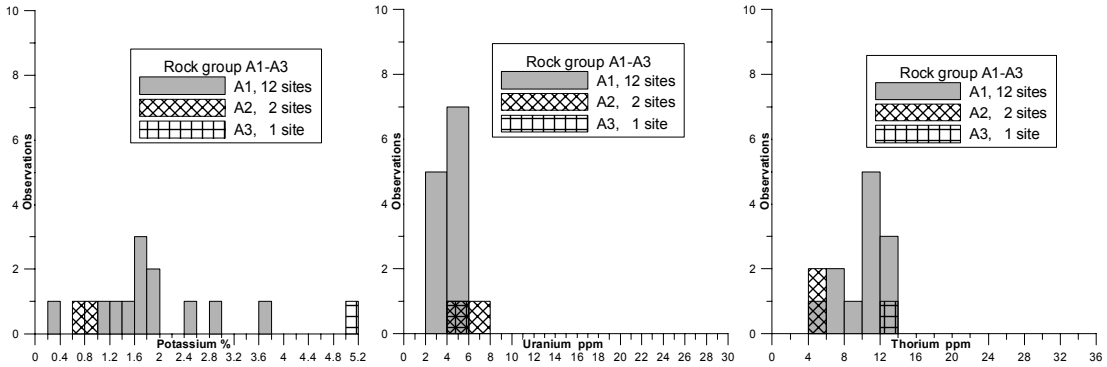


*A). Felsic to intermediate metavolcanic and metavolcanoclastic rocks (Group A1), Fe-rich mineralization (A2) and Veined gneiss (A3). Average on 12, 2 and 1 sites respectively.*

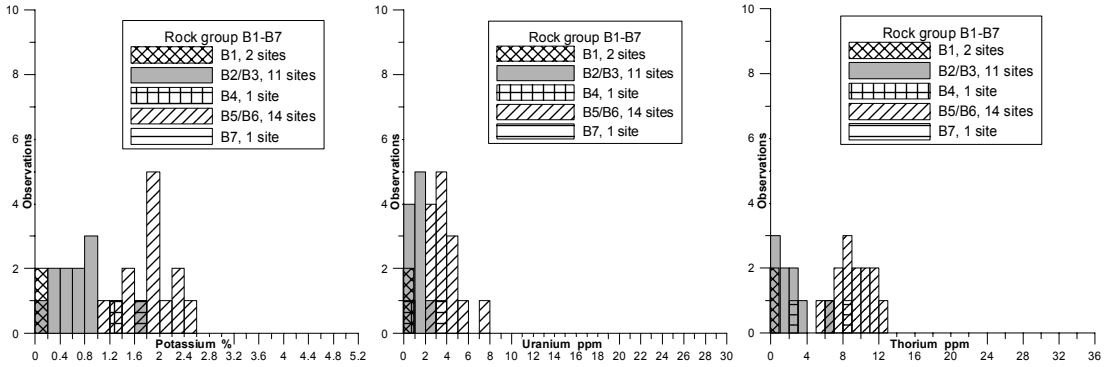


*B1-B7). Meta-ultramafic (Group B1), metagabbro-metadiorite (B2/B3), amphibolite (B4), metatonalite-metagranodiorite (B5/B6) and metagranodiorite (B7). Average on 2, 11, 1, 14 and 1 sites respectively.*

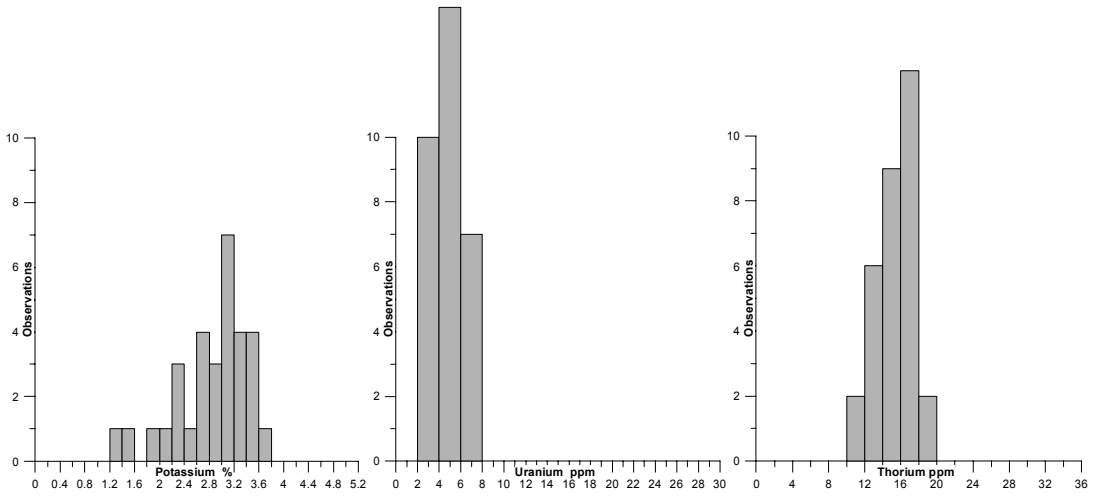


*B8/B9). Metagranodiorite – metagranite (Group B8 and B9). Averages on 31 sites.*

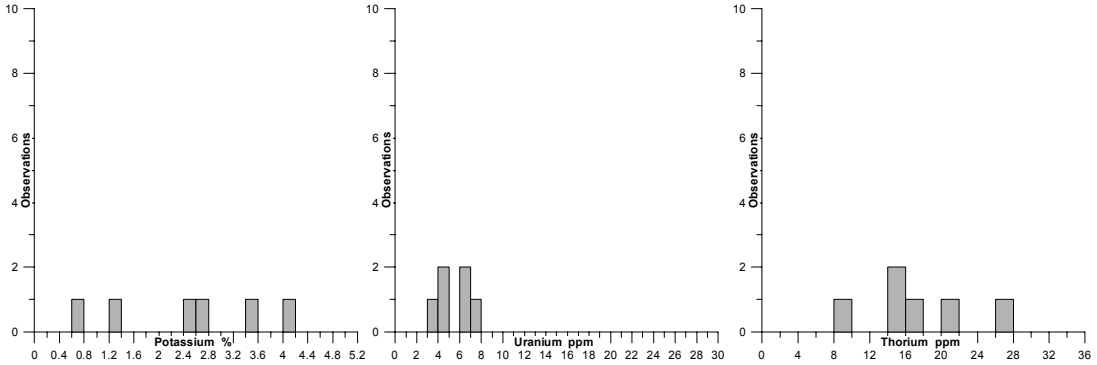


*B10). Metagranite, aplitic (Group B10). Averages on 6 sites.*

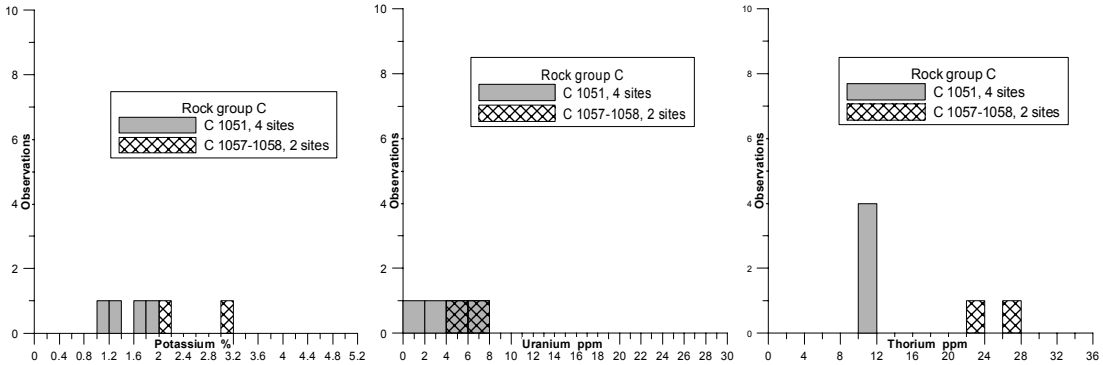


*C). Felsic granitoid, meta-intrusive rock (Group C), unspecified and metagranodiorite-metagranite. Average on 4 and 2 sites respectively.*

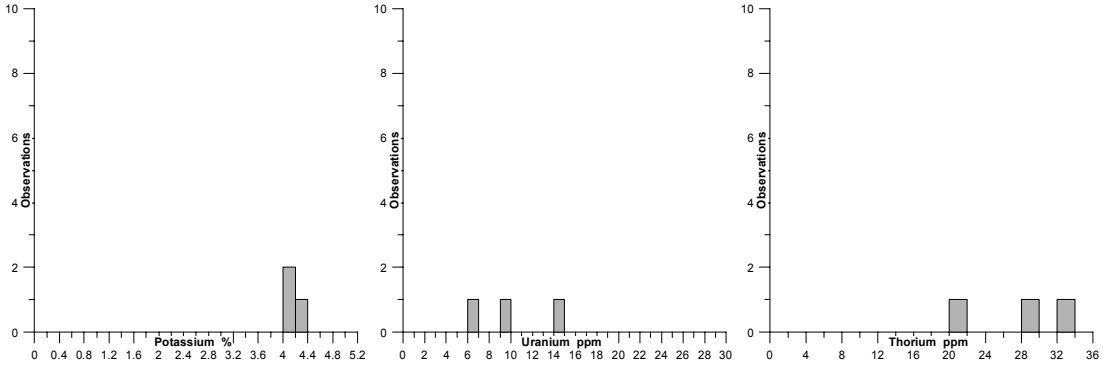


*D1). Granite (Group D1). Averages on 3 sites.*

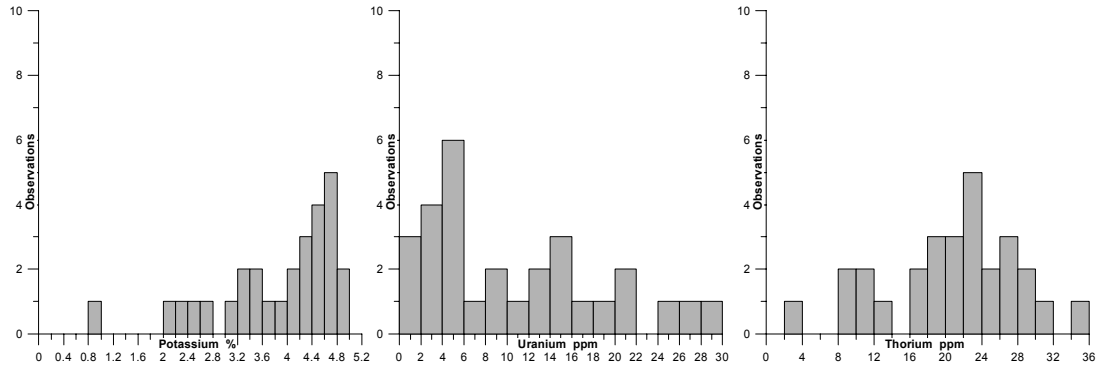


*D2). Pegmatitic granite (Group D2). 29 individual measurements at 8 sites.*

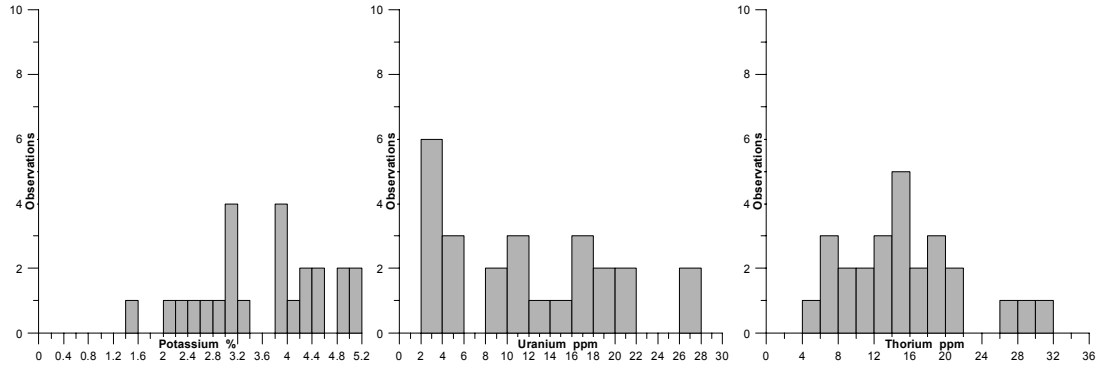


*D3). Pegmatite (Group D3). 30 individual measurements at 14 sites.*

***Figure 7-2.*** *Histogram showing the potassium (%), uranium (ppm) and thorium (ppm) content for the in situ, gamma ray spectrometry measurements. The results are presented for each of the different rock groups.*

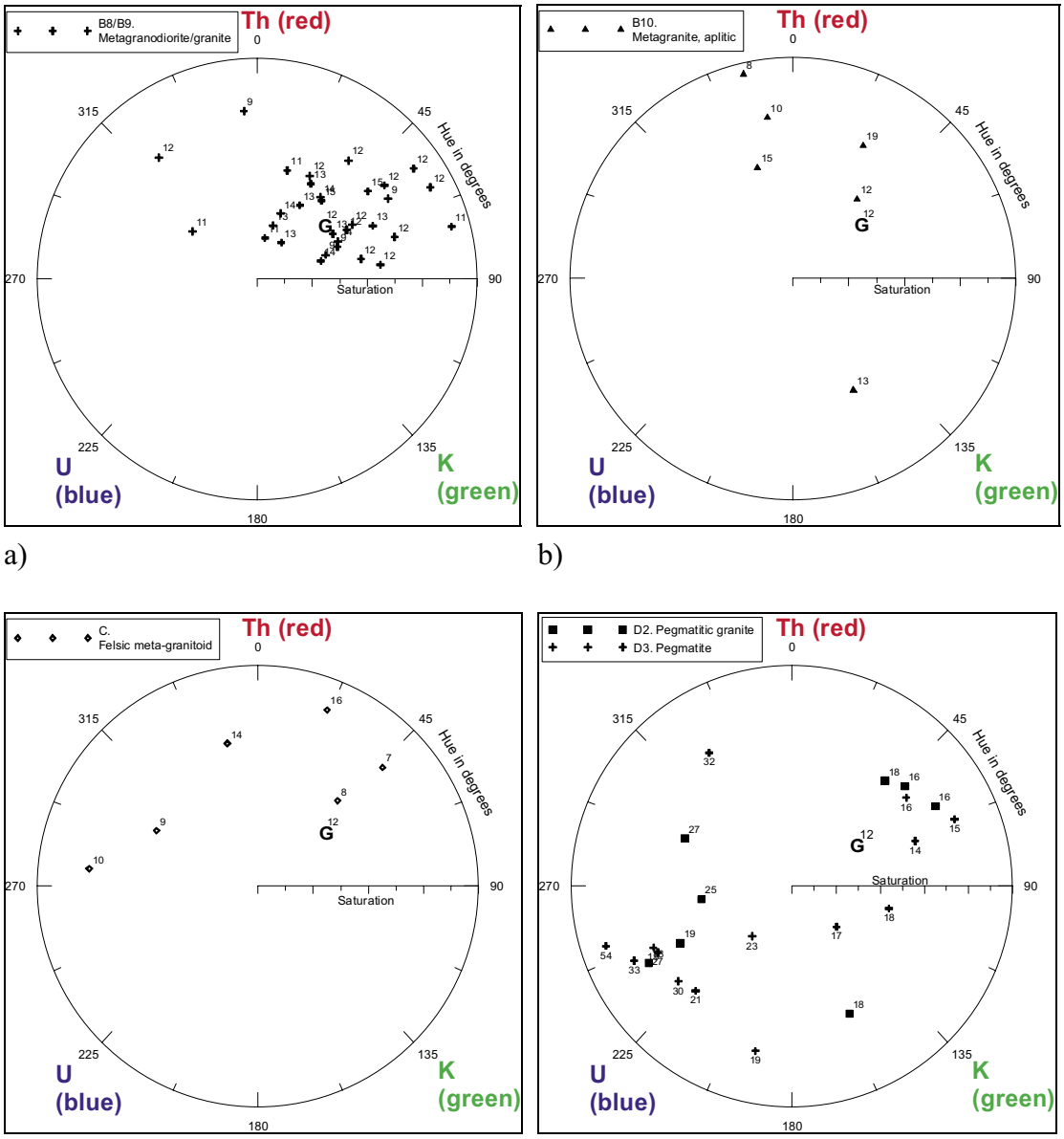


***Figure 7-3.*** *Hue-Saturation plot of in situ, gamma ray spectrometry measurements. The presentation shows the relative distribution in uranium equivalent units (Ur), between potassium, uranium and thorium. The letter* **G** *marks the position for a normal granite distribution (3% K, 5 ppm U, 15 ppm Th). Digits shows the natural exposure in microR/h.*

*a) Metagranodiorite to metagranite (Group B8/B9).*

*b) Metagranite, aplitic (Group B10).*

*c) Felsic granitoid, meta-intrusive rock (Group C).*

*d) Pegmatitic granite and pegmatite (Group D2 and D3).*

# 8 Compilation of petrophysical parameters for different sampling sites and rock types

A compilation of the petrophysical properties for the different sampling sites and rock types in the petrophysical sampling campaign in 2002 is presented in Appendix 1. A statistical compilation of the different petrophysical properties is presented in Appendix 2. A brief summary of selected petrophysical parameters (averages) for the rock groups that have sufficient amount of data (> 10 samples) to form the basis of a statistical conclusion, is presented in Table 8-1.

**Table 8-1. Compilation of petrophysical parameters for different rock groups.**

| Rock group Unit | Volume susceptibility SI | Q-value SI | Density kg/m3 | Porosity % | Resistivity Ohmm | IP mrad | K % | U ppm | Th ppm | Natural exposure microR/h |
|---|---|---|---|---|---|---|---|---|---|---|
| **A1** | 0.00381 | 0.24 | 2755 | 0.34 | 22,696 | 22.5 | 1.9 | 3.9 | 10.2 | 8.5 |
| **B2/B3** | 0.00471 | 0.15 | 2948 | 0.37 | 15,916 | 18.6 | 0.8 | 1.0 | 1.7 | 2.3 |
| **B5/B6** | 0.00149 | 0.12 | 2746 | 0.41 | 14,101 | 11.7 | 1.9 | 4.0 | 9.0 | 8.1 |
| **B8/B9** | 0.00453 | 0.16 | 2655 | 0.44 | 20,362 | 9.1 | 2.9 | 4.7 | 15.4 | 12.1 |
| **D2/D3** | 0.00284 | 0.36 | 2626 | 0.53 | 16,868 | 8.1 | 4.0 | 15.9 | 20.9 | 22.5 |

The units in Table 8-1 correspond to the following rock types (see also Chapter 3):

A1 Felsic to intermediate metavolcanic and metavolcanoclastic rocks

B2/B3 Metagabbro / Metadiorite, quartz-bearing metadiorite, metadioritoid

B5/B6 Metatonalite / Metatonalite to metagranodiorite

B8/B9 Metagranodiorite to metagranite / Metagranite

D2/D3 Pegmatitic granite / Pegmatite

Further processing and evaluation as well as co-interpretation between the different properties will be made when the results from the petrophysical sampling in 2003 are available.

# 9 Magnetic susceptibility measurements on outcrops

As part of the bedrock mapping programme /2/, data from in situ measurements of the magnetic susceptibility have been recorded for the most important rock types identified on each mapped site.

Out of 1054 geological observation points, the magnetic susceptibility has been recorded at 853 locations. At these sites, 1602 rock types have been measured and a total of 11,692 individual measurements have been recorded.

## 9.1 Data processing

Normally, 8 measurements have been recorded for each rock type and the data have been treated statistically and the geometric mean, the standard deviation and the number of measurements for each measured site and rock type have been calculated. A geographical database containing this information and connected geological information has been created.

A map showing the surface distribution of magnetic susceptibility is presented in Figure 9-1. The map is based on the most common rock type for each outcrop and, hence, this map also indicates the spatial distribution of the magnetite content in the common rocks. The susceptibilities of the most common rocks (mostly group B8/B9) within the candidate area are in general in the range of $400–1200\times10^{-5}$ SI. The metatonalite-metagranodiorite rock at Lillfjärden is very low, $0–100\times10^{-5}$ SI. The susceptibility pattern south of the candidate area is more scattered with both low and high susceptibilities.

The new mapping in 2003 will fill gaps in this map and also cover the island areas in the sea and hence, will provide better opportunities for this type of presentation.

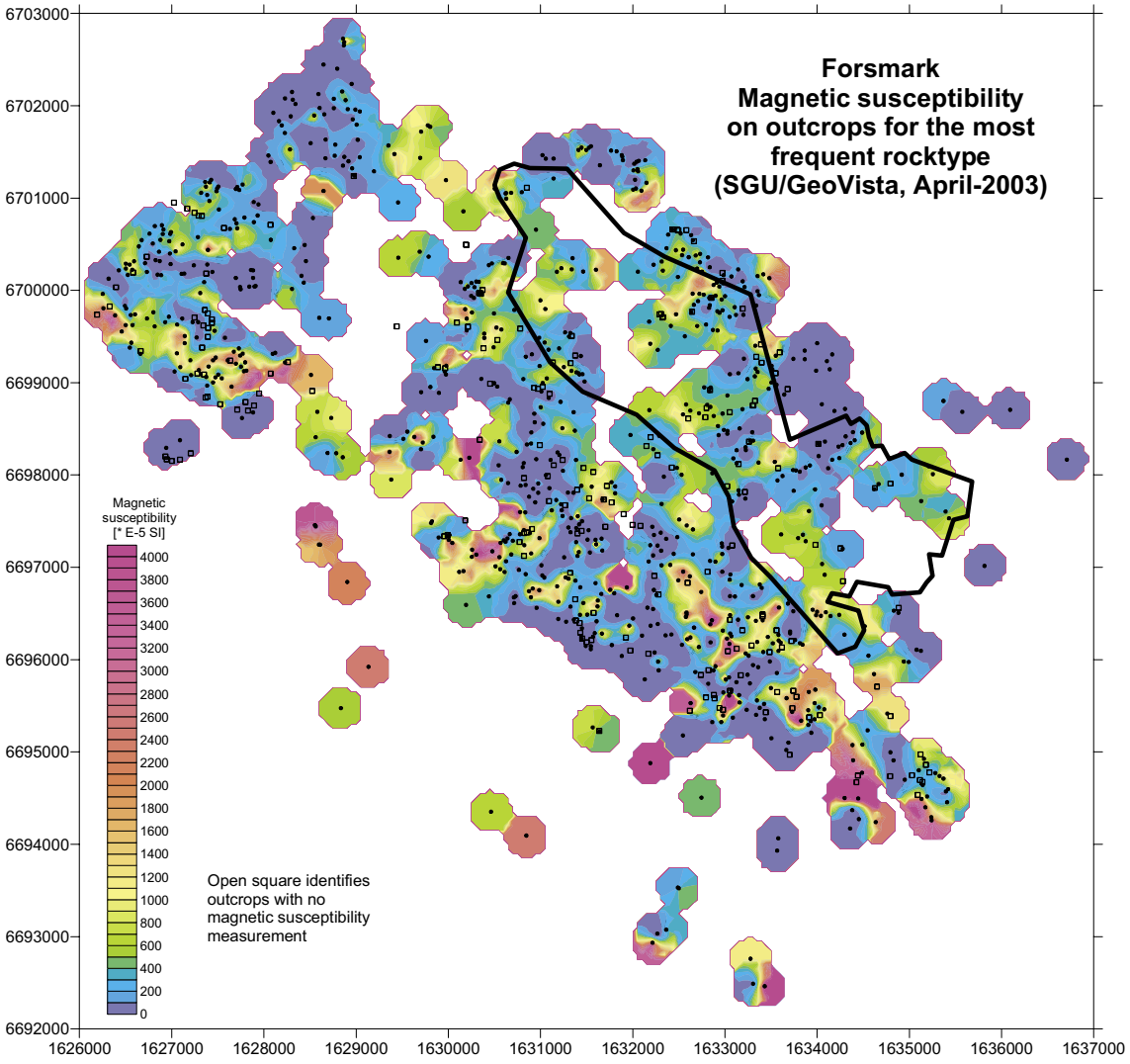


***Figure 9-1.*** *Magnetic susceptibility on outcrops, for the most frequent rock type. Open squares identifies outcrops with no magnetic susceptibility measurement. The Forsmark candidate area is outlined with a solid black line.*

## 9.2 Results

The results are discussed in conjunction with the histograms in Figure 9-2a–l.

The felsic to intermediate metavolcanic and metavolcanoclastic rocks (group A1) indicate three different populations, low (< 0.001 SI), moderate and high (> 0.01 SI), Figure 9-2a. The two low susceptibility populations are geographically scattered over the mapped area. In contrary, the outcrops with high magnetic susceptibility have so far only been noted in the southern part of the mapped area.

In spite of the fact that the number of sites is fairly limited, the meta-ultramafic rocks (group B1) indicate two populations; one population with low susceptibility (0.0004–0.001 SI), and one with moderate – high susceptibility (0.002–0.1 SI), Figure 9-2b. No characteristic geographical pattern has been identified, separating the different groups.

The metagabbro and metadioritic rocks (group B2/B3) indicate three magnetic susceptibility populations, Figure 9-2c. A low susceptibility group vary from 0.0001–0.003 SI, with a very distinct concentration on levels around 0.0004–0.001 SI, which is similar for the amphibolites in group B4. Moderate susceptibilities vary between 0.003–0.02 SI and a small group with high magnetic susceptibility vary between 0.02–0.16 SI. No characteristic geographical pattern has been identified, separating the different groups.

The amphibolites, Figure 9-2d, are dominated by a very distinct grouping of magnetic susceptibilities at 0.0004–0.001 SI. In addition to that, the distribution is widespread and varies from very low to high. Of interest is that no amphibolites with magnetic susceptibility > 0.0025 SI is identified within the Forsmark candidate area.

The metatonalite to metagranodiorite group (B5/B6), Figure 9-2e, also indicates three populations; a low susceptibility group with values varying from 0.0001 SI to 0.002 SI, moderate-high susceptibilities varying between 0.002 SI to 0.1 SI and a small group with very low magnetic susceptibilities varying between 0.00003 SI and 0.0001 SI. A metatonalite-metagranodiorite, rock unit occurring in the Lillfjärden area shows a uniform and low – very low magnetic susceptibility. Apart from that, no characteristic geographical pattern has been identified, separating the different groups.

The metagranodiorite group (B7) shows a similar distribution as the metagranodiorite-metagranite group (B8/B9), Figure 9-2f.

The metagranodiorite-metagranite group of rocks (B8/B9) have moderate – high susceptibilities, with individual peaks at 0.0063 SI and 0.0018 SI, Figure 9-2g. There is also a tendency of a tail into lower magnetic susceptibilities without any characteristic maxima. When analyzing all the individual magnetic susceptibility measurements performed, the same pattern is seen as for the outcrop site averages. The geographical distribution of the lower magnetic susceptibility trend within the Forsmark candidate area will be studied in more detail in future work.

The aplitic metagranite (B10) shows a distinct group of susceptibilities varying from 0.001 SI to 0.04 SI, with a peak at 0.0063 SI. There is also a small group with very low magnetic susceptibility, down to 0.00003 SI, Figure 9-2h.

The quartz-rich felsic (granitoid) meta-intrusive rock (group C) shows a diffuse bimodal distribution, Figure 9-2i. The rocks that certainly belong to this group show a wide grouping ranging from moderate to high susceptibility, 0.001–0.063 SI, and a more distinct group with low to very low susceptibility at 0–0.0004 SI.

Rocks that do not belong to granitoids in group C or to granites, group D1 are analyzed together and shows a very similar distribution as for group C rocks. Typically the rocks with moderate – high susceptibility are more common, Figure 9-2j.

Pegmatite granite (D2) generally shows very low to moderate magnetic susceptibility with peaks at 0.0004 SI and 0.003 SI. Typically very low susceptibilities are common, Figure 9-2k.

Pegmatite (D3) shows a similar pattern as for pegmatite granite with a peak at 0.00063 SI, Figure 9-2l. Some pegmatite outcrops give very high magnetic susceptibility readings, which are often related to dissemination of coarse magnetite grains.

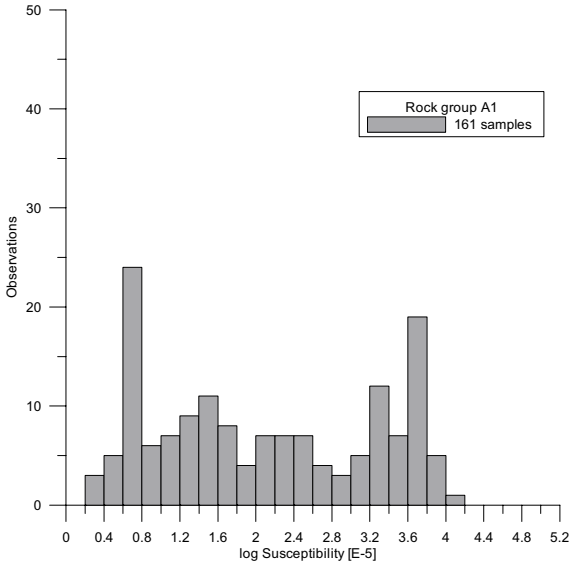


*a) Felsic to intermediate metavolcanic and metavolcanoclastic rocks (Group A1), 161 outcrop*

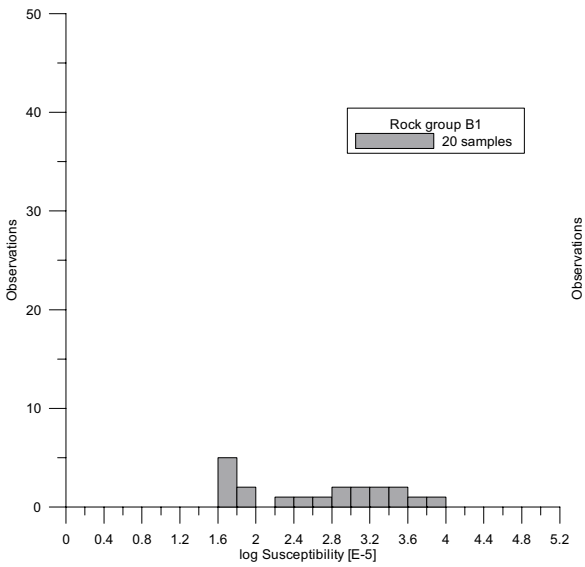


*b) meta-ultramafic rocks (B1), 20 outcrops*

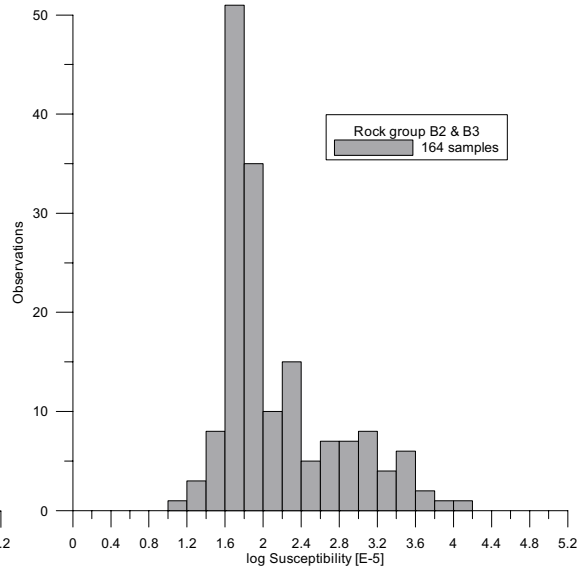


*c) metagabbro-metadiorite (B2/B3), 164 outcrops*

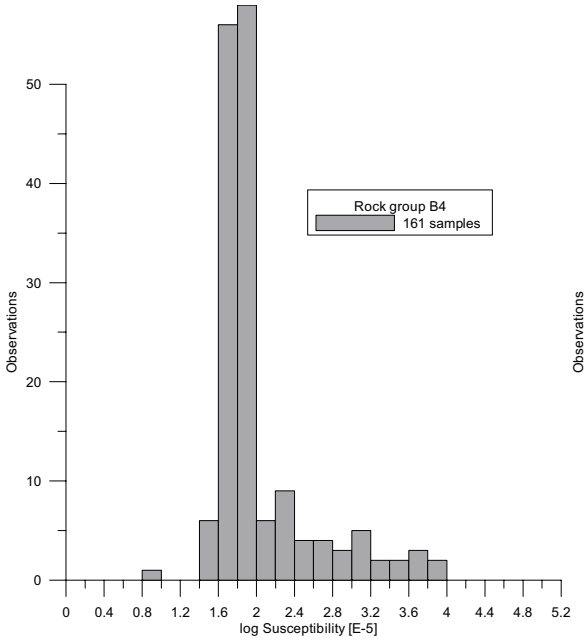


*d) amphibolite (B4), 161 outcrops*

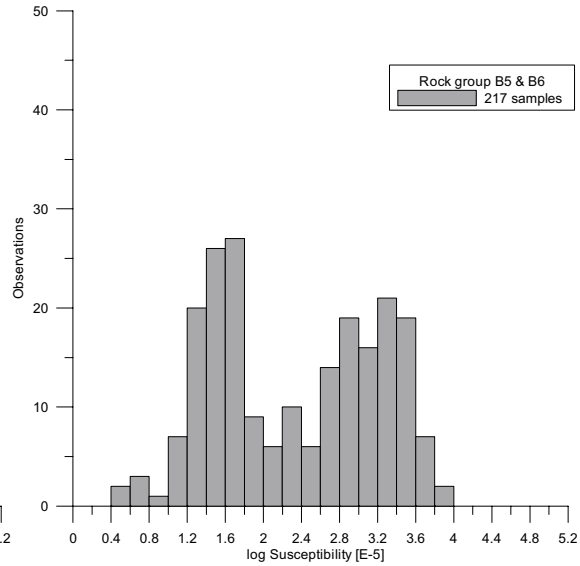


*e) metatonalite-metagranodiorite (B5/B6), 217 outcrops*

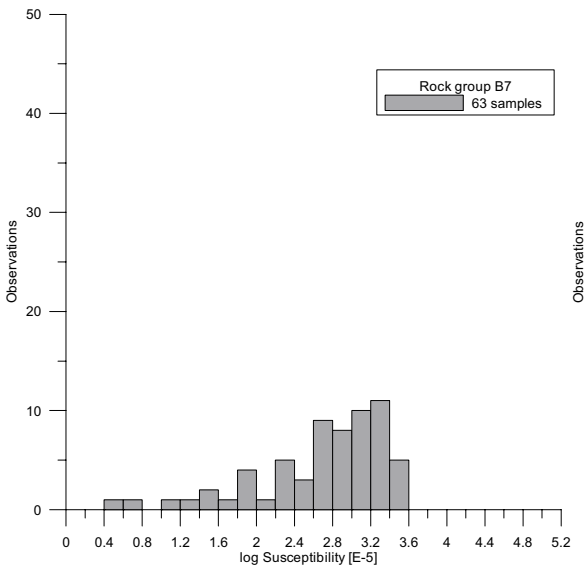


*f) metagranodiorite (B7), 63 outcrops*

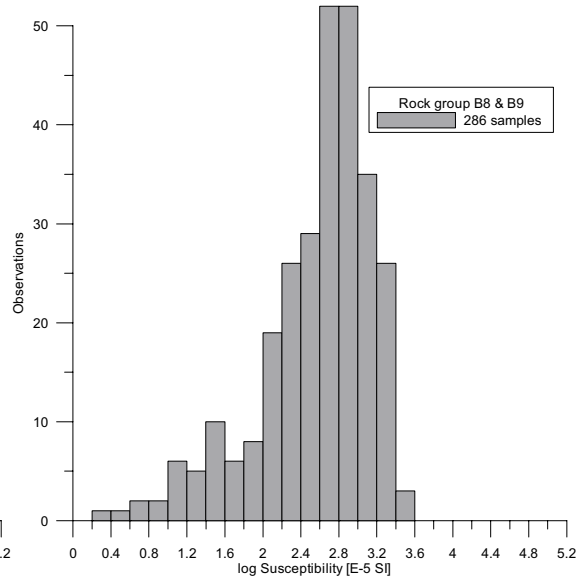


*g) metagranodiorite – metagranite (B8/B9), 286 outcrops*

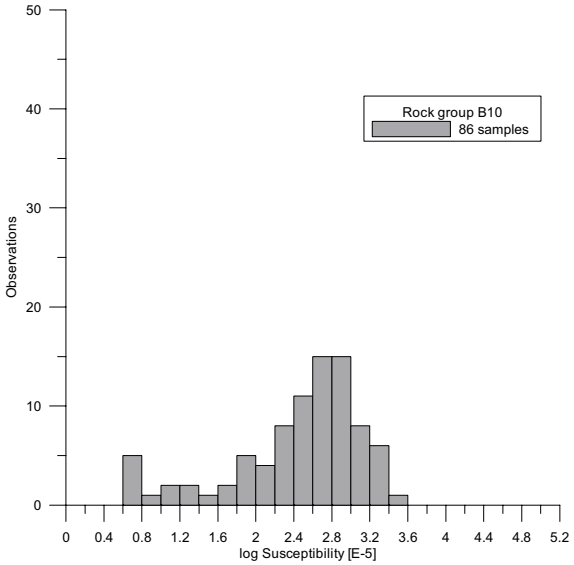


*h) metagranite, aplitic (B10), 86 outcrops*

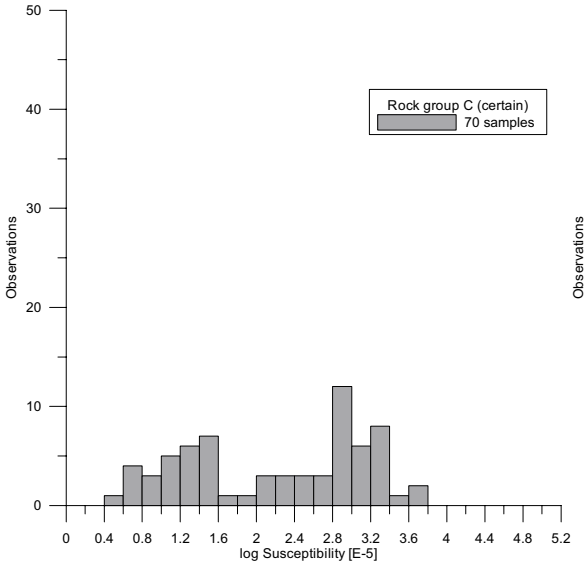


*i) felsic granitoid, meta-intrusive rock (C), 70 outcrops*

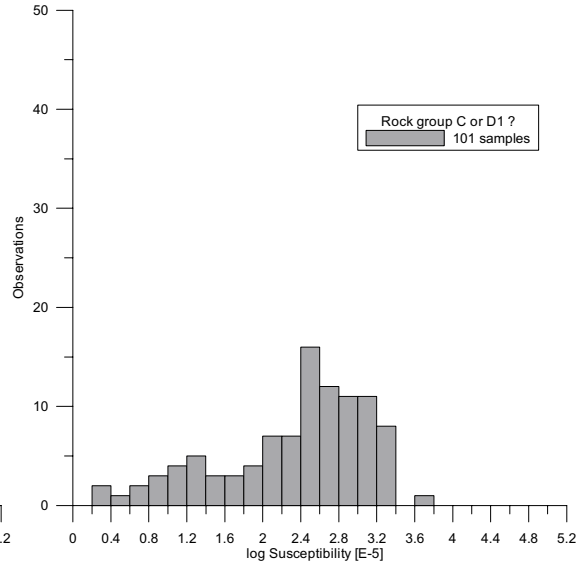


*j) granite (C or D1), uncertain provenance, 101 outcrops*

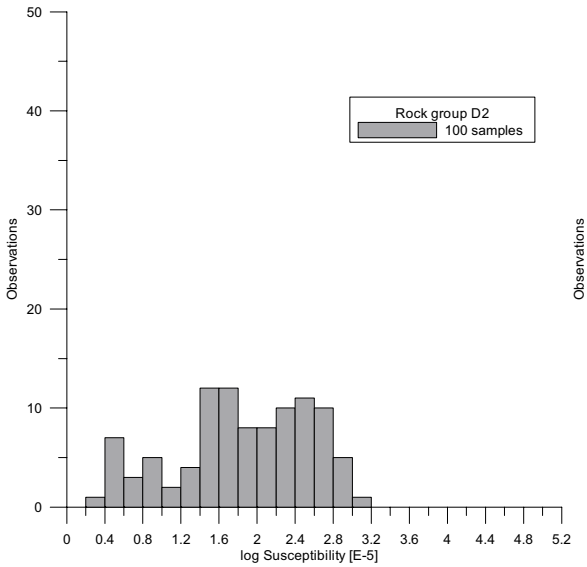


*k) pegmatitic granite (D2), 100 outcrops*

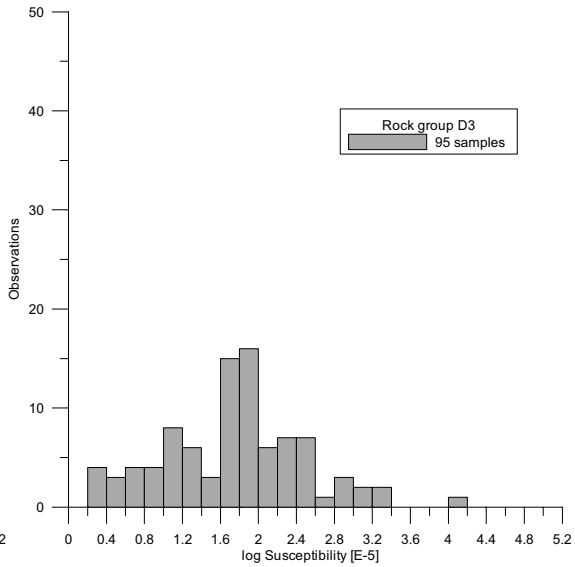


*l) pegmatite (D3), 95 outcrops*

***Figure 9-2a–l.*** *Histogram of the magnetic susceptibility (logarithm of site average) measured on outcrops. The results are presented for each of the different rock groups.*

# 10 Data delivery

The processed data and interpretation results have been delivered to SKB as described below. The SICADA field note number is Forsmark No 117. All GIS data have been documented according to “GIS – Inleverans av data”, SKB SD-081 (SKB internal controlling document).

Data have been delivered in three data formats for storage in the GIS-database and SICADA. Files that show post-processed grid-files have been delivered as georeferenced tiff-pictures and also used in the creation of figures to the report. Information that has resulted in some kind of interpreted vector; point, line or polygon information has been stored in Shape format. Petrophysical data from laboratory analysis and spectrometry field measurements have been delivered in Excel format for storage in SICADA. A listing of delivered products is shown in Appendix 3.

# 11 References


/1/ **Mattsson H, Isaksson H, Thunehed H, 2003.** Petrophysical rock sampling, measurements of petrophysical rock parameters and in situ gamma ray spectrometry measurements on outcrops carried out 2002. SKB P-03-26. Svensk Kärnbränslehantering AB.

/2/ **Stephens M B, Bergman T, Andersson J, Hermansson T, Wahlgren C-H, Albrecht L, Mikko H, 2003.** Forsmark Bedrock mapping. Stage 1 (2002) – Outcrop data including fracture data. SKB P-03-09

/3/ **Henkel H, 1991.** Petrophysical properties (density and magnetization of rock from the northern part of the Baltic Shield. Tectonophysics 192, page1–19.

/4/ **Collinson D W, 1983.** Methods in rock magnetism and paleomagnetism, Chapman and Hall, London, United Kingdom. 503 pp.

/5/ **Parasnis D S, 1997.** Principles of applied geophysics. Chapman and Hall, London, 429 pp.

/6/ **Puranen R, 1989.** Susceptibilities, iron and magnetite content of Precambrian rocks in Finland. Geological survey of Finland, Report of investigations 90, 45 pp.

/7/ **Tarling D H, Hrouda F, 1993.** The magnetic anisotropy of rocks, Chapman and Hall, London, United Kingdom. 217 pp.

/8/ **O'Reilly W**, **1984.** Rock and mineral magnetism, Chapman and Hall, New York, USA. 220 pp.

/9/ **Janak F**, **1965.** Determination of anisotropy of magnetic susceptibility of rocks, Studia geoph. et geod. 9, p 290–300.

/10/ **Bouchez J L, Gleizes G, 1995.** Two-stage deformation of the Mont-Louis-Andorra granite pluton(Variscan Pyrenees) inferred from magnetic susceptibility anisotropy. Journal of Geological Society, London 152, 669–679.

/11/ **Knight M D, Walker G P L, 1988.** Magma Flow Directions in Dikes of the Koolau Complex, Oahu, Determined From Magnetic Fabric Studies, Journal of Geophysical Research, vol 93, No B5, p 4301–4319.

/12/ **Bates M P, Mushayandebvu M F, 1995.** Magnetic fabric in the Umvimeela Dyke, satellite of the Great Dyke, Zimbabwe. Tectonophysics 242, 241–254.

/13/ **Raposo M I B, 1997.** Magnetic fabric and its significance in the Florianópolis dyke swarm, southern Brazil. Geophys. J. Int. 131, 159–170.

/14/ **Bouillin J-P, Bouchez J-L, Lespinasse P, Pêcher A, 1993.** Granite emplacement in an extensional setting: an AMS study of the magmatic structures of Monte Capanne (Elba, Italy). Earth and Planetary Science Letters, v 118, p 263–279.

/15/ **Bouchez J L, Gleizes G, Djouadi T, Rochette P, 1990.** Microstructure and magnetic susceptibility applied to emplacement kinematics of granites: the example of the Foix pluton (French Pyrenees). Tectonophysics 184, 157–171.

/16/ **Mattsson H J, Elming S-Å, 2001.** Magnetic fabrics and paleomagnetism of the Storsjön-Edsbyn deformation zone, central Sweden. Precambrian Research 107, 265–281.

/17/ **Borradaile G J, Henry B, 1997.** Tectonic applications of magnetic susceptibility and its anisotropy. Earth-Science Reviews 42, 49–93.

/18/ **Hirt A M, Lowrie W, Clendenen W S, Kligfield R, 1993.** Correlation of strain and the anisotropy of magnetic susceptibility in the Onaping formation: evidence for a near circular origin of the Sudbury Basin. Tectonophysics, v 225, p 231–254.

/19/ **Borradaile G J, Alford C, 1988.** Experimental shear zones and magnetic fabrics, Journal of structural geology 10, No 8, 895–904.

/20/ **Isaksson H, Thunehed H, Keisu M, 2004.** Interpretation of airborne geophysics and integration with topography. Stage 1 (2002). SKB P-04-29. Svensk Kärnbränslehantering AB.

/21/ **Archie G E, 1942.** The electrical resistivity log as an aid in determining some reservoir characteristics: Trans. Am. Inst. Min., Metallurg., Petr.Eng., 146, 54–62.

/22/ **Keller G V, Frischknecht F C, 1966.** Electrical methods in geophysical prospecting. Pergamon Press.

# Appendix 1

# A compilation of petrophysical properties for different sites and rock types

## Group A. Supracrustal rocks

| Group and PFM-number | Coordinates | | Geological map. Rock unit | Rock unit, order number | *Geological map. 1=BLS or SL, 2=LS* | *Geological model. Rock domain* | Magnetic properties | | | | | Density | Porosity | Electrical properties | | Gamma-ray spectrometry properties | | | |
|---|---|---|---|---|---|---|---|---|---|---|---|---|---|---|---|---|---|---|---|
| | Northing | Easting | | | | | Remanence_declination (deg) | Remanence_inclination (deg) | Remanence_intensity (A/m) | Volume_susceptibility (SI) | Q-value (SI) | Wet_density (kg/m3) | Porosity (%) | Electric resistivity (in fresh water, Ωm) | Induced polarization (phase at 0.6 Hz in fresh water, mrad) | K (%) | U (ppm) | Th (ppm) | Natural Exposure (microR/h) |
| **A1. 103076. Felsic to intermediate metavolcanic and metavolcaniclastic rocks** | | | | | | | | | | | | | | | | | | | |
| PFM000240 | 6697370 | 1630884 | 3076 | 1 | | | 115,7 | 73,2 | 0,7955 | 0,00453 | 0,44 | 2722,6 | 0,31 | 58657 | 41,1 | 1,1 | 4,1 | 11,3 | 7,7 |
| PFM000351 | 6696640 | 1631621 | 3076 | 1 | | | 86,2 | 81,3 | 0,3136 | 0,02996 | 0,13 | 2725,1 | 0,25 | 14851 | 14,0 | 1,7 | 4,1 | 10,2 | 8,2 |
| PFM000526 | 6694879 | 1632191 | 3076 | 1 | | | 134,1 | 13,1 | 3,7850 | 0,07152 | 1,20 | 2779,2 | 0,33 | 33765 | 25,3 | 2,6 | 3,0 | 7,6 | 8,2 |
| PFM000531 | 6696468 | 1633409 | 3076 | 1 | | | | | | | | | | | | 2,0 | 4,6 | 13,8 | 10,3 |
| PFM000725 | 6701464 | 1631021 | 3076 | 1 | | | 15,9 | 21,8 | 0,0018 | 0,00020 | 0,20 | 2695,4 | 0,37 | 8097 | 13,9 | 1,8 | 5,7 | 13,5 | 10,4 |
| PFM001156 | 6701371 | 1632016 | 3076 | 1 | | | 7,0 | 41,8 | 0,0005 | 0,00006 | 0,16 | 2686,5 | 0,53 | 9059 | 16,8 | 0,4 | 3,1 | 11,0 | 6,0 |
| PFM001200 | 6694369 | 1634380 | 3076 | 1 | | | 269,6 | 75,9 | 0,0231 | 0,00053 | 1,74 | 2716,5 | 0,20 | 81878 | 18,1 | 1,7 | 4,3 | 6,3 | 7,1 |
| PFM001221 | 6695616 | 1633153 | 3076 | 1 | | | 354,2 | 87,2 | 0,0007 | 0,00035 | 0,05 | 2733,3 | 0,32 | 27650 | 13,8 | 2,0 | 3,2 | 8,5 | 7,6 |
| PFM001221 | 6695616 | 1633153 | 3076 | 5 | | | 1,4 | 77,6 | 0,3816 | 0,03170 | 0,22 | 2822,3 | 0,33 | 47582 | 16,8 | | | | |
| PFM001521 | 6696685 | 1630440 | 3076 | 1 | | | 113,2 | 80,4 | 2,3030 | 0,24000 | 0,24 | 2946,4 | 0,40 | 24942 | 66,6 | 2,9 | 4,7 | 11,9 | 11,1 |
| PFM001524 | 6698414 | 1629838 | 3076 | 1 | | | 3,5 | 79,0 | 0,0502 | 0,01986 | 0,20 | 2699,7 | 0,30 | 12932 | 8,3 | 1,6 | 4,2 | 11,1 | 8,4 |
| PFM001885 | 6696272 | 1632419 | 3076 | 1 | | | 316,6 | 68,2 | 0,1400 | 0,03525 | 0,21 | 2882,0 | 0,28 | 26701 | 27,5 | 1,4 | 2,5 | 4,8 | 5,2 |
| PFM002248 | 6695208 | 1633937 | 3076 | 1 | | | 247,9 | 75,8 | 0,0002 | 0,00009 | 0,09 | 2647,8 | 0,40 | 9330 | 8,4 | 3,7 | 3,7 | 12,6 | 11,8 |
| **A2. 109014. Fe-rich mineralisation** | | | | | | | | | | | | | | | | | | | |
| PFM000336 | 6696490 | 1633408 | 9014 | 1 | | | 110,2 | 53,8 | 75,9300 | 0,12400 | 14,90 | 4224,7 | 1,24 | 168 | 232,0 | 1,0 | 5,2 | 5,9 | 6,6 |
| PFM000446 | 6697966 | 1630821 | 9014 | 1 | | | 71,0 | 3,8 | 79,7000 | 0,12220 | 15,90 | 4130,2 | 1,47 | 324 | 200,8 | 0,8 | 6,2 | 5,5 | 6,7 |
| **A3. No SKB code. Veined gneiss** | | | | | | | | | | | | | | | | | | | |
| PFM001606 | 6697443 | 1628563 | 8011 | 1 | | | 130,6 | 62,4 | 0,5328 | 0,04876 | 0,41 | 2700,9 | 0,53 | 11875 | 20,0 | 5,1 | 4,1 | 12,8 | 14,3 |
| **A4. 108019. Calc-silicate rock (skarn)** | | | | | | | | | | | | | | | | | | | |
| | | | | | | | | | | | | | | | | | | | |
| **A5. 109010. Sulphide mineralisation** | | | | | | | | | | | | | | | | | | | |
| | | | | | | | | | | | | | | | | | | | |

## Group B. Ultramafic, mafic, intermediate and quartz-rich felsic (granitoid) meta-intrusive rocks

| Group and PFM-number | Coordinates | | Geological map. Rock unit | Rock unit, order number | *Geological map. 1=BLS or SL, 2=LS* | *Geological model. Rock domain* | Magnetic properties | | | | | Density | Porosity | Electrical properties | | Gamma-ray spectrometry properties | | | |
|---|---|---|---|---|---|---|---|---|---|---|---|---|---|---|---|---|---|---|---|
| | Northing | Easting | | | | | Remanence_declination (deg) | Remanence_inclination (deg) | Remanence_intensity (A/m) | Volume_susceptibility (SI) | Q-value (SI) | Wet_density (kg/m3) | Porosity (%) | Electric resistivity (in fresh water, Ωm) | Induced polarization (phase at 0.6 Hz in fresh water, mrad) | K (%) | U (ppm) | Th (ppm) | Natural Exposure (microR/h) |
| **B1. 101004. Meta-ultramafic rock** | | | | | | | | | | | | | | | | | | | |
| PFM001201 | 6694496 | 1634445 | 1004 | 1 | | | 100,5 | 77,6 | 9,1800 | 0,10853 | 1,70 | 2785,8 | 0,88 | 228 | 353,7 | 0,0 | 0,1 | 0,0 | 0,1 |
| PFM001205 | 6694774 | 1634487 | 1004 | 1 | | | 30,7 | 61,2 | 4,6750 | 0,04572 | 2,26 | 3044,5 | 1,04 | 52 | 724,8 | 0,0 | 0,0 | 0,0 | 0,0 |
| **B2/B3. 101033. Metagabbro, metadiorite, quartz-bearing metadiorite, metadioritoid** | | | | | | | | | | | | | | | | | | | |
| PFM000229 | 6697308 | 1632363 | 1033 | 1 | | | 6,9 | 67,6 | 0,0009 | 0,00053 | 0,05 | 2879,1 | 0,37 | 13734 | 15,5 | 1,0 | 1,7 | 2,7 | 3,4 |
| PFM000233 | 6696951 | 1632971 | 1038 | 1 | | | 348,6 | 73,9 | 0,0404 | 0,01079 | 0,15 | 2738,4 | 0,27 | 29994 | 16,7 | 1,8 | 2,2 | 6,3 | 6,0 |
| PFM000243 | 6698165 | 1630133 | 1022 | 2 | | | 352,8 | 24,8 | 22,3900 | 0,01625 | 25,50 | 3074,7 | 0,35 | 14228 | 11,4 | 0,4 | 0,1 | 0,0 | 0,7 |
| PFM000253 | 6699484 | 1630390 | 1033 | 1 | | | 135,1 | 81,2 | 0,4956 | 0,01504 | 1,01 | 2871,1 | 0,34 | 32410 | 21,1 | 1,0 | 1,5 | 3,3 | 3,5 |
| PFM000518 | 6692462 | 1633431 | 1022 | 1 | | | 346,0 | 81,8 | 0,6565 | 0,05543 | 0,33 | 3119,8 | 0,36 | 29015 | 29,6 | 0,5 | 0,3 | 0,7 | 1,2 |
| PFM000522 | 6693032 | 1632267 | 1022 | 1 | | | 222,6 | 53,4 | 0,0015 | 0,00036 | 0,14 | 2882,4 | 0,39 | 34227 | 4,8 | 0,1 | 0,0 | 0,0 | 0,2 |
| PFM000780 | 6701446 | 1628872 | 1030 | 1 | | | 152,1 | 86,9 | 0,0011 | 0,00067 | 0,04 | 2928,2 | 0,36 | 11123 | 15,4 | 0,9 | 1,4 | 2,1 | 2,8 |
| PFM000850 | 6701527 | 1628282 | 1033 | 1 | | | 173,9 | 75,4 | 0,2186 | 0,03696 | 0,10 | 2941,4 | 0,44 | 8016 | 33,9 | 0,8 | 1,2 | 1,6 | 2,5 |
| PFM001235 | 6701402 | 1632065 | 1033 | 1 | | | 19,3 | 66,1 | 0,0003 | 0,00092 | 0,01 | 3023,4 | 0,46 | 10998 | 14,2 | 0,6 | 0,9 | 1,0 | 1,7 |
| PFM001515 | 6697287 | 1630699 | 1022 | 1 | | | 110,0 | 72,5 | 0,2557 | 0,05592 | 0,16 | 3017,8 | 0,25 | 16583 | 26,3 | 0,4 | 1,1 | 0,1 | 1,4 |
| PFM002087 | 6695918 | 1633360 | 1022 | 1 | | | 89,5 | 75,3 | 0,0003 | 0,00071 | 0,01 | 2951,8 | 0,54 | 5412 | 15,9 | 0,8 | 0,7 | 1,3 | 2,1 |
| **B4. 102017. Amphibolite** | | | | | | | | | | | | | | | | | | | |
| PFM001169 | 6699917 | 1632851 | 2017 | 2 | | | 16,2 | 52,9 | 0,0001 | 0,00071 | 0,00 | 2928,3 | 0,30 | 11211 | 15,3 | 1,3 | 1,1 | 2,6 | 3,4 |
| **B5/B6. 101054. Metatonalite to metagranodiorite** | | | | | | | | | | | | | | | | | | | |
| PFM000380 | 6696440 | 1631192 | 1053 | 1 | | | 303,6 | 56,1 | 0,0005 | 0,00033 | 0,04 | 2753,0 | 0,32 | 12081 | 11,3 | 1,9 | 4,0 | 9,2 | 8,2 |
| PFM000527 | 6695922 | 1629134 | 1053 | 1 | | | 161,1 | 69,2 | 0,1004 | 0,02043 | 0,10 | 2697,1 | 0,39 | 22923 | 13,1 | 2,0 | 3,4 | 9,1 | 8,0 |
| PFM000774 | 6701476 | 1629415 | 1053 | 1 | | | 169,7 | 72,7 | 0,2119 | 0,01087 | 0,36 | 2758,0 | 0,31 | 14609 | 12,5 | 1,5 | 4,3 | 8,7 | 7,7 |
| PFM000777 | 6700365 | 1629786 | 1053 | 1 | | | 310,3 | 80,4 | 0,1563 | 0,00425 | 0,71 | 2794,4 | 0,38 | 19221 | 15,6 | 1,6 | 3,3 | 6,0 | 6,3 |
| PFM000804 | 6698235 | 1627207 | 1053 | 1 | | | 30,2 | 75,2 | 0,0013 | 0,00029 | 0,09 | 2743,3 | 0,42 | 6659 | 9,9 | 2,0 | 2,8 | 8,6 | 7,5 |
| PFM000808 | 6699624 | 1626501 | 1054 | 1 | | | 144,3 | 67,9 | 0,8301 | 0,03507 | 0,38 | 2720,2 | 0,34 | 17276 | 13,1 | 1,1 | 3,5 | 7,2 | 6,1 |
| PFM000891 | 6699062 | 1627374 | 1054 | 1 | | | 254,1 | 64,8 | 0,0673 | 0,01521 | 0,12 | 2700,7 | 0,40 | 14883 | 16,0 | 2,3 | 2,7 | 10,2 | 8,4 |
| PFM001162 | 6698339 | 1634013 | 1053 | 1 | | | 13,9 | 43,8 | 0,0013 | 0,00039 | 0,09 | 2780,1 | 0,44 | 13124 | 7,0 | 2,0 | 2,8 | 7,5 | 7,1 |
| PFM001217 | 6700952 | 1629455 | 1053 | 1 | | | 187,5 | 56,3 | 0,2949 | 0,00472 | 0,66 | 2831,4 | 0,33 | 10235 | 13,2 | 1,7 | 4,9 | 8,4 | 8,2 |
| PFM001510 | 6695787 | 1632130 | 1053 | 1 | | | 8,1 | 75,5 | 0,0004 | 0,00031 | 0,03 | 2746,2 | 0,37 | 9168 | 9,3 | 2,5 | 3,6 | 11,2 | 9,5 |
| PFM001858 | 6698716 | 1634302 | 1053 | 1 | | | | | | | | | | | | 2,2 | 4,9 | 10,3 | 9,6 |
| PFM001859 | 6698693 | 1634187 | 1053 | 1 | | | 54,9 | 51,3 | 0,0003 | 0,00022 | 0,04 | 2704,0 | 0,49 | 17508 | 7,9 | | | | |
| PFM001860 | 6699145 | 1634136 | 1053 | 1 | | | 31,4 | 69,5 | 0,0002 | 0,00020 | 0,02 | 2703,1 | 0,53 | 13850 | 13,3 | 1,9 | 7,4 | 11,1 | 10,9 |
| PFM001861 | 6699427 | 1634000 | 1053 | 1 | | | 265,3 | 35,6 | 0,0012 | 0,00030 | 0,14 | 2721,9 | 0,47 | 19500 | 11,1 | 2,4 | 5,4 | 12,4 | 10,7 |
| PFM002056 | 6700134 | 1627695 | 1053 | 1 | | | 2,1 | 48,2 | 0,0041 | 0,00074 | 0,11 | 2796,4 | 0,51 | 15843 | 10,9 | 1,4 | 2,5 | 6,3 | 5,6 |

## Group B. Ultramafic, mafic, intermediate and quartz-rich felsic (granitoid) meta-intrusive rocks, continuation

| Group and PFM-number | Coordinates | | Geological map. Rock unit | Rock unit, order number | *Geological map. 1=BLS or SL, 2=LS* | *Geological model. Rock domain* | Magnetic properties | | | | | Density | Porosity | Electrical properties | | Gamma-ray spectrometry properties | | | |
|---|---|---|---|---|---|---|---|---|---|---|---|---|---|---|---|---|---|---|---|
| | Northing | Easting | | | | | Remanence_declination (deg) | Remanence_inclination (deg) | Remanence_intensity (A/m) | Volume_susceptibility (SI) | Q-value (SI) | Wet_density (kg/m3) | Porosity (%) | Electric resistivity (in fresh water, Ωm) | Induced polarization (phase at 0.6 Hz in fresh water, mrad) | K (%) | U (ppm) | Th (ppm) | Natural Exposure (microR/h) |
| **B7. 101056. Metagranodiorite** | | | | | | | | | | | | | | | | | | | |
| PFM000692 | 6696651 | 1633697 | 1056 | 1 | | | 140,8 | 73,4 | 0,1442 | 0,00673 | 0,37 | 2703,9 | 0,50 | 76646 | 23,5 | 1,7 | 3,3 | 8,3 | 7,2 |
| **B8/B9. 101057. Metagranodiorite to metagranit** | | | | | | | | | | | | | | | | | | | |
| PFM000168 | 6699705 | 1632323 | 1058 | 1 | | | 16,8 | 32,2 | 0,0611 | 0,00922 | 0,17 | 2656,1 | 0,41 | 22234 | 8,4 | 3,1 | 4,5 | 14,9 | 12,1 |
| PFM000173 | 6699400 | 1633329 | 1058 | 1 | | | 88,0 | 49,7 | 0,0502 | 0,01062 | 0,16 | 2648,3 | 0,36 | 16797 | 8,1 | 3,1 | 5,1 | 15,0 | 12,5 |
| PFM000197 | 6697201 | 1634276 | 1058 | 1 | | | 189,0 | 61,7 | 0,0285 | 0,00515 | 0,24 | 2646,4 | 0,49 | 16694 | 9,3 | 3,8 | 4,8 | 19,7 | 14,8 |
| PFM000203 | 6697357 | 1633609 | 1058 | 1 | | | 122,2 | 73,1 | 0,0984 | 0,01974 | 0,22 | 2654,5 | 0,42 | 19566 | 6,6 | 2,8 | 5,1 | 16,9 | 12,6 |
| PFM000206 | 6698933 | 1633474 | 1058 | 1 | | | 289,4 | 71,8 | 0,0128 | 0,00363 | 0,07 | 2652,1 | 0,52 | 21287 | 8,8 | 3,2 | 2,5 | 16,4 | 11,6 |
| PFM000216 | 6698919 | 1632840 | 1058 | 1 | | | 56,9 | 47,6 | 0,0378 | 0,00675 | 0,14 | 2648,0 | 0,44 | 16115 | 4,1 | 3,4 | 4,4 | 15,7 | 12,8 |
| PFM000259 | 6699183 | 1629977 | 1057 | 1 | | | 62,4 | 81,3 | 0,0362 | 0,01938 | 0,65 | 2675,5 | 0,42 | 42221 | 18,2 | 2,3 | 3,8 | 10,6 | 9,1 |
| PFM000271 | 6697873 | 1631554 | 1058 | 1 | | | 15,7 | 71,9 | 0,0201 | 0,00982 | 0,13 | 2656,8 | 0,40 | 14080 | 8,7 | 2,4 | 5,6 | 13,2 | 11,2 |
| PFM000276 | 6697997 | 1631059 | 1058 | 1 | | | 318,6 | 78,3 | 0,0027 | 0,00017 | 0,35 | 2663,6 | 0,39 | 25859 | 13,3 | 3,1 | 4,7 | 14,8 | 12,2 |
| PFM000513 | 6694094 | 1630846 | 1057 | 1 | | | 190,0 | 62,4 | 0,0003 | 0,00199 | 0,05 | 2680,7 | 0,41 | 20119 | 8,3 | 3,1 | 4,6 | 13,1 | 11,6 |
| PFM000515 | 6693531 | 1632489 | 1057 | 1 | | | 117,5 | 48,4 | 0,0277 | 0,00191 | 0,14 | 2678,9 | 0,48 | 25135 | 11,1 | 2,5 | 2,7 | 12,2 | 9,2 |
| PFM000658 | 6699102 | 1631413 | 1057 | 1 | | | 129,7 | 84,9 | 0,0361 | 0,00626 | 0,13 | 2642,2 | 0,42 | 22026 | 7,4 | 3,5 | 6,4 | 15,9 | 14,2 |
| PFM000680 | 6697848 | 1634617 | 1058 | 2 | | | 163,1 | 59,6 | 0,0145 | 0,00420 | 0,09 | 2649,3 | 0,53 | 21964 | 8,4 | 3,6 | 2,5 | 16,9 | 12,2 |
| PFM000683 | 6697604 | 1635393 | 1058 | 1 | | | 149,4 | 50,4 | 0,0451 | 0,00721 | 0,11 | 2648,0 | 0,46 | 27415 | 5,8 | 2,0 | 6,6 | 13,6 | 11,3 |
| PFM000685 | 6698095 | 1635210 | 1058 | 1 | | | 157,5 | 45,3 | 0,0758 | | | 2654,7 | 0,48 | 20049 | 9,1 | 3,2 | 3,5 | 16,4 | 12,1 |
| PFM000694 | 6698425 | 1632287 | 1056 | 1 | | | 298,5 | 73,8 | 0,0376 | 0,00506 | 0,17 | 2654,5 | 0,50 | 20526 | 6,0 | 3,3 | 3,8 | 14,1 | 11,7 |
| PFM000695 | 6698702 | 1632180 | 1058 | 1 | | | 113,3 | 34,8 | 0,1158 | 0,02148 | 0,11 | 2646,0 | 0,45 | 25212 | 7,0 | 3,5 | 6,1 | 19,3 | 15,0 |
| PFM000698 | 6699798 | 1631052 | 1058 | 1 | | | 157,4 | 73,3 | 0,0984 | 0,00790 | 0,17 | 2651,1 | 0,43 | 22813 | 8,7 | 2,3 | 4,7 | 15,9 | 11,3 |
| PFM000701 | 6700223 | 1631601 | 1058 | 1 | | | 118,5 | 65,6 | 0,0569 | 0,00771 | 0,13 | 2643,8 | 0,42 | 13785 | 7,6 | 2,9 | 4,0 | 17,5 | 12,2 |
| PFM000713 | 6700615 | 1632520 | 1058 | 2 | | | 20,2 | 42,0 | 0,0020 | 0,00007 | 0,55 | 2656,1 | 0,38 | 15736 | 11,6 | 1,3 | 3,5 | 16,1 | 9,1 |
| PFM000722 | 6701111 | 1630850 | 1058 | 1 | | | 343,2 | 61,8 | 0,0007 | 0,00017 | 0,10 | 2654,5 | 0,37 | 20518 | 6,9 | 1,5 | 6,7 | 16,7 | 11,7 |
| PFM000770 | 6701719 | 1629704 | 1058 | 1 | | | 156,3 | 84,4 | 0,0880 | 0,00817 | 0,25 | 2648,8 | 0,41 | 20787 | 9,4 | | | | |
| PFM000772 | 6701787 | 1629778 | 1058 | 1 | | | | | | | | | | | | 3,5 | 5,7 | 16,4 | 13,8 |
| PFM000890 | 6698713 | 1633190 | 1058 | 1 | | | 44,4 | 78,0 | 0,0329 | 0,00425 | 0,21 | 2649,0 | 0,52 | 13055 | 8,1 | 3,4 | 2,2 | 13,4 | 10,7 |
| PFM001159 | 6699761 | 1632635 | 1058 | 1 | | | 26,8 | 77,9 | 0,0488 | 0,00465 | 0,24 | 2655,9 | 0,40 | 20022 | 13,2 | 3,4 | 4,5 | 13,5 | 12,0 |
| PFM001173 | 6699900 | 1632964 | 1058 | 1 | | | 162,3 | 77,3 | 0,1338 | 0,01450 | 0,25 | 2648,9 | 0,35 | 10454 | 5,9 | 2,7 | 4,9 | 16,9 | 12,3 |
| PFM001180 | 6698125 | 1633127 | 1058 | 1 | | | 221,5 | 77,9 | 0,0310 | 0,00336 | 0,18 | 2645,3 | 0,47 | 23206 | 10,3 | 3,2 | 5,6 | 17,9 | 13,8 |
| PFM001183 | 6698025 | 1632858 | 1058 | 1 | | | 150,1 | 39,5 | 0,0099 | 0,00756 | 0,04 | 2648,9 | 0,50 | 29889 | 9,2 | 2,8 | 6,3 | 15,8 | 13,1 |
| PFM001213 | 6700856 | 1630163 | 1058 | 1 | | | 129,6 | 76,8 | 0,0053 | 0,00135 | 0,11 | 2654,7 | 0,34 | 18277 | 7,6 | 3,0 | 6,5 | 17,4 | 14,0 |
| PFM001251 | 6700093 | 1630330 | 1058 | 1 | | | 339,7 | 80,5 | 0,0062 | 0,00340 | 0,09 | 2679,1 | 0,44 | 45746 | 10,9 | 2,8 | 6,1 | 14,5 | 12,6 |
| PFM001864 | 6698802 | 1635370 | 1058 | 1 | | | 334,2 | 17,9 | 0,0975 | 0,00521 | 0,18 | 2647,5 | 0,51 | 11498 | 6,9 | 2,9 | 5,7 | 16,5 | 13,0 |
| PFM001879 | 6696859 | 1632494 | 1057 | 1 | | | 320,1 | 73,6 | 0,2117 | 0,02546 | 0,21 | 2666,8 | 0,53 | 21764 | 16,9 | 2,2 | 3,9 | 10,1 | 8,9 |
| **B10. 101058. Metagranite, aplitic** | | | | | | | | | | | | | | | | | | | |
| PFM000687 | 6696919 | 1634082 | 1058 | 1 | | | 97,3 | 53,6 | 0,0158 | 0,00584 | 0,09 | 2620,4 | 0,36 | 27915 | 10,5 | 4,1 | 6,4 | 27,9 | 18,9 |
| PFM000706 | 6700202 | 1632056 | 1058 | 2 | | | 90,4 | 64,4 | 0,0622 | 0,01722 | 0,10 | 2646,0 | 0,45 | 13447 | 10,5 | 2,8 | 4,9 | 15,5 | 12,1 |
| PFM000713 | 6700615 | 1632520 | 1058 | 1 | | | 91,3 | 77,0 | 0,0194 | 0,00179 | 0,31 | 2632,7 | 0,41 | 11467 | 9,4 | 1,4 | 4,1 | 16,4 | 9,7 |
| PFM000724 | 6701426 | 1631057 | 1058 | 2 | | | | | | | | | | | | 2,6 | 7,6 | 21,6 | 15,4 |
| PFM000739 | 6700227 | 1633143 | 1058 | 1 | | | 62,5 | 83,6 | 0,0195 | 0,00491 | 0,45 | 2642,6 | 0,36 | 15961 | 15,9 | 0,8 | 3,3 | 16,0 | 8,3 |
| PFM001156 | 6701371 | 1632016 | 1058 | 6 | | | | | | | | | | | | 3,6 | 6,8 | 9,4 | 12,6 |

## Group C. 101051. Quartz-rich felsic (granitoid) meta-intrusive rock, fine- to medium-grained. Occurs as dykes and lenses within rocks belonging to Groups A and B

| Group and PFM-number | Coordinates | | Geological map. Rock unit | Rock unit, order number | *Geological map. 1=BLS or SL, 2=LS* | *Geological model. Rock domain* | Magnetic properties | | | | | Density | Porosity | Electrical properties | | Gamma-ray spectrometry properties | | | |
|---|---|---|---|---|---|---|---|---|---|---|---|---|---|---|---|---|---|---|---|
| | Northing | Easting | | | | | Remanence_declination (deg) | Remanence_inclination (deg) | Remanence_intensity (A/m) | Volume_susceptibility (SI) | Q-value (SI) | Wet_density (kg/m3) | Porosity (%) | Electric resistivity (in fresh water, Ωm) | Induced polarization (phase at 0.6 Hz in fresh water, mrad) | K (%) | U (ppm) | Th (ppm) | Natural Exposure (microR/h) |
| PFM000168 | 6699705 | 1632323 | 1058 | 2 | | | | | | | | | | | | 2,2 | 6,5 | 22,5 | 14,3 |
| PFM000698 | 6699798 | 1631052 | 1051 | 5 | | | | | | 0,00014 | | | | | | | | | |
| PFM000703 | 6700277 | 1632226 | 1051 | 2 | | | 30,6 | 55,3 | 0,0221 | 0,00348 | 0,09 | 2712,4 | 0,53 | 10461 | 11,1 | 1,9 | 3,0 | 10,4 | 8,0 |
| PFM000718 | 6700543 | 1632654 | 1051 | 3 | | | 335,3 | 74,5 | 0,0025 | 0,00040 | 0,09 | 2693,7 | 0,39 | 15558 | 14,6 | 1,4 | 5,8 | 11,5 | 9,3 |
| PFM000739 | 6700227 | 1633143 | 1051 | 2 | | | 345,9 | 58,4 | 0,0824 | 0,01921 | 0,12 | 2704,9 | 0,46 | 15740 | 17,6 | 1,2 | 7,5 | 11,3 | 10,0 |
| PFM000822 | 6699696 | 1628705 | 1057 | 1 | | | 117,2 | 68,1 | 0,0432 | 0,00171 | 0,42 | 2655,0 | 0,46 | 8529 | 8,0 | 3,1 | 4,2 | 26,7 | 15,6 |
| PFM001162 | 6698339 | 1634013 | 1051 | 2 | | | 14,7 | 27,1 | 0,0005 | 0,00024 | 0,05 | 2737,6 | 0,47 | 18252 | 9,7 | 1,8 | 1,9 | 10,1 | 7,1 |

**Group D. Granite, pegmatitic granite, pegmatite. Occurs as dykes and minor intrusive bodies within rocks belonging to Groups A and B. Pegmatites display variable time relationships to Group C**

| Group and PFM-number | Coordinates | | Geological map. Rock unit | Rock unit, order number | *Geological map. 1=BLS or SL, 2=LS* | *Geological model. Rock domain* | Magnetic properties | | | | | Density | Porosity | Electrical properties | | Gamma-ray spectrometry properties | | | |
|---|---|---|---|---|---|---|---|---|---|---|---|---|---|---|---|---|---|---|---|
| | Northing | Easting | | | | | Remanence_declination (deg) | Remanence_inclination (deg) | Remanence_intensity (A/m) | Volume_susceptibility (SI) | Q-value (SI) | Wet_density (kg/m3) | Porosity (%) | Electric resistivity (in fresh water, Ωm) | Induced polarization (phase at 0.6 Hz in fresh water, mrad) | K (%) | U (ppm) | Th (ppm) | Natural Exposure (microR/h) |
| **D1. 111058. Granite** | | | | | | | | | | | | | | | | | | | |
| PFM000685 | 6698095 | 1635210 | 1058 | 4 | | | | | | | | | | | | 4,2 | 6,3 | 29,9 | 19,5 |
| PFM000713 | 6700615 | 1632520 | 1058 | 4 | | | 102,9 | 75,4 | 0,0534 | 0,00204 | 0,22 | 2631,5 | 0,48 | 13017 | 12,5 | 4,3 | 9,5 | 33,8 | 22,9 |
| PFM000722 | 6701111 | 1630850 | 1059 | 3 | | | | | | 0,00010 | | | | | | | | | |
| PFM000807 | 6699624 | 1626575 | 1058 | 7 | | | | | | | | | | | | 4,2 | 14,9 | 20,3 | 22,0 |
| **D2. 101061. Pegmatitic granite** | | | | | | | | | | | | | | | | | | | |
| PFM000198 | 6697205 | 1634253 | 1098 | 2 | | | 189,9 | 68,9 | 0,0130 | 0,00349 | 0,49 | 2622,2 | 0,51 | 14814 | 9,3 | 4,4 | 3,8 | 24,1 | 16,4 |
| PFM000245 | 6699041 | 1630358 | 1098 | 1 | | | 321,0 | 80,4 | 0,0196 | 0,00033 | 0,44 | 2630,4 | 0,58 | 33483 | 11,8 | 4,2 | 17,5 | 25,7 | 25,2 |
| PFM000446 | 6697966 | 1630821 | 1098 | 2 | | | | | | 0,00498 | | | | | | 2,1 | 18,8 | 10,8 | 18,2 |
| PFM000680 | 6697848 | 1634617 | 1098 | 1 | | | 87,7 | 71,4 | 0,2542 | 0,00498 | 0,33 | 2626,7 | 0,64 | 14129 | 6,8 | 4,7 | 2,9 | 22,2 | 15,7 |
| PFM000726 | 6699787 | 1630715 | 1098 | 1 | | | 356,3 | 68,8 | 0,1167 | 0,02028 | 0,20 | 2631,2 | 0,48 | 17936 | 4,6 | 2,9 | 16,0 | 14,7 | 18,9 |
| PFM001515 | 6697287 | 1630699 | 1098 | 2 | | | | | | | | | | | | 5,8 | 10,3 | 10,2 | 18,2 |
| PFM001869 | 6696530 | 1634832 | 1098 | 1 | | | 256,6 | 62,0 | 0,0179 | 0,00452 | 0,40 | 2620,6 | 0,45 | 10865 | 8,4 | 4,4 | 4,8 | 26,6 | 18,0 |
| PFM002056 | 6700134 | 1627695 | 1098 | 2 | | | | | | | | | | | | 3,5 | 17,7 | 33,6 | 26,7 |
| **D3. 101061. Pegmatite** | | | | | | | | | | | | | | | | | | | |
| PFM000168 | 6699705 | 1632323 | 1061 | 3 | | | | | | | | | | | | 3,9 | 3,8 | 17,0 | 13,5 |
| PFM000233 | 6696951 | 1632971 | 1061 | 3 | | | | | | | | | | | | 4,4 | 8,3 | 15,4 | 16,6 |
| PFM000259 | 6699183 | 1629977 | 1061 | 2 | | | | | | | | | | | | 4,9 | 14,5 | 20,6 | 22,9 |
| PFM000513 | 6694094 | 1630846 | 1061 | 2 | | | | | | | | | | | | 5,0 | 27,4 | 18,0 | 30,2 |
| PFM000680 | 6697848 | 1634617 | 1061 | 5 | | | | | | 0,00057 | | | | | | 5,3 | 7,0 | 17,2 | 17,6 |
| PFM000685 | 6698095 | 1635210 | 1061 | 3 | | | | | | | | | | | | 4,7 | 2,3 | 20,4 | 14,9 |
| PFM000725 | 6701464 | 1631021 | 1098 | 2 | | | | | | | | | | | | 3,5 | 25,8 | 18,8 | 27,2 |
| PFM000726 | 6699787 | 1630715 | 1061 | 3 | | | | | | | | | | | | 3,0 | 61,7 | 36,4 | 54,3 |
| PFM000822 | 6699696 | 1628705 | 1061 | 3 | | | | | | | | | | | | 3,1 | 17,2 | 51,6 | 31,5 |
| PFM001162 | 6698339 | 1634013 | 1061 | 3 | | | | | | | | | | | | 5,1 | 14,7 | 6,9 | 19,0 |
| PFM001213 | 6700856 | 1630163 | 1061 | 2 | | | | | | | | | | | | 2,3 | 17,7 | 13,6 | 18,8 |
| PFM001524 | 6698414 | 1629838 | 1061 | 3 | | | | | | | | | | | | 3,2 | 36,1 | 19,7 | 33,4 |
| PFM001858 | 6698716 | 1634302 | 1061 | 2 | | | | | | | | | | | | 4,4 | 4,0 | 23,2 | 16,3 |
| PFM001885 | 6696272 | 1632419 | 1061 | 2 | | | | | | | | | | | | 4,0 | 17,8 | 12,7 | 21,0 |

# Appendix 2

# A compilation of petrophysical properties for different rock type groups

**Group A. Supracrustal rocks**

| A1. (103076) Felsic to intermediate metavolcanic and meta-volcanoclastic rock | | [unit] | Arithmetic mean | Arithmetic standard deviation (α95 for remanence directions) | Geometric mean | Geometric standard deviation above average | Geometric standard deviation below average | Count |
|---|---|---|---|---|---|---|---|---|
| Magnetic properties | Remanence_ declination | deg. | 32,5 | 19,4 | | | | 12 |
| | Remanence_ inclination | deg. | 80,6 | 19,4 | | | | 12 |
| | Remanence_ intensity | A/m | | | 0,0404 | 1,2074 | 0,0391 | 12 |
| | Volume_sus ceptibility | SI | | | 0,00381 | 0,06541 | 0,00360 | 12 |
| | Q-value | SI | | | 0,24 | 0,41 | 0,15 | 12 |
| Density | Wet_density | kg/m3 | 2755 | 88 | | | | 12 |
| Porosity | Porosity | % | 0,34 | 0,08 | | | | 12 |
| Electrical properties | Electric resistivity (in fresh water) | ohmm | | | 22696 | 26316 | 12186 | 12 |
| | Induced polarization (phase at 0.6 Hz in fresh water) | mrad | 22,5 | 16,6 | | | | 12 |
| Gamma-ray spectrometry | K | % | 1,9 | 0,9 | | | | 12 |
| | U | ppm | 3,9 | 0,9 | | | | 12 |
| | Th | ppm | 10,2 | 2,8 | | | | 12 |
| | Natural Exposure | microR/ h | 8,5 | 2,0 | | | | 12 |

**Group A. Supracrustal rocks**

| A2. (109014) Fe-rich mineralisation | | [unit] | Arithmetic mean | Arithmetic standard deviation (α95 for remanence directions) | Geometric mean | Geometric standard deviation above average | Geometric standard deviation below average | Count |
|---|---|---|---|---|---|---|---|---|
| Magnetic properties | Remanence_ declination | deg. | 106,7 | 75,0 | | | | 2 |
| | Remanence_ inclination | deg. | 27,6 | 75,0 | | | | 2 |
| | Remanence_ intensity | A/m | | | 77,7922 | 2,7117 | 2,6204 | 2 |
| | Volume_sus ceptibility | SI | | | 0,12310 | 0,00128 | 0,00127 | 2 |
| | Q-value | SI | | | 15,39 | 0,72 | 0,69 | 2 |
| Density | Wet_density | kg/m3 | 4177 | 67 | | | | 2 |
| Porosity | Porosity | % | 1,36 | 0,16 | | | | 2 |
| Electrical properties | Electric resistivity (in fresh water) | ohmm | | | 233 | 138 | 87 | 2 |
| | Induced polarization (phase at 0.6 Hz in fresh water) | mrad | 216,4 | 22,1 | | | | 2 |
| Gamma-ray spectrometry | K | % | 0,9 | 0,1 | | | | 2 |
| | U | ppm | 5,7 | 0,7 | | | | 2 |
| | Th | ppm | 5,7 | 0,3 | | | | 2 |
| | Natural Exposure | microR/ h | 6,7 | 0,1 | | | | 2 |

**Group B. Ultramafic, mafic, intermediate and quartz-rich felsic (granitoid) meta-intrusive rocks**

| B2/B3. (101033) Metagabbro, metadiorite, quartz-bearing metadiorite, metadioritoid | | [unit] | Arithmetic mean | Arithmetic standard deviation (α95 for remanence directions) | Geometric mean | Geometric standard deviation above average | Geometric standard deviation below average | Count |
|---|---|---|---|---|---|---|---|---|
| Magnetic properties | Remanence_ declination | deg. | 13,5 | 15,9 | | | | 11 |
| | Remanence_ inclination | deg. | 83,3 | 15,9 | | | | 11 |
| | Remanence_ intensity | A/m | | | 0,0254 | 1,0713 | 0,0249 | 11 |
| | Volume_sus ceptibility | SI | | | 0,00471 | 0,03135 | 0,00409 | 11 |
| | Q-value | SI | | | 0,15 | 1,13 | 0,13 | 11 |
| Density | Wet_density | kg/m3 | 2948 | 107 | | | | 11 |
| Porosity | Porosity | % | 0,37 | 0,08 | | | | 11 |
| Electrical properties | Electric resistivity (in fresh water) | ohmm | | | 15916 | 13540 | 7316 | 11 |
| | Induced polarization (phase at 0.6 Hz in fresh water) | mrad | 18,6 | 8,4 | | | | 11 |
| Gamma-ray spectrometry | K | % | 0,8 | 0,4 | | | | 11 |
| | U | ppm | 1,0 | 0,7 | | | | 11 |
| | Th | ppm | 1,7 | 1,9 | | | | 11 |
| | Natural Exposure | microR/ h | 2,3 | 1,6 | | | | 11 |

**Group B. Ultramafic, mafic, intermediate and quartz-rich felsic (granitoid) meta-intrusive rocks**

| B5/B6. (101054) Metatonalite to metagranodiorite | | [unit] | Arithmetic mean | Arithmetic standard deviation (α95 for remanence directions) | Geometric mean | Geometric standard deviation above average | Geometric standard deviation below average | Count |
|---|---|---|---|---|---|---|---|---|
| Magnetic properties | Remanence_ declination | deg. | 26,8 | 14,5 | | | | 14 |
| | Remanence_ inclination | deg. | 84,4 | 14,5 | | | | 14 |
| | Remanence_ intensity | A/m | | | 0,0081 | 0,1551 | 0,0077 | 14 |
| | Volume_sus ceptibility | SI | | | 0,00149 | 0,00881 | 0,00128 | 14 |
| | Q-value | SI | | | 0,12 | 0,25 | 0,08 | 14 |
| Density | Wet_density | kg/m3 | 2746 | 42 | | | | 14 |
| Porosity | Porosity | % | 0,41 | 0,07 | | | | 14 |
| Electrical properties | Electric resistivity (in fresh water) | ohmm | | | 14101 | 5530 | 3972 | 14 |
| | Induced polarization (phase at 0.6 Hz in fresh water) | mrad | 11,7 | 2,6 | | | | 14 |
| Gamma-ray spectrometry | K | % | 1,9 | 0,4 | | | | 14 |
| | U | ppm | 4,0 | 1,3 | | | | 14 |
| | Th | ppm | 9,0 | 1,9 | | | | 14 |
| | Natural Exposure | microR/ h | 8,1 | 1,6 | | | | 14 |

**Group B. Ultramafic, mafic, intermediate and quartz-rich felsic (granitoid) meta-intrusive rocks**

| B8/B9. (101057) Metagranodiorite to metagranite | | [unit] | Arithmetic mean | Arithmetic standard deviation (α95 for remanence directions) | Geometric mean | Geometric standard deviation above average | Geometric standard deviation below average | Count |
|---|---|---|---|---|---|---|---|---|
| Magnetic properties | Remanence_ declination | deg. | 97,4 | 10,5 | | | | 31 |
| | Remanence_ inclination | deg. | 81,4 | 10,5 | | | | 31 |
| | Remanence_ intensity | A/m | | | 0,0248 | 0,0907 | 0,0195 | 31 |
| | Volume_sus ceptibility | SI | | | 0,00453 | 0,01352 | 0,00339 | 31 |
| | Q-value | SI | | | 0,16 | 0,13 | 0,07 | 31 |
| Density | Wet_density | kg/m3 | 2655 | 11 | | | | 31 |
| Porosity | Porosity | % | 0,44 | 0,06 | | | | 31 |
| Electrical properties | Electric resistivity (in fresh water) | ohmm | | | 20362 | 7713 | 5594 | 31 |
| | Induced polarization (phase at 0.6 Hz in fresh water) | mrad | 9,1 | 3,1 | | | | 31 |
| Gamma-ray spectrometry | K | % | 2,9 | 0,6 | | | | 31 |
| | U | ppm | 4,7 | 1,3 | | | | 31 |
| | Th | ppm | 15,4 | 2,2 | | | | 31 |
| | Natural Exposure | microR/ h | 12,1 | 1,6 | | | | 31 |

**Group B. Ultramafic, mafic, intermediate and quartz-rich felsic (granitoid) meta-intrusive rocks**

| B10. (101058) Metagranite, aplitic | | [unit] | Arithmetic mean | Arithmetic standard deviation (α95 for remanence directions) | Geometric mean | Geometric standard deviation above average | Geometric standard deviation below average | Count |
|---|---|---|---|---|---|---|---|---|
| Magnetic properties | Remanence_ declination | deg. | 91,4 | 15,9 | | | | 4 |
| | Remanence_ inclination | deg. | 69,9 | 15,9 | | | | 4 |
| | Remanence_ intensity | A/m | | | 0,0247 | 0,0214 | 0,0115 | 4 |
| | Volume_sus ceptibility | SI | | | 0,00546 | 0,00832 | 0,00330 | 4 |
| | Q-value | SI | | | 0,18 | 0,24 | 0,10 | 4 |
| Density | Wet_density | kg/m3 | 2635 | 11 | | | | 4 |
| Porosity | Porosity | % | 0,39 | 0,04 | | | | 4 |
| Electrical properties | Electric resistivity (in fresh water) | ohmm | | | 16190 | 7662 | 5201 | 4 |
| | Induced polarization (phase at 0.6 Hz in fresh water) | mrad | 11,6 | 2,9 | | | | 4 |
| Gamma-ray spectrometry | K | % | 2,6 | 1,3 | | | | 6 |
| | U | ppm | 5,5 | 1,7 | | | | 6 |
| | Th | ppm | 17,8 | 6,3 | | | | 6 |
| | Natural Exposure | microR/ h | 12,8 | 3,9 | | | | 6 |

**Group C. Quartz-rich felsic (granitoid) meta-intrusive rock, fine- to medium-grained. Occurs as dykes and lenses within rocks belonging to Groups A and B**

| C. (101051) Group C rocks | | [unit] | Arithmetic mean | Arithmetic standard deviation (α95 for remanence directions) | Geometric mean | Geometric standard deviation above average | Geometric standard deviation below average | Count |
|---|---|---|---|---|---|---|---|---|
| Magnetic properties | Remanence_ declination | deg. | 17,5 | 28,8 | | | | 5 |
| | Remanence_ inclination | deg. | 63,3 | 28,8 | | | | 5 |
| | Remanence_ intensity | A/m | | | 0,0099 | 0,0746 | 0,0087 | 5 |
| | Volume_sus ceptibility | SI | | | 0,00107 | 0,00583 | 0,00091 | 6 |
| | Q-value | SI | | | 0,12 | 0,14 | 0,06 | 5 |
| Density | Wet_density | kg/m3 | 2701 | 30 | | | | 5 |
| Porosity | Porosity | % | 0,46 | 0,05 | | | | 5 |
| Electrical properties | Electric resistivity (in fresh water) | ohmm | | | 13187 | 4961 | 3605 | 5 |
| | Induced polarization (phase at 0.6 Hz in fresh water) | mrad | 12,2 | 3,9 | | | | 5 |
| Gamma-ray spectrometry | K | % | 1,9 | 0,7 | | | | 6 |
| | U | ppm | 4,8 | 2,2 | | | | 6 |
| | Th | ppm | 15,4 | 7,3 | | | | 6 |
| | Natural Exposure | microR/ h | 10,7 | 3,5 | | | | 6 |

**Group D. Granite, pegmatitic granite, pegmatite. Occurs as dykes and minor intrusive bodies within rocks belonging to Groups A and B. Pegmatites display variable time relationships to Group C**

| D1. (111058) Granite | | [unit] | Arithmetic mean | Arithmetic standard deviation (α95 for remanence directions) | Geometric mean | Geometric standard deviation above average | Geometric standard deviation below average | Count |
|---|---|---|---|---|---|---|---|---|
| Magnetic properties | Remanence_ declination | deg. | | | | | | |
| | Remanence_ inclination | deg. | | | | | | |
| | Remanence_ intensity | A/m | | | | | | |
| | Volume_sus ceptibility | SI | | | | | | |
| | Q-value | SI | | | | | | |
| Density | Wet_density | kg/m3 | | | | | | |
| Porosity | Porosity | % | | | | | | |
| Electrical properties | Electric resistivity (in fresh water) | ohmm | | | | | | |
| | Induced polarization (phase at 0.6 Hz in fresh water) | mrad | | | | | | |
| Gamma-ray spectrometry | K | % | 4,2 | 0,1 | | | | 3 |
| | U | ppm | 10,2 | 4,3 | | | | 3 |
| | Th | ppm | 28,0 | 6,9 | | | | 3 |
| | Natural Exposure | microR/ h | 21,5 | 1,8 | | | | 3 |

**Group D. Granite, pegmatitic granite, pegmatite. Occurs as dykes and minor intrusive bodies within rocks belonging to Groups A and B. Pegmatites display variable time relationships to Group C**

| D2/D3. (101061) Pegmatitic granite and Pegmatite | | [unit] | Arithmetic mean | Arithmetic standard deviation (α95 for remanence directions) | Geometric mean | Geometric standard deviation above average | Geometric standard deviation below average | Count |
|---|---|---|---|---|---|---|---|---|
| Magnetic properties | Remanence_ declination | deg. | 276,9 | 22,0 | | | | 5 |
| | Remanence_ inclination | deg. | 86,0 | 22,0 | | | | 5 |
| | Remanence_ intensity | A/m | | | 0,0423 | 0,1160 | 0,0310 | 5 |
| | Volume_sus ceptibility | SI | | | 0,00284 | 0,00883 | 0,00215 | 7 |
| | Q-value | SI | | | 0,36 | 0,15 | 0,11 | 5 |
| Density | Wet_density | kg/m3 | 2626 | 5 | | | | 5 |
| Porosity | Porosity | % | 0,53 | 0,08 | | | | 5 |
| Electrical properties | Electric resistivity (in fresh water) | ohmm | | | 16868 | 8881 | 5818 | 5 |
| | Induced polarization (phase at 0.6 Hz in fresh water) | mrad | 8,1 | 2,7 | | | | 5 |
| Gamma-ray spectrometry | K | % | 4,0 | 1,0 | | | | 22 |
| | U | ppm | 15,9 | 13,5 | | | | 22 |
| | Th | ppm | 20,9 | 9,9 | | | | 22 |
| | Natural Exposure | microR/ h | 22,5 | 9,1 | | | | 22 |

## Group A, B and D. Rock types with only one observation

| Group | Count | Magnetic properties | | | | | Density | Porosity | Electrical properties | | Gamma-ray spectrometry properties | | | |
|---|---|---|---|---|---|---|---|---|---|---|---|---|---|---|
| | | Remanence_declination (deg) | Remanence_inclination (deg) | Remanence_intensity (A/m) | Volume_susceptibility (SI) | Q-value (SI) | Wet_density (kg/m3) | Porosity (%) | Electric resistivity (in fresh water, Ωm) | Induced polarization (phase at 0.6 Hz in fresh water, mrad) | K (%) | U (ppm) | Th (ppm) | Natural Exposure (microR/h) |
| **Group A. Supracrustal rocks** | | | | | | | | | | | | | | |
| A3. No SKB code. Veined gneiss | 1 | 130,6 | 62,4 | 0,5328 | 0,04876 | 0,413 | 2700,9 | 0,53 | 11875 | 20,0 | 5,1 | 4,1 | 12,8 | 14,3 |
| A4. 108019. Calc-silicate rock (skarn) | 0 | | | | | | | | | | | | | |
| A5. 109010. Sulphide mineralisation | 0 | | | | | | | | | | | | | |
| | | | | | | | | | | | | | | |
| **Group B. Ultramafic, mafic, intermediate and quartz-rich felsic (granitoid) meta-intrusive rocks** | | | | | | | | | | | | | | |
| B1. 101004. Meta-ultramafic rock | 1 | 30,7 | 61,2 | 4,6750 | 0,04572 | 2,260 | 3044,5 | 1,04 | 52 | 724,8 | 0,0 | 0,0 | 0,0 | 0,0 |
| B4. 102017. Amphibolite | 1 | 16,2 | 52,9 | 0,0001 | 0,00071 | 0,004 | 2928,3 | 0,30 | 11211 | 15,3 | 1,3 | 1,1 | 2,6 | 3,4 |
| B7. 101056. Metagranodiorite | 1 | 140,8 | 73,4 | 0,1442 | 0,00673 | 0,369 | 2703,9 | 0,50 | 76646 | 23,5 | 1,7 | 3,3 | 8,3 | 7,2 |
| | | | | | | | | | | | | | | |
| **Group D. Granite, pegmatitic granite, pegmatite. Occurs as dykes and minor intrusive bodies within rocks belonging to Groups A and B. Pegmatites display variable time relationships to Group C** | | | | | | | | | | | | | | |
| D1. 111058. Granite | 1 | 102,9 | 75,4 | 0,0534 | 0,00204 | 0,22 | 2631,5 | 0,48 | 13017 | 12,5 | | | | |

# Appendix 3

## Delivered data

### Shape-files

| Filename | Filetype | Information type | Content |
|---|---|---|---|
| fm_kmax_point | Shape | Petrophysic | Magnetic anisotropy- lineation |
| fm_kmin_point | Shape | Petrophysic | Magnetic anisotropy- foliation |
| fm_l_f_p_t_point | Shape | Petrophysic | Magnetic anisotropy- Parameters describing the shape of magnetical susceptibility ellipsoid |
| fm_s_r_q_d_p_point | Shape | Petrophysic | Magnetic susceptibility, density, remanence, Q-value, porosity |
| fm_res_ip_point | Shape | Petrophysic | Electrical properties measured on samples. |
| fm_gammaspek_rockgroup_point | Shape | Petrophysic | Site average on K, U and Th, calculated for each outcrop and rocktype |
| fm_hallsusc_point | Shape | Petrophysic | Site average on susceptibility, calculated for each outcrop and rocktype. Supplementary data from SGU bedrock database. |



### Tiff-files

| Filename | Filetype | Information type | Content |
|---|---|---|---|
| FM_HallSusc_map | Tiff | Petrophysic | Site average on susceptibility, calculated for each outcrop and most frequent rocktype (rockno=1). Interpolated to a 10m grid using Krieging (Surfer ver.8, Golden Software Inc) |

### Grid- and xls-files

| Filename | Filetype | Information type | Content |
|---|---|---|---|
| mag_sus_anisotropi_sitemeandata | xls | Petrophysic | Site average on magnetic susceptibility anisotropy, calculated for each outcrop and rocktype |
| Q_value | xls | Petrophysic | Calculated Q-value |
| outcrop_magnetic susceptibility_sitemean | xls | Petrophysic | Site average on susceptibility, calculated for each outcrop and rocktype |